

**IN THE UNITED STATES PATENT AND TRADEMARK OFFICE**

Applicant : Lin et al.  
App. No. : 10/815,905  
Filed : March 31, 2004  
For : INTERFEROMETRIC MODULATION  
PIXELS AND MANUFACTURING  
METHOD THEREOF  
Examiner : Hoang Q. Tran  
Art Unit : 2874  
Conf. No. : 9293

**CERTIFICATE OF EFS WEB  
TRANSMISSION**

I hereby certify that this correspondence, and any other attachment noted on the automated Acknowledgement Receipt, is being transmitted from within the Pacific Time zone to the Commissioner for Patents via the EFS Web server on:

December 11, 2009

(Date)

  
Jeremy R. Pierce, Reg. No. 59,034**ON APPEAL TO THE BOARD OF PATENT APPEALS AND INTERFERENCES**  
**APPELLANT'S BRIEF**

**Mail Stop Appeal Brief – Patents**  
**COMMISSIONER FOR PATENTS**  
P.O. Box 1450  
Alexandria, VA 22313-1450

Dear Sir:

The Appellants appeal the rejection of Claims 20-28 in the above-referenced patent application. These claims were rejected in a Final Office Action dated July 22, 2009. Appellants filed a Pre-Appeal Brief Request for Review and a Notice of Appeal on September 21, 2009. The panel determined that Claims 20-28 remained rejected, and the decision was mailed on November 13, 2009, providing a one-month time period for filing an appeal brief.

**I. REAL PARTY IN INTEREST**

Pursuant to 37 C.F.R. 41.37(c)(1), Appellants hereby notify the Board of Patent Appeals and Interferences that the real party in interest is the assignee of record for this application, Qualcomm MEMS Technologies, Inc., 5775 Morehouse Drive, San Diego, CA 92121-1714.

**II. RELATED APPEALS AND INTERFERENCES**

Appellants are unaware of any other related appeals or interferences.

**III. STATUS OF THE CLAIMS**

Claims 20-28 are finally rejected. Claims 1-19 are withdrawn from consideration. Accordingly, Claims 20-28 are the subject of this appeal. The claims at issue are attached hereto as Appendix A.

**IV. STATUS OF AMENDMENTS**

No amendments were submitted subsequent to the July 22, 2009 Final Office Action.

**V. SUMMARY OF THE CLAIMED SUBJECT MATTER**

The claimed subject matter is directed to an interferometric modulation pixel that comprises a first electrode (205, 210, 215) and a movable second electrode (245) situated above and parallel to the first electrode. *See* Specification, page 6, lines 9-10 and Figure 2D. The interferometric modulation pixel comprises two supports (235) between the first electrode (205, 210, 215) and the second electrode (245), such that a cavity is formed between the first and the second electrodes. *See* Specification, page 6, lines 10-12 and Figure 2D. The interferometric modulation pixel comprises a hydrophobic layer (250) on a cavity-side surface of the first electrode (205, 210, 215). *See* Specification, page 6, lines 12-13 and Figure 2D. The hydrophobic layer (250) is formed on the first electrode (205, 210, 215) to maintain the distance between the first electrode and the second electrode (245) such that the second electrode is not pulled toward the first electrode due to adsorbed moisture in the cavity. Specification, page 4, lines 14-18.

**VI. GROUND OF REJECTION TO BE REVIEWED ON APPEAL**

A. The Examiner has rejected pending Claims 20, 21, 23, and 26-28 under 35 U.S.C. §103(a) as being unpatentable over U.S. Patent No. 5,835,255 to Miles ("Miles") in view of Matsumoto et al., "Novel Prevention Method of Stiction Using Silicon Anodization for SOI Structure," Sensors and Actuators, A72 (1999) 153-159 ("Matsumoto"). *See* Final Office Action dated July 22, 2009, pages 2-4.

B. The Examiner also has rejected pending Claims 22, 24, and 25 as being unpatentable over Miles in view of Matsumoto and further in view of U.S. Patent No. 6,335,224 to Peterson et al. ("Peterson"). See Final Office Action dated July 22, 2009, pages 4-5.

## VII. APPELLANTS' ARGUMENT

### A. Rejection of Claims 20, 21, 23, and 26-28 over Miles in view of Matsumoto

The Examiner's rejection contains clear error because the Examiner has not established a *prima facie* case of obviousness since the combination of references proposed by the Examiner does not provide a reasonable expectation of success. To support a conclusion that a claim would have been obvious, M.P.E.P. § 2143.02 requires that "one skilled in the art could have combined the elements as claimed by known methods with no change in their respective functions." The prior art can only be modified or combined to reject claims as obvious if there is a reasonable expectation of success. *In re Merck & Co., Inc.*, 800 F.2d 1091, (Fed. Cir. 1986).

Miles discloses an optical display device that functions by modulating light. One of the stated features of the light modulating device disclosed by Miles is that such a device provides "high resolution, full-color images" (Miles, column 3, line 5). The Miles device is dependent upon its ability to reflect and modulate light (*see* Miles, column 2, lines 30-56). In fact, Miles states that lower layer 502 and upper layer 506/508 in the optical device are both mirror layers (Miles, column 13, lines 27-30).

The ability of the mirrors to reflect light properly is further described by Miles at, for example, column 1, line 62 – column 2, line 7 (see below, emphasis added).

The predetermined impedance characteristic may include reflection of incident electromagnetic radiation in the visible spectrum, e.g., the proportion of incident electromagnetic radiation of a given frequency band that is, on average, <sup>65</sup> reflected by each of the modulation elements. The modulation element may be responsive to a particular electrical

2

condition to occupy either a state of higher reflectivity or a state of lower reflectivity, and the control circuitry may generate a stream of pulses having a duty cycle corresponding to the proportion of incident radiation that is reflected and places the modulation element in the higher state of reflectivity during each the pulse and in the lower state of reflectivity in the intervals between the pulses. The charac-

It is clear that the Miles device is not simply a micromechanical device. Rather, the Miles device is an optical device whose function depends upon its ability to reflect and modulate light in a particular manner.

The Examiner relies on Matsumoto for the proposition that one of ordinary skill in the art could insert a self-assembled monolayer ("SAM") or a fluorocarbon film into the device of Miles. However, Matsumoto does not address the important aspects of an optical device's ability to reflect and modulate light. Matsumoto discloses a "study made on the application of silicon anodization process to prevent both 'after-rinse stiction' and 'in-use stiction' for SOI sensors" (Matsumoto, p. 153). While the disclosed SOI sensors are micromechanical devices, there is no indication that their performance is dependent on their optical properties. Nor does Matsumoto provide any discussion regarding an SOI sensor's ability to modulate or reflect light. Matsumoto merely states that the "formation of [a] hydrophobic surface such as SAM or fluorocarbon film is one of the effective methods to prevent stiction although these methods require additional fabrication process or specific equipment" (Matsumoto, p. 154).

However, Matsumoto does not provide any reason for one of ordinary skill in the art to use either of the self-assembled monolayer ("SAM") or the fluorocarbon film in an optical device, and is silent with regard to whether such use on the reflective surfaces of an optical device would likely be successful. Therefore, Matsumoto provides no reasonable expectation of success for modifying an optical device to include a hydrophobic layer, because it fails to account for the effect such modification one skilled in the art would have expected such a layer to have on optical performance.

Appellants note that several references of record support the proposition that, at the time of the invention, neither fluorocarbon films nor SAMs would necessarily have been considered compatible with optical devices that modulate light. For example, U.S. Patent No. 5,730,792 to

Camilletti et al. describes fluorocarbon polymers as “opaque materials or obstructing agents” at column 5, lines 24-47. Additionally, U.S. Patent No. 6,020,047 to Everhart discloses that SAMs both reflect and transmit visible light such that “[r]ainbow diffraction colors were observed with transmitted white light” at column 7, lines 61-67.

The evidence of record, unrebutted by the Examiner, establishes that fluorocarbons and SAM's can negatively affect the ability of a mirror layer, such as the mirror layer described by Miles, to reflect light, and Matsumoto does not contradict this evidence. The Miles device would not function properly, *e.g.* to provide high resolution, full-color images in the manner described by Miles, if the mirror layers did not properly reflect light. Therefore, there is no *prima facie* obviousness in view of the evidence of record because the combination of references proposed by the Examiner does not provide a reasonable expectation of success.

The Examiner made several arguments in the Final Office Action, each of which are addressed below. First, in the “Response to Arguments” section on page 5 of the Final Office Action, the Examiner stated that “[A]pplicant argues that the prior art to Miles is not a micromechanical device.” This is an inaccurate characterization of the argument actually made by Appellants. As outlined above, Appellants previously argued that “the Miles device is not simply a micromechanical device. Rather, the Miles device is an optical device whose function depends upon its ability to reflect and modulate light” (emphasis added). Appellants were pointing out that, importantly, the micromechanical device of Miles heavily relied on its optical function and ability to reflect and modulate light. The Examiner did not rebut this aspect of Miles.

Instead, on page 6 of the Final Office Action, the Examiner cited to column 15, lines 16-67 of Miles and asserted that “the mirror of Miles is capable of both transmitting and reflecting.” The Examiner then argued that “adding an additional film using SAM base materials and techniques would not prevent the device of Miles from functioning since the SAM base material is capable of both transmitting and reflecting. The level of T/R can be adjusted by one of ordinary skill in the art.” Appellants respectfully disagree. The Examiner's conclusion that transmittance and reflection can simply be adjusted upon the addition of an opaque layer that interferes with or scatters light is a conclusory statement that is unsupported by any evidence. In fact, the only evidence that is of record, U.S. Patent Nos. 5,730,792 to Camilletti et al. and

6,020,047 to Everhart, establishes that fluorocarbons and SAM's can negatively affect the ability of a mirror layer.

The "T/R" plots in Miles refer to the ability of the optical devices to transmit and reflect visible light in the driven and undriven states (column 14, lines 46-55). However, there is simply nothing in either Miles or Matsumoto that teaches a person having ordinary skill in the art how to adjust both the transmission and reflectivity of a material upon the addition of an opaque fluorocarbon or SAM-based film.

The Examiner's assertion that a "SAM base material is capable of both transmitting and reflecting" is misleading because it amounts to nothing more than a *non sequitur*. Many materials, such as paper, reflect and transmit light, but one would not put paper over a mirror and expect it to function properly. Likewise, even with knowledge that a SAM would reflect and transmit light, the more important inquiry is *how* one of skill in the art would expect a SAM to transmit and reflect light. Appellants previously submitted the Everhart reference as evidence for the proposition that a SAM reflects and transmits diffraction patterns and that rainbow diffraction colors were observed with transmitted white light. Thus, based on Everhart one skilled in the art would have expected that the SAM layer proposed by the Examiner would scatter light into multiple wavelengths in a manner completely in conflict with the teachings of Miles, which discloses a device that provides "high resolution, full-color images" (Miles, column 3, line 5). Miles does not provide any disclosure as to how one of ordinary skill in the art could control transmittance and reflectance of such a scattered diffraction pattern. Nor does the Examiner support that assertion with any evidence of record.

Rather, the evidence that is of record clearly indicates that one of ordinary skill in the art at the time of the invention would not have had a reasonable expectation of success to modify the optical device of Miles, which heavily relies on its ability to control and modulate light, by adding an opaque or light scattering layer that could interfere with the light modulation. Therefore, Appellants respectfully request reconsideration and reversal of this rejection.

B. Rejection of Claims 22, 24, and 25 over Miles in view of Matsumoto and Peterson

Peterson does not cure the defects of Miles and Matsumoto discussed above. Since the factual findings of record strongly support non-obviousness of the claims over the cited references, the Examiner's failure to address and rebut Appellants' evidence and arguments

**Application No. : 10/815,905**  
**Filed : March 31, 2004**

constitutes clear error. Therefore, Appellants respectfully request reconsideration and reversal of this rejection.

C. Conclusion

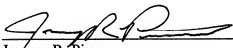
In view of the arguments presented above, Appellants submit that Claims 20-28 are allowable. Appellants therefore respectfully request that the Board reverse the rejections of the pending claims as unpatentable under 35 U.S.C. §103(a).

Please charge any additional fees, including any fees for additional extension of time, or credit overpayment to Deposit Account No. 11-1410.

Respectfully submitted,

KNOBBE, MARTENS, OLSON & BEAR, LLP

Dated: 12/11/2009

By:   
Jeremy R. Pierce  
Registration No. 59,034  
Attorney of Record  
Customer No. 20995  
(619) 235-8550

**VIII. APPENDIX A – CLAIMS ON APPEAL**

20. An interferometric modulation pixel, comprising:  
a first electrode;  
a movable second electrode being situated above the first electrode and being parallel to the first electrode;  
two supports between the first electrode and the second electrode to form a cavity between the first and the second electrodes; and  
a hydrophobic layer on a cavity-side surface of the first electrode.
21. The interferometric modulation pixel of claim 20, wherein the hydrophobic layer comprises a hydrophobic organic compound having at least a hydrogen atom being capable of forming hydrogen bonds with oxygen or nitrogen atoms or a hydrophobic resin.
22. The interferometric modulation pixel of claim 20, wherein the hydrophobic organic compound comprises silanes including hexamethyl disilane or silanols including trimethyl silanol.
23. The interferometric modulation pixel of claim 20, wherein the first electrode comprises an insulating layer.
24. The interferometric modulation pixel of claim 23, wherein the insulating layer comprises silicon oxide or silicon nitride.
25. The interferometric modulation pixel of claim 23, wherein the hydrophobic layer is positioned on the insulating layer.
26. The interferometric modulation pixel of claim 20, wherein the first electrode comprises a transparent conductive layer, a light-absorption layer and an insulating layer.
27. The interferometric modulation pixel of claim 20, wherein the movable second electrode is a light-reflection electrode.
28. The interferometric modulation pixel of claim 20, wherein the hydrophobic layer prevents the first electrode from adsorbing water molecules.



**Application No. : 10/815,905**  
**Filed : March 31, 2004**

**IX. APPENDIX B – EVIDENCE**

Attached hereto is a copy of the evidence cited in Appellants' Brief. The list of evidence below is accompanied by a statement setting forth where in the record that evidence was entered into the record by the Examiner.

<b>Item</b>	<b>Reference</b>	<b>Submitted</b>	<b>Entered</b>
1	U.S. Patent No. 5,835,255 to Miles	Submitted in an Information Disclosure Statement mailed on April 30, 2004.	Considered by the Examiner in the Office Action mailed on May 10, 2007.
2	Matsumoto et al., "Novel Prevention Method of Stiction Using Silicon Anodization for SOI Structure," Sensors and Actuators, A72 (1999) 153-159.	Submitted in an Information Disclosure Statement on June 13, 2008.	Considered by the Examiner in the Office Action mailed on January 23, 2009.
3	U.S. Patent No. 6,335,224 to Peterson et al.		Cited by the Examiner in the Office Action mailed on May 10, 2007.
4	U.S. Patent No. 5,730,792 to Camilletti et al.	Submitted in an Information Disclosure Statement on April 22, 2009.	Considered by the Examiner in the Office Action mailed on July 22, 2009.
5	U.S. Patent No. 6,020,047 to Everhart	Submitted in an Information Disclosure Statement on April 22, 2009.	Considered by the Examiner in the Office Action mailed on July 22, 2009.

**Application No. : 10/815,905**  
**Filed : March 31, 2004**

**X. APPENDIX C – RELATED PROCEEDINGS**

None – there are no decisions rendered by a court or the Board in any related proceedings identified above.



US00583255A

**United States Patent** [19][11] **Patent Number:** **5,835,255****Miles**[45] **Date of Patent:** **Nov. 10, 1998**[54] **VISIBLE SPECTRUM MODULATOR ARRAYS**

5,022,745 6/1991 Zaykowski et al. .... 350/608

[75] **Inventor:** **Mark W. Miles, Boston, Mass.**

5,044,736 9/1991 Jaskie et al. .... 359/291

[73] **Assignee:** **Etalon, Inc., Boston, Mass.**

(List continued on next page.)

[21] **Appl. No.:** **238,750**[22] **Filed:** **May 5, 1994****OTHER PUBLICATIONS****Related U.S. Application Data**

[63] Continuation-in-part of Ser. No. 32,711, Mar. 17, 1993, abandoned, which is a continuation of Ser. No. 794,819, Nov. 18, 1991, abandoned, which is a continuation of Ser. No. 489,794, Mar. 5, 1990, abandoned, which is a continuation of Ser. No. 296,896, Jan. 12, 1989, abandoned, which is a continuation of Ser. No. 166,774, Mar. 4, 1988, abandoned, which is a continuation of Ser. No. 855,116, Apr. 23, 1986, abandoned.

"Light over Matters", Jun. 1993, Circle No. 36.  
Miles, Mark, W., "A New Reflective FPD Technology Using Interferometric Modulation", Society for Information Display '97 Digest, Session 7.3.  
Newsbreaks, "Quantum-trench devices might operate at terahertz frequencies", Laser Focus World May 1993.  
Winton, John M., "A novel way to capture solar energy", Chemical Week, May 15, 1985.

(List continued on next page.)

[51] **Int. Cl.<sup>6</sup>** ..... **G02B 26/00**[52] **U.S. Cl.** ..... **359/291; 359/578**[58] **Field of Search** ..... 359/528, 529,  
359/290, 291, 522

*Primary Examiner*—Georgia Y. Epps  
*Assistant Examiner*—Dawn-Marie Bey  
*Attorney, Agent, or Firm*—Fish & Richardson PC

**ABSTRACT**[56] **References Cited****U.S. PATENT DOCUMENTS**

2,534,846 12/1950 Ambrose et al. .... 178/5.2  
3,439,973 4/1969 Paul et al. .... 350/370  
3,443,854 5/1969 Weiss ..... 350/395  
3,653,741 4/1972 Marks ..... 350/370  
3,813,265 5/1974 Marks ..... 350/395  
3,955,880 5/1976 Lierke ..... 359/291  
4,099,854 7/1978 Decker et al. .... 350/370  
4,228,437 10/1980 Shelton ..... 343/009  
4,377,324 3/1983 Durand et al. .... 350/166  
4,389,096 6/1983 Hort et al. .... 350/339 R  
4,403,248 9/1983 Te Velde ..... 358/62  
4,445,050 4/1984 Marks ..... 307/145  
4,519,676 5/1985 te Velde ..... 350/269  
4,531,126 7/1985 Sadones ..... 343/009  
4,663,083 5/1987 Marks ..... 350/375  
4,681,403 7/1987 Te Velde et al. .... 350/334  
4,748,366 5/1988 Taylor .  
4,790,635 12/1988 Apsley ..... 350/356  
4,982,184 1/1991 Kirkwood .

Light in the visible spectrum is modulated using an array of modulation elements, and control circuitry connected to the array for controlling each of the modulation elements independently, each of the modulation elements having a surface which is caused to exhibit a predetermined impedance characteristic to particular frequencies of light. The amplitude of light delivered by each of the modulation elements is controlled independently by pulse code modulation. Each modulation element has a deformable portion held under tensile stress, and the control circuitry controls the deformation of the deformable portion. Each deformable element has a deformation mechanism and an optical portion, the deformation mechanism and the optical portion independently imparting to the element respectively a controlled deformation characteristic and a controlled modulation characteristic. The deformable modulation element may be a non-metal. The elements are made by forming a sandwich of two layers and a sacrificial layer between them, the sacrificial layer having a thickness related to the final cavity dimension, and using water or an oxygen based plasma to remove the sacrificial layer.

**46 Claims, 26 Drawing Sheets**

## U.S. PATENT DOCUMENTS

5,075,796	12/1991	Schildkraut et al.	
5,124,834	6/1992	Cusano et al.	359/291
5,153,771	10/1992	Link et al.	359/286
5,168,406	12/1992	Nelson	
5,231,532	7/1993	Magel et al.	359/295
5,233,459	8/1993	Bozler et al.	359/230
5,311,360	5/1994	Bloom et al.	
5,381,253	1/1995	Sharp et al.	
5,401,983	3/1995	Jokerst et al.	
5,459,610	10/1995	Bloom et al.	
5,497,172	3/1996	Doherty et al.	
5,500,635	3/1996	Mott	
5,500,761	3/1996	Goossen et al.	359/290
5,579,149	11/1996	Moret et al.	
5,619,059	4/1997	Li et al.	
5,636,052	6/1997	Arney et al.	
5,703,710	12/1997	Brinkman et al.	
5,710,656	1/1998	Goossen	

## OTHER PUBLICATIONS

Aratani, K., et al., "Surface micromachined tuneable interferometer array", *Sensors and Actuators*, 1994, pp. 17-23.  
 Johnson, "Optical Scanners", *Microwave Scanning Antennas*, vol. 1, p. 251 et seq.  
 Akasaka, "Three-Dimensional IC Trends", *Proceedings of IEEE*, vol. 74, No. 12, Dec. 1986, pp. 1703-1714.  
 Stone, "Radiation and Optics, An Introduction to the Classical Theory", McGraw-Hill, pp. 340-343.  
 Jackson, "Classical Electrodynamics", John Wiley & Sons Inc., pp. 568-573.  
 Gosch, "West Germany Graps the Lead in X-Ray Lithography", *Electronics*, Feb. 5, 1987, pp. 78-80.

Howard, "Nanometer-Scale Fabrication Techniques", *VLSI Electronics: Microstructure Science*, vol. 5, 1982, pp. 145-153, pp. 166-173.

Jerman et al., "A Miniature Fabry-Perot Interferometer with a Corrugated Silicon Diaphragm Support", *Sensors and Actuators A*, vol. 29, p. 151, 1991.

Raley et al., "A Fabry-Perot Microinterferometer for Visible Wavelengths", *IEEE Solid-State Sensor and Actuator Workshop*, Jun. 1992, Hilton Head, SC.

Aratani, et al., "Process and Design Considerations for Surface Micromachined Beams for a Tuneable Interferometer Array in Silicon", *Proc. IEEE Microelectromechanical Workshop*, Fort Lauderdale, FL, Feb. 7-10, p. 230, 1993.

Walker, et al., "Electron-beam-tunable Interference Filter Spatial Light Modulator", *Optics Letters* vol. 13, No. 5, p. 345, 1988.

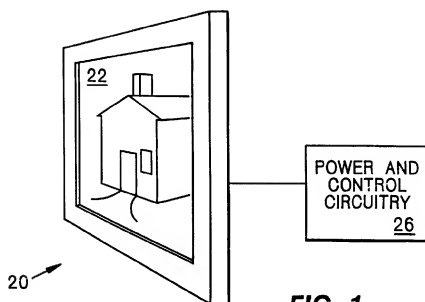
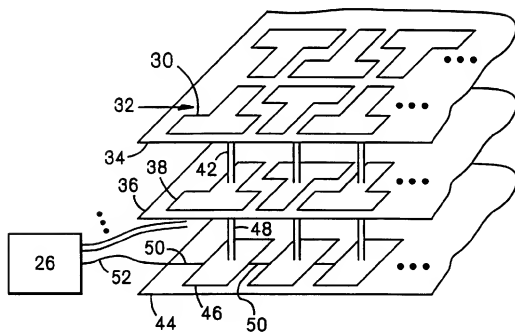
Goossen et al., "Silicon Modulator Based on Mechanically-Active Anti-Reflection Layer with 1Mbit/sec Capability for Fiber-in-the-Loop Applications", *IEEE Photonic Technology Letters*, Sep. 1994.

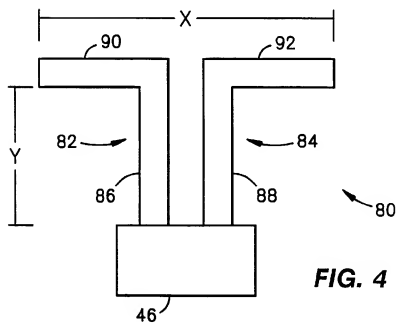
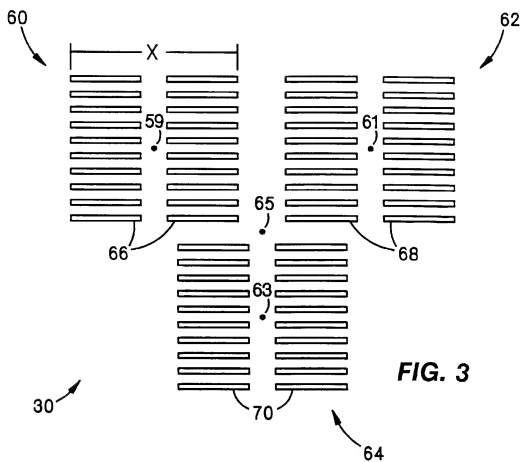
Goossen et al., "Possible Display Applications of the Silicon Mechanical Anti-Reflection Switch", *Society for Information Display*, 1994.

Sperger et al., "High Performance Patterned All-Dielectric Interference Colour Filter for Display Applications", *SID Digest* 1994.

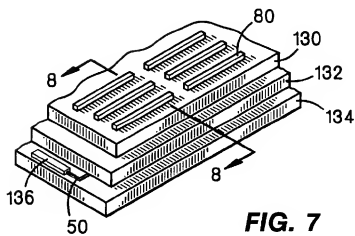
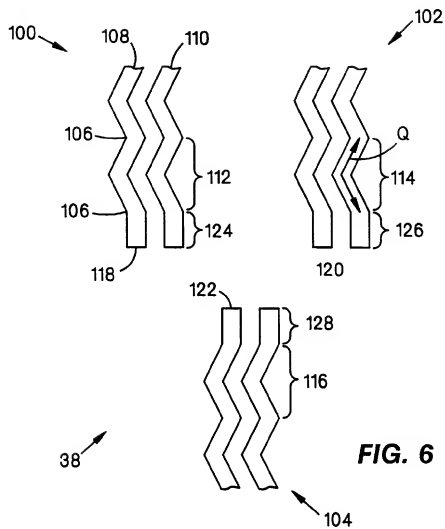
Conner, "Hybrid Color Display Using Optical Interference Filter Array", *SID Digest* 1993, pp. 577-580.

Wu, "Design of a Reflective Color LCD Using Optical Interference Reflectors", *ASIA Display '95*, Oct. 16, pp. 929-931.

**FIG. 1****FIG. 2**

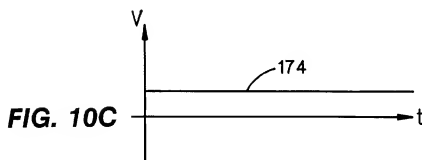
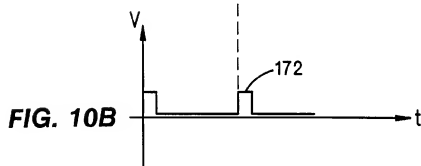
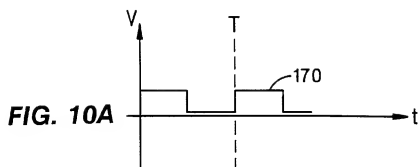


**FIG. 5**

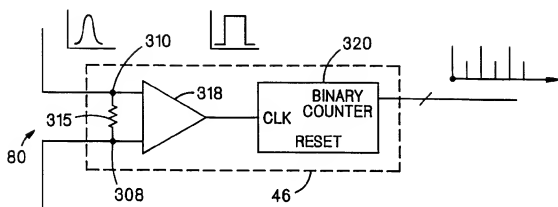
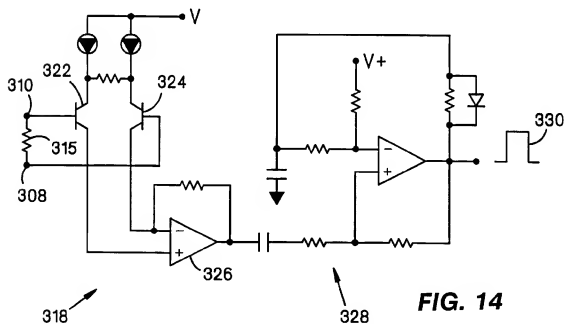


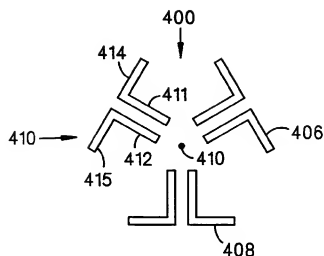
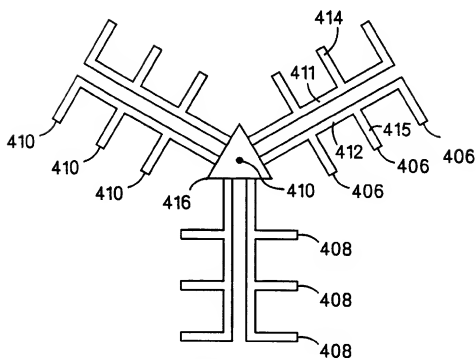


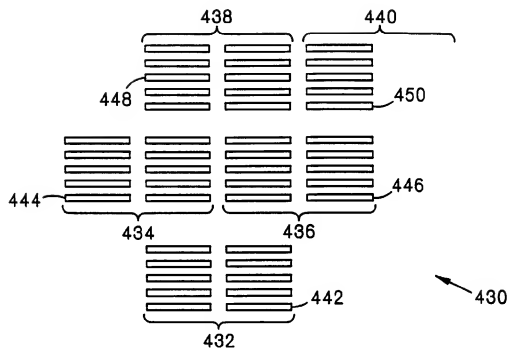
**FIG. 9**

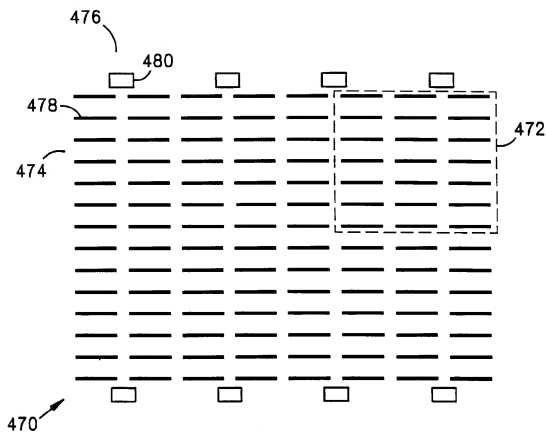
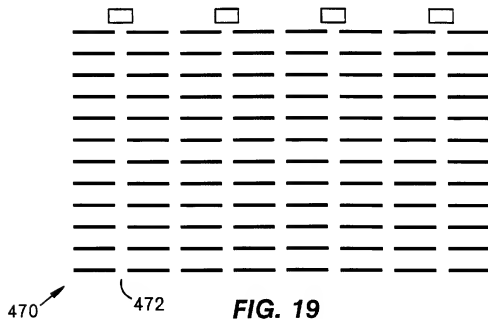


**FIG. 12**

**FIG. 13****FIG. 14**

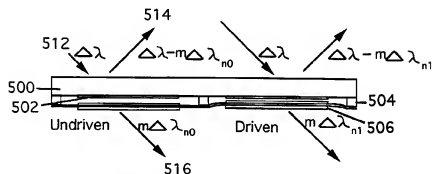
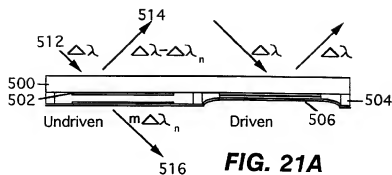
**FIG. 15****FIG. 16**

**FIG. 17**

**FIG. 18****FIG. 19**

**FIG. 20D**





eq. 1

$$T = \frac{T_a T_b}{[1 - (R_a^* R_b^*)^{1/2}]^2} \left[ 1 + \frac{4 R_a^* R_b^*}{[1 - (R_a^* R_b^*)^{1/2}]^2} \sin^2 \left( \frac{\phi_a + \phi_b}{2} - \delta \right) \right]^{-1}$$

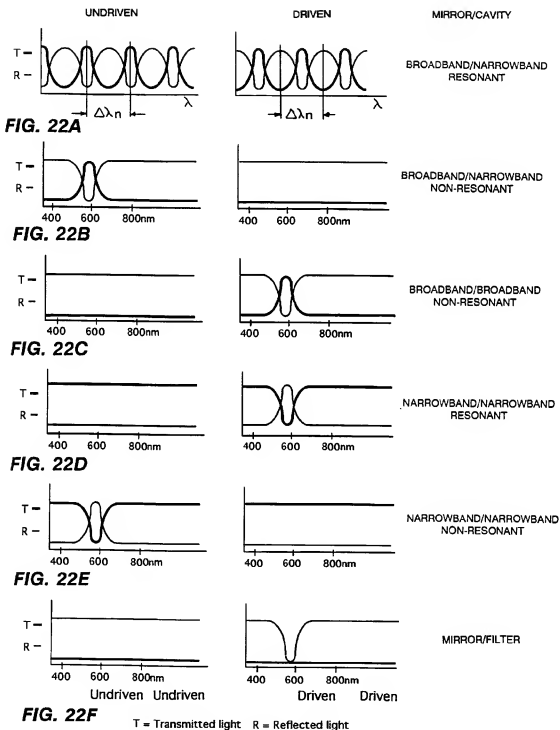
eq. 2

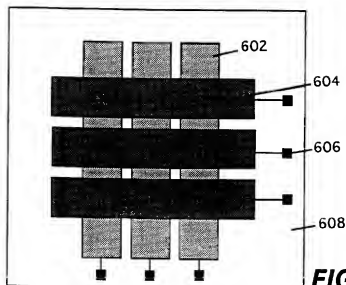
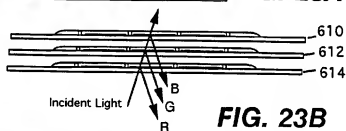
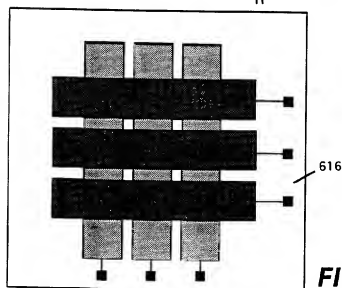
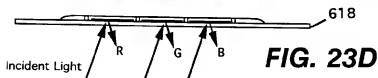
$$\delta = (2\pi n_s d_s \cos \theta_s) / \lambda_s \quad \text{phase thickness}$$

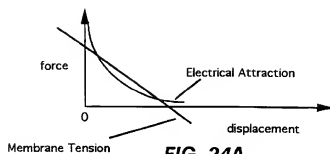
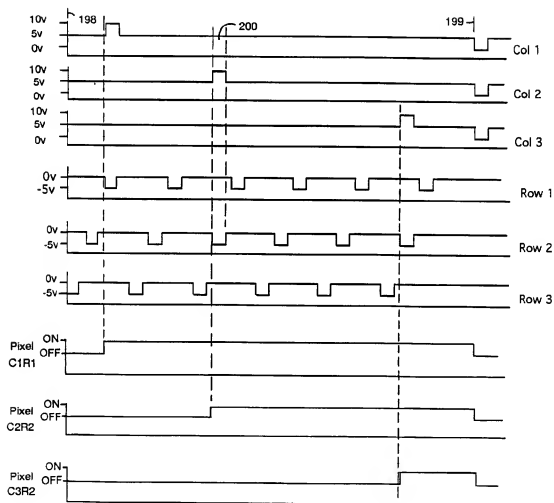
eq. 3

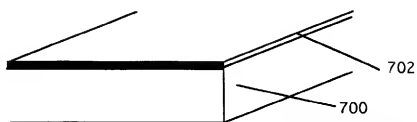
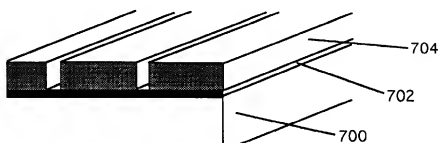
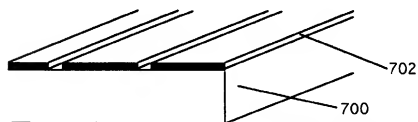
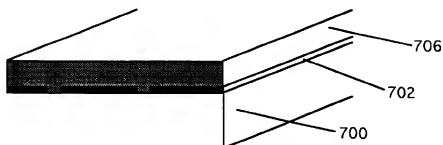
$$T = T_b \quad \text{for } T_a \text{ approaching } 0$$

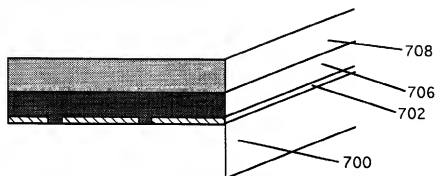
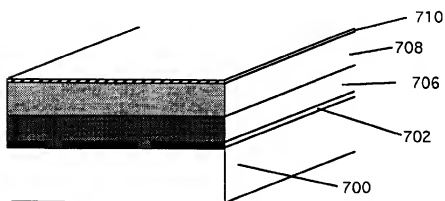
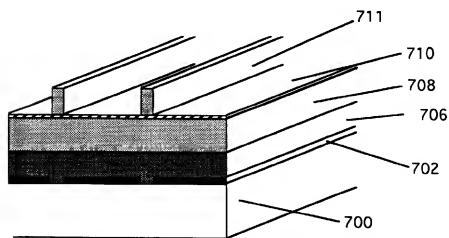
**FIG. 21B**

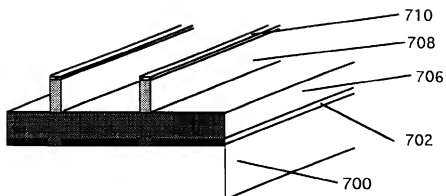
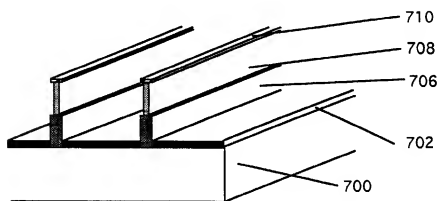
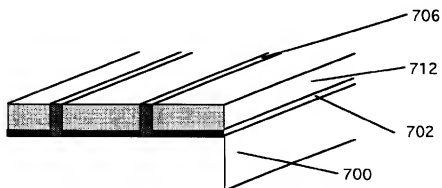


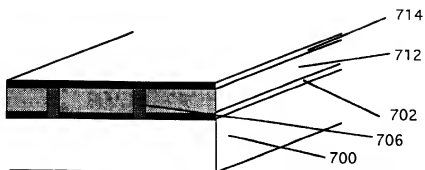
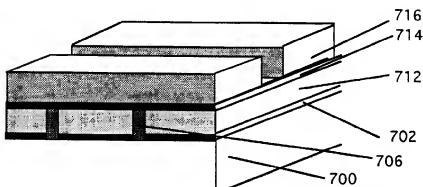
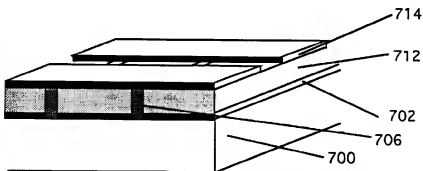
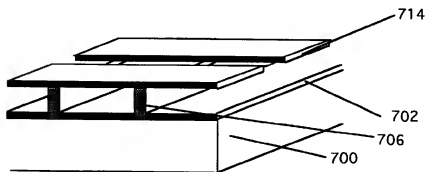
**FIG. 23A****FIG. 23B****FIG. 23C****FIG. 23D**

**FIG. 24A****FIG. 24B**

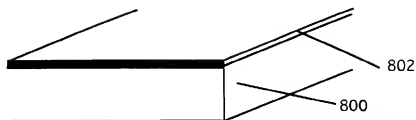
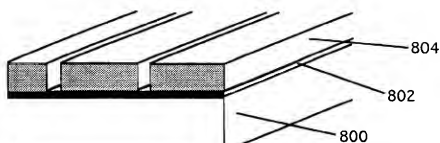
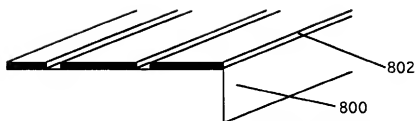
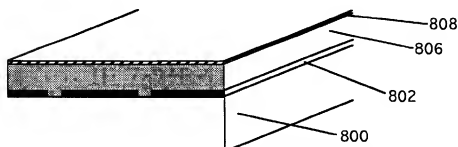
**FIG. 25A****FIG. 25B****FIG. 25C****FIG. 25D**

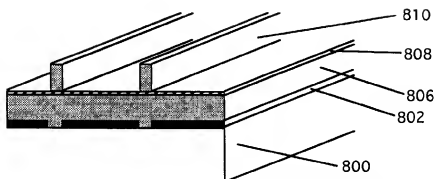
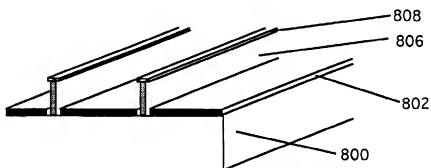
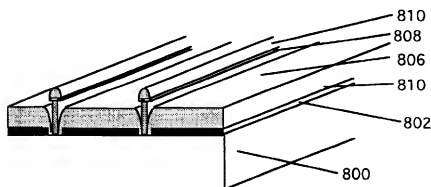
**FIG. 25E****FIG. 25F****FIG. 25G**

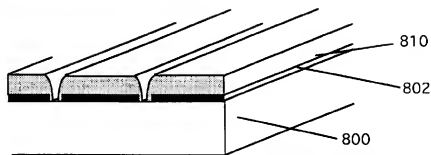
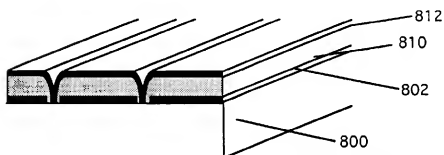
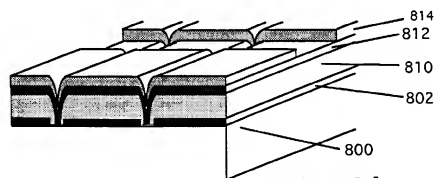
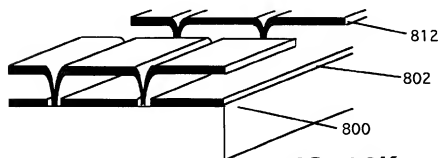
**FIG. 25H****FIG. 25I****FIG. 25J**

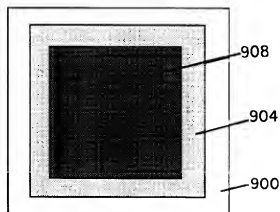
**FIG. 25K****FIG. 25L****FIG. 25M****FIG. 25N**

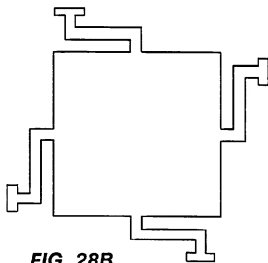
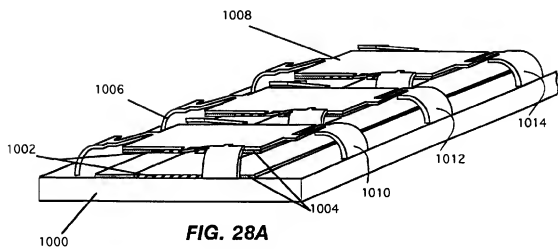


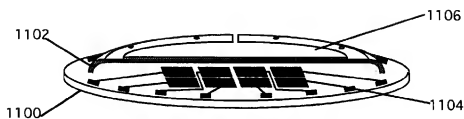
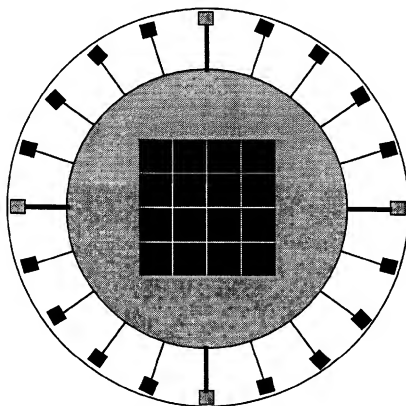
**FIG. 26A****FIG. 26B****FIG. 26C****FIG. 26D**

**FIG. 26E****FIG. 26F****FIG. 26G**

**FIG. 26H****FIG. 26I****FIG. 26J****FIG. 26K**

**FIG. 27A****FIG. 27B****FIG. 27C****FIG. 27D**



**FIG. 29A****FIG. 29B**

## VISIBLE SPECTRUM MODULATOR ARRAYS

This is a continuation-in-part of U.S. Ser. No. 08/032, 711, filed Mar. 17, 1993, now abandoned; which was a continuation of U.S. Ser. No. 07/794,819, filed Nov. 18, 1991, now abandoned; which was a continuation of U.S. Ser. No. 07/489,794, filed Mar. 5, 1990, now abandoned; which was a continuation of U.S. Ser. No. 07/296,896, filed Jan. 12, 1989, now abandoned; which was a continuation of U.S. Ser. No. 07/166,774, filed Mar. 4, 1988, now abandoned; which was a continuation of U.S. Ser. No. 06/855,116, filed Apr. 23, 1986, now abandoned, and incorporated herein by reference.

### BACKGROUND

This invention relates to modulator arrays.

Visible spectrum modulator arrays, such as backlit LCD computer screens, have arrays of electro-optical elements corresponding to pixels. Each element may be electronically controlled to alter light which is aimed to pass through the element. By controlling all of the elements of the array, black and white or, using appropriate elements, color images may be displayed. Non-backlit LCD arrays have similar properties but work on reflected light. These and other types of visible spectrum modulator arrays have a wide variety of other uses.

### SUMMARY OF THE INVENTION

In general, in one aspect, the invention features modulation of light in the visible spectrum using an array of modulation elements, and control circuitry connected to the array for controlling each of the modulation elements independently, each of the modulation elements having a surface which is caused to exhibit a predetermined impedance characteristic to particular frequencies of light.

Implementations of the invention may include the following features. The surface may include antennas configured to interact with selected frequencies of light, or the surface may be a surface of an interference cavity. The impedance characteristic may be reflection of particular frequencies of light, or transmission of particular frequencies of light. Each of the modulation elements may be an interference cavity that is deformable to alter the cavity dimension. The interference cavity may include a pair of cavity walls (e.g., mirrors) separated by a cavity dimension. One of the mirrors may be a broadband mirror and the other of the mirrors may be a narrow band mirror. Or both of the mirrors may be narrow band mirrors, or both of the mirrors may be broad band, non-metallic mirrors. The cavity may have a cavity dimension that renders the cavity resonant with respect to light of the frequency defined by the spectral characteristics of the mirrors and intrinsic cavity spacing in an undeformed state. One of the mirrors may be a hybrid filter. One (or both) of the walls may be a dielectric material, a metallic material, or a composite dielectric/metallic material. The cavity may be deformable by virtue of a wall that is under tensile stress. The control circuitry may be connected for analog control of the impedance to light of each element. The analog control may be control of the degree of deformity of the deformable wall of the cavity.

The predetermined impedance characteristic may include reflection of incident electromagnetic radiation in the visible spectrum, e.g., the proportion of incident electromagnetic radiation of a given frequency band that is, on average, reflected by each of the modulation elements. The modulation element may be responsive to a particular electrical

condition to occupy either a state of higher reflectivity or a state of lower reflectivity, and the control circuitry may generate a stream of pulses having a duty cycle corresponding to the proportion of incident radiation that is reflected and places the modulation element in the higher state of reflectivity during each the pulse and in the lower state of reflectivity in the intervals between the pulses. The characteristic may include emission of electromagnetic radiation in the visible spectrum. The characteristic may include the amount of electromagnetic radiation in the visible spectrum that is emitted, on average, by the antennas. The characteristic may be incident electromagnetic radiation in the visible spectrum. The modulation elements may include three sub-elements each associated with one of three colors of the visible spectrum. The modulation element may be responsive to a particular electrical condition to occupy either a state of higher transmissivity or a state of lower transmissivity, and the control circuitry may generate a stream of pulses having a duty cycle corresponding to the proportion of incident radiation that is transmitted and places the modulation element in the higher state of transmissivity during each the pulse and in the lower state of transmissivity in the intervals between the pulses. The characteristic may include the proportion of incident electromagnetic radiation of a given frequency band that is, on average, transmitted by each of the modulation elements.

The visible spectrum may include ultraviolet frequencies, or infrared frequencies.

In general, in another aspect of the invention, the control circuitry may be connected to the array for controlling the amplitude of light delivered by each of the modulation elements independently by pulse code modulation.

In general, in another aspect, the invention features a modulation element having a deformable portion held under tensile stress, and control circuitry connected to control the deformation of the deformable portion.

Implementations of the invention may include the following features. The modulation element may be self-supporting or held on separate supports. The deformable portion may be a rectangular membrane supported along two opposite edges by supports which are orthogonal to the membrane. The deformable portion, under one mode of control by the control circuitry, may be collapsed onto a wall of the cavity. The control circuitry controls the deformable portion by signals applied to the modulation element, and the deformation of the control portion may be subject to hysteresis with respect to signals applied by the control circuitry.

In general, in another aspect, the invention features modulating light in the visible spectrum using a deformable modulation element having a deformation mechanism and an optical portion, the deformation mechanism and the optical portion independently imparting to the element respectively a controlled deformation characteristic and a controlled modulation characteristic.

Implementations of the invention may include the following features. The deformation mechanism may be a flexible membrane held in tensile stress, and the optical portion may be formed on the flexible membrane. The optical portion may be a mirror. The mirror may have a narrow band, or a broad band, or include a hybrid filter.

In general, in another aspect, the invention broadly features a non-metal deformable modulation element.

In general, in another aspect, the invention features a process for making cavity-type modulation elements by forming a sandwich of two layers and a sacrificial layer

between them, the sacrificial layer having a thickness related to the final cavity dimension, and using water or an oxygen based plasma to remove the sacrificial layer.

Among the advantages of the invention are the following.

Very high-resolution, full-color images are produced using relatively little power. The embodiment which senses the image incident on the array has relatively low noise. Their color response characteristics are tunable by selection of the dimensions of the antennas. The antenna or cavity embodiments are useful in portable, low power, full color displays, especially under high ambient light conditions. Phase controlled reflective embodiments are useful in passive light scanning such as optical disk readers without moving parts. The emissive embodiments also could be used as display devices especially in low-ambient-light conditions.

Because of the dielectric materials used in some embodiments, the devices have the advantage of being extremely light efficient, making them especially appropriate for high intensity projection displays, and reducing or eliminating the need for backlighting in low ambient light applications. In addition, more accurate color representations are possible, as well as designs optimized for the IR and UV. Mechanical hysteresis precludes the need for active drivers, and this coupled with their geometric simplicity and monolithic nature brings defect losses down significantly. The devices are also exceptionally fast, low power, and non-polarizing. The fact that they can be reflective and/or transmissive enhances their flexibility.

The process for fabrication as represented in some embodiments relies on benign chemicals, minimizing waste disposal problems, and facilitating the fabrication of devices on a variety of substrates (e.g., plastics or integrated circuits) using a larger variety of materials. Devices on plastic substrates have the potential of being extremely inexpensive. All of the manufacturing technologies used are mature, further reducing manufacturing costs.

Other advantages and features of the invention will become apparent from the following description and from the claims.

### DESCRIPTION

FIG. 1 is a perspective view of a display device.

FIG. 2 is a perspective schematic exploded view of a representative portion of the screen of FIG. 1.

FIG. 3 is an enlarged top view of a tri-dipole of FIG. 2.

FIG. 4 is a schematic view of a single dipole antenna of FIG. 3.

FIG. 5 is a schematic perspective view, broken away, of a portion of the screen of FIG. 1.

FIG. 6 is an enlarged top view of an individual tri-bus of FIG. 2.

FIG. 7 is an enlarged perspective view of a representative portion of the screen of FIG. 1.

FIG. 8 is a cross-sectional view along 8—8 of FIG. 7.

FIG. 9 is a diagram of a portion of a control circuit of FIG. 2, and a corresponding dipole antenna of FIG. 3.

FIGS. 10A, 10B, 10C are representative graphs of the input voltage to the bias source of FIG. 9.

FIG. 11 is a diagram of portions of the control modules for a row of pixels.

FIG. 12 is a circuit diagram of an oscillator.

FIG. 13 is a schematic diagram of a circuit module of FIG. 2, a corresponding dipole antenna of FIG. 3, and a graphical representation of the output of a binary counter.

FIG. 14 is a circuit diagram of the pulse counter of FIG. 13.

FIGS. 15, 16, 17, 18, and 19 are top views of alternative dipole arrangements.

FIGS. 20A through 20D are perspective views of a cavity device.

FIGS. 21A and 21B are side views of the cavity device.

FIGS. 22A through 22F are graphs of frequency responses of the cavity device in different states.

FIGS. 23A and 23B are top and cutaway side views, respectively, of a display.

FIGS. 23C and 23D are top and cutaway side views, respectively, of another display.

FIG. 24A is a graph of an electromechanical response of the cavity device.

FIG. 24B is a graph of an addressing and modulation scheme for a display.

FIGS. 25A through 25N and FIGS. 26A through 26K are perspective views of the device during assembly.

FIGS. 27A through 27C are side views of dielectric mirrors.

FIG. 27D is a top view of a dielectric mirror.

FIGS. 28A, 28B are perspective and top views of a linear tunable filter.

FIGS. 29A, 29B are perspective and top views of a deformable mirror.

Referring to FIG. 1, device 20 includes a screen 22 for displaying or sensing a high resolution color image (or a succession of color images) under control of power and control circuitry 26. The image is made up of a densely packed rectangular array of tiny individual picture elements (pixels) each having a specific hue and brightness corresponding to the part of the image represented by the pixel. The pixel density of the image depends on the fabrication process used but could be on the order of 100,000 pixels per square centimeter.

Referring to FIG. 2, each pixel is generated by one so-called tri-dipole 30. The boundary of each tri-dipole is T-shaped. The tri-dipoles are arranged in rows 32 in an interlocking fashion with the "Ts" of alternating tri-dipoles oriented in one direction and the "Is" of intervening tri-dipoles along the same row oriented in the opposite direction. The rows together form a two-dimensional rectangular array of tri-dipoles (corresponding to the array of pixels) that are arranged on a first, external layer 34 of screen 22. The array may be called an electrically alterable optical planar array, or a visible spectrum modulator array.

On a second, internal layer 36 of screen 22 so-called tri-busses 38 (shown as T-shaped blocks in FIG. 2) are arranged in an interlocking two-dimensional array 40 corresponding to the layout of the tri-dipoles on layer 34 above. Each tri-dipole 30 is connected to its corresponding tri-bus 38 by a multi-conductor link 42 running from layer 34 to layer 36 in a manner described below.

On a third, base layer 44 of screen 22 a set of circuit modules 46 are arranged in a two-dimensional rectangular array corresponding to the layouts of the tri-dipoles and tri-busses. Each circuit module 46 is connected to its corresponding tri-bus 38 by a six-conductor link 48 running from layer 36 to layer 44 in a manner described below.

Each circuit module 46 electronically controls the optical characteristics of all of the antennas-of its corresponding tri-dipole 30 to generate the corresponding pixel of the image on screen 22. Circuit modules 46 are connected, via



conductors 50 running along layer 44, to an edge of layer 44. Wires 52 connect the conductors 50 to control and power circuitry 26 which coordinates all of the circuit modules 46 to 25 generate the entire image.

Referring to FIG. 3, each tri-dipole 30 has three dipole sections 60, 62, 64. The center points 59, 61, 63 of the three sections are arranged at 120 degree intervals about a point 65 at the center of tri-dipole 30. Each section 60, 62, 64 consists of a column of dipole antennas to 66, 68, 70, respectively, only ten dipole antennas are shown in each section in FIG. 3, but the number could be larger or smaller and would depend on, e.g., the density with which control circuits 46 can be fabricated, the tradeoff between bandwidth and gain implied by the spacing of the antennas, and the resistive losses of the conductors that connect the antennas to the control circuit 46. Only the two arms of each dipole antenna are exposed on layer 34, as shown in FIG. 3. The dipole antennas of a given section all have the same dimensions corresponding to a particular resonant wavelength (color) assigned to that section. The resonant wavelengths for the three sections 60, 62, 64 are respectively 0.45 microns (blue), 0.53 microns (green), and 0.6 microns (red).

Referring to FIG. 4, each dipole antenna 80 schematically includes two Ls 82, 84 respectively made up of bases 86, 88, and arms 90, 92. The bases of each antenna 80 are electrically connected to the corresponding circuit module 46. The span (X) of arms 90, 92 is determined by the desired resonant wavelength of dipole antenna 80; for example, for a resonant wavelength of  $\lambda$ , X would be  $\lambda/2$ . Dipole antennas 66, 68, 70 have X dimensions of 0.225 microns ( $\lambda/4$ ), 0.265 microns ( $\lambda/2$ ), and 0.3 microns ( $\lambda/2$ ), respectively. The effective length (Y) of bases 86, 88 from arms 90, 92 to circuit module 46 is also a function of the dipole antenna's resonant wavelength; for a resonant wavelength of  $\lambda$ , Y is a multiple of  $\lambda$ .

Referring to FIG. 5, each of the bases 86, 88 physically is made up of four segments; (1) one of the conductors 96 of link 42, (2) a portion 112 of tri-bus 38, (3) a short connecting portion 124 of tri-bus 38, and (4) one of the conductors 94 of link 48, which together define a path (e.g., the path shown as dashed line 97) with an effective length of Y from the arm (e.g., 92) to the circuit module 46.

The placement of link 42 perpendicular to the surface of layer 34 allows arms 90, 92 (formed on the surface of layer 34) to be spaced at an actual spacing Z that is closer than  $\lambda/2$ , the minimum required effective Y dimension of bases 86, 88. Spacing Z may be chosen based on the bandwidth/gain tradeoff, and for example may be one quarter of the resonant wavelength for the dipole antennas of a given section (i.e.,  $\lambda/4$ , or 0.1125 microns ( $\lambda/4$ ), 0.1325 microns ( $\lambda/4$ ) and 0.15 microns ( $\lambda/4$ ) for antennas 66, 68, 70, respectively).

Referring to FIG. 6, each tri-bus 38 is formed of aluminum on layer 36 and has three zigzag shaped bus pairs 100, 102, 104 for respectively connecting dipole antennas of the corresponding sections 60, 62, 64 of tri-dipole 30. Bus pairs 100, 102, 104 are connected to individual dipole antennas 66, 68, 70 via conductors of link 42 (FIG. 2) that are joined to the bus pairs at points, e.g., 106.

Each bus pair 100, 102, 104 has two parallel buses 108, 110. Bus 108 electrically connects together the arms of the dipole antenna 5 of the corresponding section and, independently, the related bus 110 electrically connects together the arms 92 of the dipole antennas of that same section.

Points 106 delineate a series of fragments 112, 114, 116 on each of the three bus pairs 100, 102, 104, respectively. Each

fragment forms part of one or more of the bases 86, or 88 and therefore contributes to the effective Y dimension.

The lengths (Q) of fragments 112, 114, 116 are one-half of the resonant wavelengths (i.e.  $\lambda/2$ ) of the sections 60, 62, 64, or 0.225 microns ( $\lambda/2$ ), 0.265 microns ( $\lambda/2$ ), and 0.3 microns ( $\lambda/2$ ), respectively.

The conductors of link 48 (FIG. 2) are attached to tri-bus 38 at points 118, 120, 122 at the ends of buses 108, 110. Between points 118, 120, 122 and the first points 106 on also forms buses 108, 110 are fragments 124, 126, 128, which also form portions of the bases 86, 88 and are included to adjust the effective Y dimensions of those bases to be integer multiples of  $\lambda/2$ . The lengths of the three fragments 124, 126, 128 are 0.1125 microns, 0.1525 microns, and 0.1875 microns, respectively.

Referring to FIG. 7, each dipole antenna 80 is physically formed (of aluminum) on an insulating semiconductor (e.g. silicon dioxide of silicon nitride) substrate 130 (part of layer 34) by x-ray or electron beam lithography or other technique suitable for forming submicron-sized structures.

Tri-buses 38 (not seen in FIG. 7) are formed on the upper-side of a second insulating semiconductor substrate 132 (part of layer 36). Circuit modules 46 (not seen in FIG. 7) are part of a third insulating semiconductor substrate 134 (part of layer 44) and are connected by conductors 80 to gold contact pads 136 (only one shown, not to scale) formed on the edge of substrate layer 134.

Referring to FIG. 8, circuit module 46 is formed in and on substrate 134 by any one of several monolithic processes. A section 138 of the substrate 134, which has been previously coated with an insulating semiconductor oxide layer 140, is repeatedly masked (whereby small windows are opened in the oxide layer, exposing the semiconductor beneath) and exposed to n and p dopants to form the desired circuit elements (not shown in detail in FIG. 8).

The individual circuit elements are connected to each other and to external contact pad 136 (FIG. 7) by aluminum conductors 142, 50, respectively. To form the connections, holes 144 are opened in oxide layer 140 and a sheet of aluminum is deposited, filling holes 144. Using a masking technique similar to the one described above the unwanted aluminum is removed, leaving only conductors 142, 50.

Semiconductor substrate layer 132 is deposited directly on top of the remaining exposed oxide layer 140 and conductors 142, 50. Holes 146 (one shown) (opened using a suitable lithographic technique) are channels for the electrical conductors 147 of links 48, which connect tri-bus 38 and circuit module 46. Tri-bus 38 is etched from a sheet of aluminum deposited onto the surface of layer 132. The deposition process fills holes 146, thereby forming the conductors of links 48.

Substrate layer 130 is deposited onto the surface of substrate layer 132 and tri-bus 38. The arms of dipole antennas 80 are formed by depositing a sheet of aluminum onto the surface of layer 130 and etching away the unwanted metal. During the deposition process holes 148 are filled thereby forming the conductors 149 of links 42 between the arms of dipole antenna 80 and tri-bus 38.

The conductors 149 are the uppermost parts of bases 86, 88 (FIG. 4) of dipole antennas 66, 68, 70; the lengths of conductors 149 together with the lengths of fragments 112, 114, 116 (FIG. 6), the lengths of fragments 124, 126, 128, and the lengths of the conductors 147 determine the effective Y dimension of bases 86, 88.

The length of the conductors 149 is determined by the thickness of the substrate 130 through which links 42 pass.

Substrate 130 and links 42 are 0.05625 microns (i.e. lambda<sub>0</sub>/8) thick. This thickness is achieved by controlling the deposition rate of the semiconductor material as layer 130 is formed.

The length of the conductors 149 is determined by the thickness of the substrate layer 132 through which they pass. This layer and links 48 are therefore also 0.05625 microns 20 thick.

The Y dimensions for the dipole antennas 66, 68, 70 of sections 60, 62, 64 therefore are as follows:

(a) For section 60, Y equals the sum of 0.05625 microns (length of the conductor in link 42, lambda<sub>0</sub>/8)+n \* 0.225 microns (where 0.225 microns=lambda<sub>0</sub>/2, the length of a fragment 112, and n=the number of fragments 112 in each base 86, 88 of the nth dipole antenna 66n)+0.1125 microns (length of fragment 124, lambda<sub>0</sub>/4)+0.05625 microns (length of the conductor in link 48, lambda<sub>0</sub>/8), and that sum equals (n+1) \* (lambda<sub>0</sub>/2).

(b) For section 62, Y equals the sum of 0.05625 microns (length of link 42, lambda<sub>0</sub>/8)+n \* 0.265 microns (where 0.265 microns=lambda<sub>0</sub>/2, the length of a fragment 114, and n=the number of fragments 114 in each base 86, 88 of the nth dipole antenna 68n)+0.1125 microns (length of fragment 126, (lambda<sub>0</sub>/2)-(lambda<sub>0</sub>/4))+0.05625 microns (length of the conductor in link 48, lambda<sub>0</sub>/8), and that sum equals (n+1)\*(lambda<sub>0</sub>/2).

(c) For section 64, Y equals the sum of 0.05625 microns (length of conductor in link 42, lambda<sub>0</sub>/8)+n \* 0.3 microns (where 0.3 microns=lambda<sub>0</sub>/2, the length of a fragment 116, and n equals the number of fragments 116 in each base 86, 88 of the nth dipole antenna 70n)+0.1875 microns (the length of fragment 128, (lambda<sub>0</sub>/2)-(lambda<sub>0</sub>/4))+0.05625 microns (length of conductor in link 48), and that sum equals (n+1) \* (lambda<sub>0</sub>/2).

Referring again to FIG. 1, in some embodiments, the displayed image is not emitted from device 20 but is comprised of ambient light (or light from a source, not 25 shown) selectively reflected by the tri-dipoles 30 of screen 22.

In that case, each tri-dipole 30 receives ambient light having a broad spectrum of wavelengths and is controlled by the corresponding circuit module to reflect only that portion of the ambient light manifesting the hue and brightness of the desired corresponding pixel.

The hue generated by tri-dipole 30 depends on the relative intensities of the light reflected by sections 60, 62, 64. The overall brightness of that hue of light in turn depends on the absolute intensities of the light radiation reflected by sections 60, 62, 64. Thus, both the hue and brightness of the light generated by tri-dipole 30 can be controlled by regulating the intensity of the light reflected by the dipole antennas in each section of the tri-dipole; this is done by controlling the reflectivity of each dipole antenna, i.e., the percentage of the light of the relevant wavelength for that dipole antenna which is reflected.

The desired percentage is attained not by regulating the amount of light reflected at any given instant but by arranging for the antenna to be fully reflective in each of a series of spaced apart time slots, and otherwise non-reflective. Each dipole antenna, in conjunction with its circuit module, has only two possible states: either it reflects all of the light (at the antenna's resonant frequency), or it reflects none of that light. The intensity is regulated by controlling the percentage of total time occupied by the time slots in which the dipole antenna occupies the first state.

Each dipole antenna is controlled to be reflective or not by controlling the impedance of the dipole antenna relative to

the impedance of the medium (e.g., air) through which the light travels. If the medium has an effective impedance of zero, then the relationship of the reflectivity of the dipole antenna to zero (the controlled impedance of the dipole antenna) can be derived as follows. If we define a three-axis system x-y-z in which the x and y axes are in the plane of the array and the z axis is the axis of propagation of the incident and reflected waves, where z=0 is the surface of the array, then the incident plus reflected wave for z<0 may be represented as:

$$\vec{E} = \vec{E}_t e^{-jk_z z} + \vec{E}_r e^{+jk_z z} \quad (1)$$

$$\vec{H} = \frac{\nabla \times \vec{E}}{-j\omega\mu_0} = \hat{y} \frac{1}{\eta_0} [E_t e^{-jk_z z} - E_r e^{+jk_z z}] \quad (2)$$

where  $\vec{E}$  (overbar) is the complex amplitude of the electric field of the sum of the transmitted wave and the reflected wave;  $\vec{E}_t$  is the complex amplitude of the electric field of the transmitted 20 wave;  $\vec{E}_r$  is the complex amplitude of the electric field of the reflected wave;  $\hat{x}$  (hat) is the orientation of the electric field of the wave;  $\hat{H}$  is the amplitude of the magnetic field;  $\hat{y}$  (hat) is the orientation of the magnetic field;  $\mu_0$  is the permeability of free space;  $\epsilon_0$  is the permittivity of free space;  $k = \omega \sqrt{\mu_0 \epsilon_0}$  is the wavenumber; and  $\eta = \sqrt{\mu_0 / \epsilon_0}$  is the impedance of free space. For z>0 (i.e., within free space) only the transmitted wave exists and is represented by

$$\vec{E} = \vec{E}_t e^{-jk_z z} \quad (3)$$

$$\vec{H} = \hat{y} \frac{1}{\eta} E_t e^{-jk_z z} \quad (4)$$

$\vec{E}$  (overbar) is the complex amplitude the transmitted wave at z=0,  $k_z = \sqrt{k^2 - k_x^2}$  is its wavenumber,  $\eta = \sqrt{\mu_0 / \epsilon_0}$  is the impedance of the medium, i.e. z>0. Boundary conditions (z=0) for tangential electric fields are imposed on equations 1 and 2 and they are combined to yield,

$$\vec{E}_t + \vec{E}_r = \vec{E}_0 \quad (5)$$

In the same way, continuity for tangential magnetic fields (z=0) at the boundary yields,

$$\hat{y} (1/\eta_0) (\vec{E}_t - \vec{E}_r) = \hat{y} (1/\eta) \vec{E}_0 \quad (6)$$

Dividing equation 5 and 6 by  $\vec{E}_0$  and  $\vec{E}_0/\eta_0$  respectively gives the following two equations:

$$1 + \vec{E}_r/\vec{E}_0 = \vec{E}_t/\vec{E}_0 \quad (7)$$

$$1 - \vec{E}_r/\vec{E}_0 = \eta(\eta_0/\eta) (\vec{E}_t/\vec{E}_0) \quad (8)$$

$\vec{E}_r/\vec{E}_0$  is called  $\Gamma$  and is the complex reflection coefficient while  $\vec{E}_t/\vec{E}_0 = T$  is called the complex transmission coefficient, and  $\eta/\eta_0 = \eta_n$  is the normalized wave impedance. Solving for T and  $\Gamma$  yields

$$\Gamma = \frac{\vec{E}_r}{\vec{E}_0} = \frac{2}{1 + \eta_n \eta_n^*} - \frac{2\eta_n}{\eta_n + 1} \quad (9)$$

$$\Gamma = \frac{\vec{E}_r}{\vec{E}_0} = T - 1 = \frac{\eta_n - 1}{\eta_n + 1} \quad (10)$$

For matched impedance values,  $\eta_n = \eta_n^*$ , the reflection coefficient is zero, and T=1 (i.e., no reflection), and in the case of a load at the boundary, a matched antenna, there is complete absorption.

As  $\eta_n$  approaches zero or infinity, the reflection coefficient approaches plus or minus one, implying total reflection.

Referring to FIG. 9, the impedance  $Z_d$  of dipole antenna 80 is controlled by a variable resistance PIN diode 160

connected across bases 86, 88, PIN line 162 to the output of a bias high voltage or a low voltage based on a line 168 from power and the output of bias source 164 is a high voltage, the resistance R of PIN diode 160 (and hence the impedance ( $E_p$ ) of the dipole antenna is zero causing full reflection; when the output of bias source 164 is a low voltage 98, resistance R is set to a value such that the resulting impedance  $Z_{in}$  is matched to  $Z_0$  (the impedance of the air surrounding the antenna), causing zero reflection.

To generate an entire image on screen 20, power and control circuitry 26 receives a video signal (e.g. a digitized standard RGB television signal) and uses conventional techniques to deliver corresponding signals to modules 46 which indicate the relative desired intensities of light reflected from all sections 60, 62, 64 of all of the tri-dipoles in the array at a given time. Circuit modules 46 use conventional techniques to deliver an appropriate stream of input control signal pulses to each bias source 164 on line 168.

The pulse stream on each line 168 has a duty cycle appropriate to achieve the proper percentages of reflectance for the three Sections of each tri-dipole. Referring to FIGS. 10A, 10B, and 10C, for example, pulse stream 170 has a period T and a 50% duty cycle. For the first 50% of each period T the input to bias source 164 is high and the corresponding output of source 164 is a high voltage. During this portion of the cycle dipole antenna 80 will reflect all received light having the dipole antenna's resonant wavelength. For the second 50% of the cycle the output of source 164 will be low and dipole antennas 80 will absorb the received light. In FIGS. 10B, 10C, pulse streams 172, 174 represent a 30% duty cycle and a 100% duty cycle respectively; with a 30% duty cycle the effective intensity of the light radiation of the dipole antennas of the section will be 30%; for a duty cycle of 100%, the effective intensity is 100%.

For example, if a particular pixel of the image is to be brown, the relative intensities required of the three red, 25 green, and blue sections 60, 62, 64 may be, respectively, 30, 40, and 10. The input signals to the bias sources 164, carried on lines 168, would then have duty cycles, respectively, of 30%, 40%, and 10%. An adjacent pixel which is to be a brown of the same hue but greater brightness might require duty cycles of 45%, 60%, and 15%.

Referring to FIG. 11, to accomplish the delivery of the pulse width modulated signals from circuitry 26 to the pixel circuit modules 46, each circuit module 46 in the row includes storage 180, 182 for two bits. The bit 1 storage elements 180 of the modules 46 in the row are connected together to create one long shift register with the pulse width modulated signals being passed along the row data line 184 from pixel to pixel. If, for example, the period of the modulated signals is 1 millisecond and there are ten different intensity levels, then an entire string of bits (representing the on or off state of the respective pixels in the row during the succeeding  $\frac{1}{10}$  millisecond) is shifted down the row every  $\frac{1}{10}$  millisecond. At the end of the initial  $\frac{1}{10}$  millisecond all of the bits in elements 180 are shifted to the associated elements 182 by a strobe Pulse on strobe line 186. The content of each element 182 is the input to the driver 188 for the appropriate one of the three colors of that pixel, which in turn drives the corresponding section 60, 62, 64 of the tri-dipole. The rate at which data is shifted along the shift registers is determined by the number of elements on a given row, the number of rows, the number of intensity levels, and the refresh rate of the entire array.

In another embodiment, the light comprising the image is emitted by tri-dipoles 30 rather than being produced by

reflected ambient light. In that case, each tri-dipole generates the light for a single pixel with a hue and brightness governed by the intensities of the light emitted by each of the three sections 60, 62, 64.

Each dipole antenna within a tri-dipole is caused to emit light at the resonant wavelength of that antenna by stimulating it using a signal whose frequency corresponds to the resonant wavelength. Thus, the sections 60, 62, 64 will emit blue ( $\lambda_{b0}$ ), green ( $\lambda_{g0}$ ), and red ( $\lambda_{r0}$ ) light respectively when provided with signals whose frequencies equal, respectively,  $\lambda_{b0}/2\pi$ ,  $\lambda_{g0}/2\pi$ , and  $\lambda_{r0}/2\pi$ .

For an idealized dipole, the current I and current density  $\vec{J}(\vec{r})$  are described by

$$I = I_0 \cos(kz) \quad (11)$$

$$\vec{J}(\vec{r}) = I_0 \delta(\vec{r} - \vec{r}_0) \quad (12)$$

where  $\vec{r}_0$  is the charge density;  $\hat{z}$  indicates the direction of the current (along the z-axis);  $\omega$  angular frequency; and d is the distance between ideal point charges representing the dipole. The vector potential  $\vec{A}(\vec{r})$  in polar coordinates is given by

$$\vec{A} = \frac{\mu_0 I_0}{4\pi r} \left[ \cos\theta - \frac{1}{k} \frac{\partial}{\partial r} \left( \frac{\sin\theta}{r} \right) \right] \quad (13)$$

where  $\theta$  represents the angle relative to the dipole;  $\theta(\hat{r})$  is the angular orientation of the wave;  $\mu_0$  is the permeability of free space; r is radius from the dipole;  $\hat{r}$  is radial orientation of the wave;  $A_r$  is the radial component of the vector potential; and k is a factor which is used to represent sinusoidally varying waves. The H field is given by where  $\phi$  is elevation, with respect to the dipole. The E field is given by,

The far-field equation is given by

$$\vec{H} = \frac{1}{\mu_0 r} \left[ \frac{\partial}{\partial \theta} \left( r \sin\theta \frac{\partial}{\partial r} \left( \frac{1}{r} \right) \right) \right] \quad (14)$$

$$= \frac{\partial}{\partial \theta} \left[ \left( 1 + \frac{1}{kr} \right) \sin\theta \right] \quad (15)$$

$$\vec{E} = \frac{1}{\mu_0 c} \frac{\partial}{\partial r} \left[ \left( 1 + \frac{1}{kr} \right) \sin\theta \right] \quad (16)$$

$$\vec{H} = \frac{1}{\mu_0 c} \frac{\partial}{\partial r} \left[ \left( 1 + \frac{1}{kr} \right) \sin\theta \right] \quad (16)$$

$$\vec{E} = \frac{1}{\mu_0 c} \frac{\partial}{\partial r} \left[ \left( 1 + \frac{1}{kr} \right) \sin\theta \right] \quad (16)$$

Equation (16) describes the radiation pattern away from a dipole antenna at distances significantly greater than the wavelength of the emitted electromagnetic wave. It is a very broad radiation pattern providing a wide field of view at relevant distances.

Referring to FIG. 12, the dipole antennas 66, 68, 70 of each section 60, 62, 64 are driven by signals (e.g., sinusoidal) with frequencies of  $5 \times 10^{14}$  Hz,  $5.6 \times 10^{14}$  Hz, and  $6.6 \times 10^{14}$  Hz for red, green, and blue, respectively. These signals are supplied by three monolithic oscillators 200 (one

shown) within circuit module 46, each tuned to one of the three required frequencies.

In circuit 200 (an a stable multivibrator), the center pair of coupled transistors 202, 204 are the primary active elements and will oscillate if the circuit admittance is set appropriately. Diodes 206, 208, 210, 212 provide coupling capacitance's between the transistors and the inductors 214, 216 are used to tune the operating frequency.

In a third embodiment, an image of the object is focused by a conventional lens (not shown in FIG. 1) onto screen 22, which then acts as an image sensor. The tri-dipoles of screen 22, controlled by power and control circuitry 26, generate electrical signals corresponding to pixels of the received image. The signals are then processed by a processor which, in conventional fashion, delivers a derived RGB video signal which can then be transmitted or stored.

The signals generated for each tri-dipole are generated by the corresponding circuit module 46 and represent the hue and brightness of the light radiation received at that tri-dipole.

Each section of tri-dipole 30 can only be used to measure light having the resonant wavelength of its respective dipole antennas, however, because most colors can be expressed as a combination of red, green, and blue, circuit module 46 can, by independently measuring the intensity of the light radiation received at each section 60, 62, 64, derive a signal which specifies the hue and intensity of the received pixel.

Referring to FIG. 13, dipole antenna 80 will absorb incident light radiation at its resonant wavelength when its reflection coefficient ( $\Gamma_r$ ) is zero, which occurs when its controlled impedance ( $Z_c$ ) matches the impedance of the medium ( $Z_o$ ). In those circumstances, a voltage pulse is produced across the ends 308, 310 of dipole 80 for each incident photon. The relative magnitude of the light radiation received by each dipole antenna can thus be measured by counting the average number of pulses across ends 308, 310 over a given time period.

In this embodiment, circuit module 46 includes a terminating load resistor 315 connected across ends 308, 310. The controlled impedance of the combination of dipole antenna 80 and resistor 315, described by the equations set forth below, is equal to  $Z_o$ .

The voltage of the pulse across resistor 315 (created by an incident photon) is illustrated by the sine wave graph above register 15 and is described generally by the following equation

$$V(z) = V_0 e^{-\alpha z} - j\omega C + \Gamma_r e^{j\omega z} \quad (17)$$

Because  $Z_L = Z_o$ ,  $\Gamma_L = 0$ , and equation 17 simplifies to

$$V(z) = V_0 e^{-\alpha z} \quad (18)$$

A pulse detector 318 amplifies and sharpens the resulting pulse to a square wave form as shown, which is then used as the clock (CLK) input 319 to a binary counter 320. The output of the binary counter is sampled at a regular rate; collectively the samples form a digital signal representing the intensity of received light radiation over time. Each time counter 320 is sampled, it is reset to zero by a pulse on control line 322. Counter 320 thus serves as a digital integrator that indicates how much light arrived in each one of a succession of equal length time periods.

Referring to FIG. 14, in pulse detector 318 the pair of transistors 322, 324 serve as a high impedance differential stage whose output (representing the voltage difference between points 308, 310) is delivered to an amplifier 326. Amplifier 326 serves as a high-bandwidth gain stage and

delivers a single sided output pulse to a conditioning circuit 328 that converts slow rising pulses to square pulses 330 for driving counter 320.

In another embodiment, the array of tri-dipoles is operated as a phased array. The operation of phased arrays is discussed more fully in Amitay, et al., *Theory and Analysis of Phased Array Antennas*, 1972, incorporated herein by reference. By controlling the spacing of successive tri-dipoles across the array and the relative phases of their operation, wave cancellation or reinforcement can be used to control the direction in three dimensions and orientation of the radiation. Beams can thus be generated or scanned. In the case of an array used to sense incoming radiation, the array can be made more sensitive to radiation received from selected directions.

Other embodiments are also possible. For example, referring to FIG. 15, each section of tri-dipole 400 array be a single dipole antenna 406, 407, 408. The tri-dipole antennas are then arranged about a center Point 410 at 120 degree intervals in a radial pattern. Bases 411, 412, as well as arms 414, 415, of the dipole antennas, are all formed on the same surface.

Referring to FIG. 16, each section may consist of multiple dipole antennas 406, 407, 408 connected by attaching the bases 411, 412 of each succeeding dipole antenna to the inner ends of arms 414, 415 of the preceding dipole antenna. Circuit modules 416 are formed on the surface of layer 413.

Referring to FIG. 17, a multi-dipole 430 could have five sections 432, 434, 436, 438, 440 composed of dipole antennas 442, 444, 446, 448, 450, respectively. The dipole antennas of the different sections would have different resonant wavelengths. Other multi-dipoles might have any number of sections.

The scanning of pixels could be done other than by pulse width modulation, for example, using charge coupled devices to shift packets of charge along the rows of pixels.

Referring to FIGS. 18, 19, other arrangements of dipole antennas may be used in order to match the area required for the control circuit modules.

Referring to FIG. 18, each section 470 of a tri-dipole in the reflective mode could be formed of a number of subsections (e.g., 472) arranged in two rows 474 and a number of columns 47. The antennas 478 in each subsection 472 are all served by a single PIN diode circuit 480 located at the peripheral edge of section 470 at the end of the subsection on the layer below the antenna layer. All circuits 480 for the entire Section 470 are in turn served by a single bias source 164 (FIG. 9). This arrangement reduces the number of bias sources required for the entire array of tri-dipoles. FIG. 19 shows an alternate arrangement in which there is but one row of subsections each served by a single PIN diode circuit at the end of the row.

In order to reduce the number of conductors 50, selected tri-dipoles could be used to receive control signals transmitted directly by light and to pass those control signals to the control circuits of nearby active tri-dipoles.

The dipoles could be mono-dipoles comprised of only a single dipole antenna, all with the same resonant wavelength.

Dipole antennas 470 could be randomly arranged on the surface of layer 472 of screen 22.

A different color regime, e.g. cyan-magenta-yellow, could be substituted for RGB.

Spiral, biconical, slotted, and other antenna configurations could be substituted for the dipole configuration.

The array could be three-dimensional.

The successive tri-dipoles in the array can be oriented so that their respective antennas are orthogonal to each other to enable the array to interact with radiation of any arbitrary polarization.

The PIN diodes could be replaced by other impedance controlling elements. Such elements might include quantum well transistors, superconducting junctions, or transistors based on vacuum microelectronics. Further improvement could be achieved by reducing the complexity of the third layer containing control circuitry. The electronics required to get control signals to the circuitry could be eliminated by the use of laser or electron beams to provide such signals. This would have the advantage of allowing for arrays of even higher density.

The array could be fabricated on a transparent substrate, thus facilitating transmissive operation.

In other embodiments, the antenna arrays alone (without control circuitry or connection buses) may be fabricated on one-half of a microfabricated interferometric cavity. The antenna array can be considered a frequency selective mirror whose spectral characteristics are controlled by the dimensions of the antennas. Such a cavity will transmit and reflect certain portions of incident electromagnetic radiation depending on (a) the dimensions of the cavity itself and (b) the frequency response of the mirrors. The behavior of interferometric cavities and dielectric mirrors is discussed more fully in Macleod, H. A., *Thin Film Optical Filters*, 1969, incorporated by reference.

Referring to FIG. 20a, two example adjacent elements of a larger array of this kind include two cavities 498, 499 fabricated on a transparent substrate 500. A layer 502, the primary mirror/conductor, is comprised of a transparent conductive coating upon which a dielectric or metallic mirror has been fabricated. Insulating supports 504 hold up a second transparent conducting membrane 506. Each array element has an antenna array 508 formed on the membrane 506. The two structures, 506 and 508, together comprise the secondary mirror/conductor. Conversely, the antenna array may be fabricated as part of the primary mirror/conductor. Secondary mirror/conductor 506/508 forms a flexible membrane, fabricated such that it is under tensile stress and thus parallel to the substrate, in the undriven state.

Because layers 506 and 502 are parallel, radiation which enters any of the cavities from above or below the array can undergo multiple reflections within the cavity, resulting in optical interference. Depending on the dimensions of the antenna array, as explained above, the interference will determine its effective impedance, and thus its reflective and/or transmissive characteristics. Changing one of the dimensions, in this case the cavity height (i.e., the spacing between the inner walls of layers 502, 506), will alter the optical characteristics. The change in height is achieved by applying a voltage across the two layers at the cavity, which, due to electrostatic forces, causes layer 506 to collapse. Cavity 498 is shown collapsed (7 volts applied), while cavity 499 is shown uncollapsed (0 volts applied).

In another embodiment, FIG. 20b, each cavity may be formed by a combination of dielectric or metallic mirrors on the two layers, and without the antennas formed on either layer. In this case the spectral characteristics of the mirror are determined by the nature and thickness(es) of the materials comprising it.

In an alternative fabrication scheme, FIG. 20c, each cavity is fabricated using a simpler process which precludes the need for separately defined support pillars. Here, each secondary mirror/conductor, 506, is formed in a U-shape with the legs attached to the primary layer; each secondary mirror/conductor thus is self-supporting.

In yet another scheme, FIG. 20d, the cavity has been modified to alter its mechanical behavior. In this version, a stiffening layer, 510, has been added to limit deformation of

the membrane while in the driven state. This assures that the two mirrors will remain parallel as a driving voltage is gradually increased. The resulting device can be driven in analog mode (e.g., cavity 511 may be driven by 5 volts to achieve partial deformation of the cavity) so that continuous variation of its spectral characteristics may be achieved.

Referring to FIGS. 21A and 21B, the modulation effect on incident radiation is shown. The binary modulation mode is shown in FIG. 21A. In the undriven state (shown on the left) incident light 512 (the delta lambda represents a range of incident frequencies, e.g., the range of visible light) contains a spectral component which is at the resonant frequency of the device in the undriven state. Consequently this component (delta lambda n) is transmitted, 516, and the remaining components (at nonresonant frequencies, delta lambda lambda minus delta lambda n) are reflected, 514. This operation is in the nature of the operation of a fabry-perot interference cavity.

When the device is driven and the geometry altered to collapse (right side of figure), the resonant frequency of the device also changes. With the correct cavity dimensions, all of the incident light (delta lambda n) is reflected.

FIG. 21A shows a binary mode of operation while FIG. 21B shows an analog mode, where a continuously variable voltage may be used to cause a continuously variable degree of translation of secondary mirror/conductor 506. This provides a mechanism for continuous frequency selection within an operational range because the resonant frequency of the cavity can be varied continuously. In the left side of FIG. 21A, the transmitted wavelengths are delta lambda n n zero, while in the right hand side they are delta lambda lambda n zero.

The equations which explain the performance of the cavity are set forth at the bottom of FIG. 21B. Equation 1 defines the transmission T through a fabry-perot cavity. T<sub>a</sub>, T<sub>b</sub>, R<sub>a</sub>, R<sub>b</sub> are the transmittances and reflectances of the primary (a) and secondary (b) mirrors. Phi a and Phi b are the phase changes upon reflection at the primary and secondary mirrors, respectively. Delta is the phase thickness. Equation 2 defines the phase thickness in terms of the cavity spacing ds, the index of refraction of the spacer ns, and the angle of incidence, theta s. Equation 3 shows that the transmission T becomes the transmission of the second mirror when the transmission of the first mirror approaches 0.

There are a number of particular frequency response modes which would be useful in applying the invention to displays. FIGS. 22A through 22F illustrate some of the possibilities and relate to the equations of FIG. 21B. These are idealized plots which illustrate transmission and reflectivity (T/R) of the cavity for wavelengths in the visible range in driven and undriven states for each of the driven and undriven response modes. The different modes are achieved by using different combinations of mirrors and cavity spacings.

The spectral characteristics of the mirrors used can be referred to as broad-band and narrow-band. The mirrors are optimized for the visible range with a broad band mirror operating across the entire visible range (i.e., reflecting over a minimum range of 400 nm to 700 nm). Such a mirror is denoted in the stack formula 1.671/0.775(ERS) 0.833M (ERS)1.671 where ERS denotes an equal ripple filter. The ERS filter has layers which are a quarter wavelength thick, and their refractive indices are n0=1.671, n1=1.986, n2=1.663, n3=2.122, n4=1.562, n5=2.240, n6=1.495, n7=2.316, n8=1.460, n9=2.350, n10=1.450. A narrow-band filter optimized for the color green would reflect only over

the range of 500 nm to 570 nm, and transmit everywhere else. Such a filter is described by the stack formula  $1C1\ 2C2\ (3A/2\ 3B1\ 3A/2)2\ (3A/2\ 3B\ 3A/2)6\ (3A/2\ 3B1\ 3A/2)2\ 1I.52$  where the refractive indices are  $nA=0.156$ ,  $nC2=nB1=1.93$ , and  $nB=2.34$ .

The cavity spacing (i.e., cavity height) in both driven and undriven states can be set to a predetermined value by the film thicknesses used in its construction. These two values determine whether a cavity is resonant or non-resonant. For a resonant cavity, the spacing is determined such that the undriven state coincides with the resonant peak of the narrower of the two mirrors. When a device is non-resonant, it must be driven in order for the device to become resonant.

For example, if the undriven cavity spacing were 535 nm then, because this coincides with the center of the previously defined narrow-band mirror, there would be a transmission peak at this frequency. Peak spacing for this cavity is 267 nm so the other peaks, which would occur in the standard Fabry-Perot fall outside of range of the narrow band mirror. This would be considered a resonant cavity because the peak occurs in the undriven state. Driving the cavity so that the spacing were 480 nm would result in no transmission peak because all of the cavity peaks are outside the range of the narrow-band mirror. For all practical purposes the narrow-band mirror does not exist at this frequency and therefore the transmission peak disappears.

FIG. 22A shows a T/R plot of a cavity having broad band mirrors on both layers of the cavity. When undriven, this results in transmission/reflection peaks which occur at wavelengths which are approximately integral multiples of the cavity spacing (the notation  $n\ \delta\ \lambda$  in FIG. 21A denotes the fact that there may be a series of peaks). This is classic fabry-perot behavior. In the driven state (shown to the right in FIG. 22A), the cavity resonance is shifted out of the visible range causing the device to act like a broadband mirror.

FIG. 22B shows a T/R plot for a cavity having one broad band and one narrow band mirror. This device has a resonant cavity, causing a transmission peak at the center of the narrow-band mirror's passband when the device is in the undriven state. Driving the device (right hand side of FIG. 22B) shifts the cavity resonance away from that of the narrow band mirror, and the device acts like a broadband mirror.

In FIG. 22C, the cavity is like that of FIG. 22B, except the cavity is non-resonant which results in broadband mirror cavity behavior in the undriven state. When driven, the cavity spacing shifts into resonance, causing a transmission peak centered on the narrow-band mirror.

FIG. 22D shows the performance of a resonant cavity with two narrow-band mirrors. When undriven, there is a transmission peak centered on the mirrors' response. Since the mirrors are narrow-band, the overall cavity response is that of a broad-band transmitter. Driving the device out of resonance (i.e. active) results in a reflective peak at the narrow-band center frequency.

Like FIG. 22D, the cavity of FIG. 22E has two narrow band mirrors, but it is a non-resonant cavity. Consequently its behavior is opposite that of the cavity portrayed in FIG. 22D.

Thus, when one of the mirrors is narrow banded, mirror a for example, the transmission approaches zero for frequencies outside its range. This is essentially the transmission of mirror b. When both of the mirrors are narrow banded, the transmission becomes a maximum outside the frequency range. In either case, the spurious peaks typical of a fabry-perot are avoided. The result is a device which can be described as a single mode resonant cavity.

When both of the mirrors are narrow banded, then fabry-perot type behavior occurs only when the cavity spacing is correct. Making the mirrors narrow enough allows only a single peak to occur. Then it is unnecessary to be concerned about spurious peaks that might occur within the visible range.

FIG. 22F is for a cavity with a simpler design involving only a metallic mirror on one wall and a hybrid filter on the other wall. The hybrid filter is a combination of a narrow bandpass filter (outer surface) and an induced absorber (inner surface). The induced absorber is a simple structure which can consist of one or more dielectric or dielectric and metallic films. The function of the absorber is to cause incident light of a specified frequency range to be absorbed by a reflective surface (i.e. mirror). One such design can be achieved with a single film of refractive index  $n=1.65$  and a thickness of 75.8 nm. The induced absorber only functions when it is in contact with the mirror, otherwise it is inconsequential.

In the undriven state, the hybrid filter (a green centered narrow bandpass/induced absorber) reflects everything, but the green light, which is unaffected by the induced absorber and subsequently reflected by the metallic mirror. Thus the overall cavity response is like that of a broad-band mirror. When in the driven state, the hybrid filter comes into contact with the metallic mirror. The absorber couples the green light into the mirror, and the result is an absorption peak at that wavelength.

Referring to FIG. 23A, a red  $3\times 3$  pixel (i.e., 9 cavities) subtractive mode display array based on the cavity device using the N—N (narrow band-narrow band) configuration of FIG. 22D is shown. The cavity pixels are formed at the intersections of primary mirror/conductors 602 and secondary mirror/conductors 604. The display is fabricated on substrate 608 and driven via contact pads 606 connected to each conductor/mirror 604.

A full nine-pixel display comprises three replications of the array of FIG. 23A arranged on top of one another and fabricated on separate substrates or color planes 610, 612, 614, as shown in FIG. 23B. Each of the individual color planes interacts only with and reflects one color (e.g., red, green, or blue), while passing all other colors. This is done by selecting the mirror spectral characteristic and cavity spacing in each color plane appropriately. The color planes are physically aligned and electrically driven through the contact pads to produce full color images. The image would be viewed from below in FIG. 23B.

Referring to FIGS. 23C and 23D, a single layer composite approach is shown. Such a device would be more complicated to fabricate (though the mirror designs are simpler) but may suffer from inferior resolution. In this case, all three colors reside on the same array 616. Devices using either the R—B, R—N, N—N, or the M—F (B—broad band, N—narrow band, M—mirror, H—F—hybrid filter) configuration are used for this display.

Either the three plane or the single plane approach may be used in either transmissive and reflective modes. Pixel size and overall display size can be altered to make the displays useful in many different display and spatial light modulator applications. These include direct view and projection displays, optical computing, holographic memory, and any other situation where a one or two dimensional modulator of light can be used.

Because these structures depend on electrostatic attraction, which varies in an exponential fashion with cavity spacing, while the mechanical restoring force of the membrane varies linearly with cavity spacing, they exhibit

hysteresis. As seen in FIG. 24A, the straight line labelled membrane tension shows that the restoring force on the membrane varies inversely linearly with distance (i.e., cavity spacing). That is, the smaller the spacing, the stronger the mechanical force tending to restore the original, at rest spacing. On the other hand, electrical attraction between the two layers of the cavity (the curved line) varies exponentially with smaller spacing, that is, as the two layers get closer there is an exponential increase in the attractive force between them. This causes a hysteresis effect as follows. With a low driving voltage applied, the secondary mirror/conductor experiences a displacement towards the substrate until the force of restoration balances the electrical attraction. However if the voltage is raised past a point known as a collapse threshold the force of restoration is completely overcome and the membrane is pressed tightly against the substrate. The voltage can then be lowered again to some degree without affecting the position of the membrane. Only if the voltage is then lowered significantly or eliminated will the membrane be released. Because the membrane is under tensile stress, it will then pull itself away from the substrate when the voltage is released. This hysteresis can be used to achieve matrix addressing of a two-dimensional array, as explained with reference to FIG. 24B.

The display can be addressed and brightness controlled using control pulse sequences in the driving voltage. Shown is a timing diagram for a 3x3 pixel array analogous to that shown in FIG. 23A. During operation, a continuous series of ~5 volts scanning pulses is applied to the rows (rows 1-3) of the pixel array in a sequential fashion, as seen in the charts labelled "Row". The pulses appear at the same frequency on each of the rows but the pulses for different rows are staggered. These pulses are insufficient in their own right to cause the membrane to collapse. The columns (cols. 1-3) of the pixel array (see charts labelled "Col") are maintained at a bias voltage of 5 volts so that the nominal voltage across each unactivated pixel is 5 volts. At times when the scan pulses are delivered to that pixel, the nominal row and column potentials are 5 and ~5 volts respectively, resulting in a cavity voltage of 10 volts. With a 10 volts potential applied to the row and a ~5 volts potential to the column, the total voltage across the cavity becomes 15 volts which is sufficient to drive the secondary mirror/conductor into the collapsed state, where it will remain until the end of the scan when all of the column voltages are pulsed to zero. The three charts at the bottom of FIG. 24B show the on and off states of the three pixels identified there by row and column numbers.

The intensity or brightness of a pixel may be varied by changing the fraction of the scan during which the pixel is activated. The scan cycle begins at 198 and ends at 199. The frequency of the scan pulses is such that six pulses of a given row fall within the scan cycle, providing an opportunity to activate a pixel at any one of six times during each cycle. Once the pixel is activated it stays on until the end of the cycle. Therefore six different intensities are possible for each pixel. For the scan shown, pixel C1R1 is at full brightness, pixel C2R2 is at 1/2 brightness, and pixel C3R2 is at 1/3 brightness. All pixels are cleared at the end of the scan and the cycle begins again. Since these structures can be driven at frequencies as high as 50 kHz, this method of brightness control is practical. Assuming six brightness levels, there would be a possibility of more than 8 thousand row scans per second.

Two processes for fabricating the arrays will be discussed; others may also be possible.

Referring to FIG. 25A, substrate 700 is first cleaned using standard procedures. The substrate may be of many different

materials including silicon, plastic, mylar, or quartz. The primary requirement is that the material be able to support an optically smooth, though not necessarily flat, finish. A preferred material would likely be glass, which would permit both transmissive and reflective operation in the visible range.

The substrate is then coated with the primary conductor/mirror layer(s) 702. This can be achieved using a physical vapor deposition (PVD) method such as sputtering or e-beam evaporation. Other possible methods include chemical vapor deposition and molecular beam epitaxy. The dimensions and nature of the layer(s) depend on the specific configuration desired. Detailed examples are discussed below.

Referring to FIG. 25B, a photoresist 704 has been patterned on the primary conductor/mirror. The photoresist may be of a positive or negative type. The standard procedure for this step involves spinning of the resist, softbaking at 90 °C, exposing through an appropriate mask, developing to produce the pattern, and hardbaking at 130 °C.

Referring to FIG. 25C, the photoresist pattern is defined in the primary conductor/mirror by an etching process. This step can be achieved either by wet chemical means or by plasma or reactive ion etching (RIE). The choice of etching technique depends on the nature of the conductor/mirror. In the case of an aluminum conductor/mirror, chlorine gas may be used to perform the etch, with a standard chamber power of 100 watts producing an etch rate of 100 angstroms/min. Some mirror materials may resist RIE and in such cases a technique such as ion milling may be used. All RIE steps are performed at a pressure of 30 mtorr unless otherwise noted. All plasma etch steps are performed at a pressure of 100 mtorr unless otherwise noted. The photoresist is removed using standard solvents.

Alternatively, the conductor/mirror may be defined using the well-known procedure called lift-off. This procedure is used to define a layer in a subsequent step and is described below.

Referring to FIG. 25B, support rail material 706, has been deposited using one of the methods mentioned previously. This material should be an insulator, for example silicon dioxide or silicon nitride. The material should be deposited uniformly, and at a thickness equal to thickness of the spacer layer, which will be deposited later. This thickness should in general be at least a multiple of the wavelength of light of interest. A thickness of 0.5 microns would place such a device near the middle of the visible spectrum.

Referring to FIG. 25E, photoresist layer 708 is spun on and hardbaked. Since this layer will not be photolithographically defined, other polymeric materials may be used instead. The only requirement is that they dissolve in solvents such as acetone or methanol, and be able to withstand a vacuum. This is the first step in defining a lift-off stencil.

Referring to FIG. 25F, template layer 710 has been deposited using one of the methods of PVD. The layer is of silicon dioxide though other materials are possible. Ideally the material should be etched using a process which does not affect the underlying resist. Buffered Oxide Etch (BOE) which consists of Hydrofluoric acid diluted 7:1 with water can perform this step in 15 seconds. The layer need only be a thousand angstroms thick.

In FIG. 25G, photoresist layer 712 has been spun-on and patterned in a manner already discussed.

Referring to FIG. 25H, using a combination of BOE and RIE, the pattern of resist layer 711 has been transferred to layers 710 and 708. In the first step, the BOE is used to etch through the silicon dioxide layer 710. An oxygen plasma is

used to etch through resist layer 708, and to remove resist layer 711. Plasma etching differs from RIE in that it tends to be less anisotropic, yielding profiles that are not purely vertical.

Referring to FIG. 25I, using an oxygen plasma, resist layer 708 has been slightly underetched in order to facilitate removal of the lift-off stencil. RIE using a carbon tetrafluoride chemistry (CF<sub>4</sub>:O<sub>2</sub> 6:4) is then applied to etching through layer 706.

Referring to FIG. 25J, spacer layer 712 is deposited using PVD techniques. This material can be any number of different compounds which can be deposited using this technique. There are two key requirements for such a material. The first is that the material be soluble in water but not in solvents such as acetone or methanol. Example materials include lithium fluoride, aluminum fluoride, and sodium chloride. The second is that it be deposited with extreme uniformity and thickness control.

The former allows resulting structures to be underetched without damage by using water as the final etchant. Water is an extremely benign solvent, and makes possible the incorporation of many different mirror, conductor, and structural materials in the final device.

The latter insures that subsequent layers conform to the variations of the substrate and therefore primary conductor/mirror. This parallelism is essential for the optical behavior of the resonant cavity devices.

The spacer may also be composed of a polymeric material such as hardbaked photoresist or polyimide. To achieve the required thickness uniformity, a technique other than spinning must be used to deposit the polymer. Two such techniques include extrusion and capillary coating. The consequence of using such a spacer is that all subsequent process steps must be low temperature in nature to prevent outgassing and shrinkage of this layer. In this case, the spacer is ultimately removed using an oxygen plasma.

The stencil is subsequently removed using an ultrasonic acetone bath and methanol rinse. This also removes or lifts off excess deposited spacer material and is what constitutes the final step of the lift-off process.

Alternatively, by using negative photoresist and an oppositely polarized mask, a natural overhang may be produced via overexposure. The same may be accomplished with positive photoresist using a technique known as image-reversal. This would preclude the need to put down a sacrificial photoresist layer and a subsequent SiO<sub>2</sub> layer.

Referring to FIG. 25K, secondary conductor/mirror layer (s) and support membrane (714) are deposited. The nature of the conductor/mirror is dependent on the application. The support membrane must have a tensile residual stress. Tensile stress is required for two reasons. First so that the resulting membranes will be flat and therefore parallel to the substrate in the quiescent state. Secondly, such structures have a tendency to stick when the membranes come in contact with the substrate. Sufficient tensile stress is required pull the membrane away when the drive voltage is reduced.

The membrane must have the appropriate optical characteristics as well. For visible light this would mean transparency in the visible region. Silicon nitride is one candidate for this role for it can be deposited using plasma enhanced chemical vapor deposition (PECVD) with controlled stress. Other candidates include silicon dioxide, magnesium fluoride and calcium fluoride, all of which can be deposited using e-beam evaporation with a resulting tensile stress.

In FIG. 25L, photoresist layer 716 has been spun-on and patterned in a manner described above.

In FIG. 25M, using RIE or ion milling, layer(s) 714 have been etched according to the pattern of resist layer 716.

Referring to FIG. 25N, the final etch is accomplished by placing the device in water for a period of time. The water is agitated, and when the devices are fully etched they are dried.

One variation on this step involves the use of n-butyl alcohol to displace the water when the etch is finished. The devices are then placed in a chamber at approximately 32 degrees centigrade to cause the alcohol to freeze. After this step the devices are placed into a vacuum chamber where the air is then evacuated. This causes the alcohol to sublime and can reduce membrane sticking during the drying phase.

Another alternative process has initial steps of assembly shown in FIGS. 26A through 26C, analogous to those shown in FIGS. 25A through 25C.

Thereafter, in FIG. 26D, photoresist or polymer layer 806 is spun on and a stencil layer, 208, of silicon dioxide is deposited using PVD. This layer must be thicker than the spacer layer to be deposited.

In FIG. 26E, resist layer 810 has been spun-on and patterned using standard procedures.

In FIG. 26F, this step uses BOE and an oxygen plasma etch to define a lift-off stencil.

In FIG. 26G, the spacer material is chosen and deposited as described in FIG. 25J.

In FIG. 26H, the stencil is subsequently removed using an ultrasonic acetone bath and methanol rinse.

The step shown in FIG. 26I is analogous to that shown in FIG. 25K.

In FIG. 26J, photoresist layer 814 has been spun-on and patterned.

In FIG. 26K, using RIE or ion milling, layer(s) 812 have been etched according to the pattern of resist layer 214.

The final etch is accomplished in a manner described above.

All of the materials used for the mirrors must be deposited in such a way that their stress can be controlled. Ideally, they are deposited as "stress balanced" which means that the overall stress of the film or film stack is zero. Since the ultimate goal is that the support membrane conductor/mirror combination have an overall tensile stress, conductor/mirror films with compressive stress may be accommodated by having a high stress support membrane. The technique of ion assisted e-beam deposition (IABD) precludes the need for such accommodation. Using this technique, the residual stress of almost any film of interest may be controlled by bombarding the substrate with a stream of neutral ions during the deposition process. This make possible the total mechanical decoupling of the support material from the optical material. As a result, emphasis can be placed on depositing an optically neutral support membrane with ideal mechanical characteristics. In the same manner, a "mechanically neutral" (i.e. stressless) conductor/mirror can be deposited with ideal optical characteristics.

Referring to FIG. 27A, the simplest conductor/mirror configuration for an individual cavity is formed from a layer 900 that is either the substrate for the primary conductor/mirror, or the support membrane if this is the secondary. Layer 902 is a metallic film with a thickness on the order of several hundred angstroms. The film can be of aluminum, silver, or any number of metals, based on the spectral, and resistive properties as well as the ease with which the metal can be etched.

The use of a metal as both mirror and conductor simplifies fabrication. Unfortunately the spectral characteristics of the metallic layer cannot be tailored, and the performance limits devices to very specific kinds of behavior. Layer 904 is an insulator and/or reflection enhancement film. This can be



formed by oxidizing the metal, if aluminum is being used, in an oxygen plasma thus forming a thin layer of aluminum oxide. Alternatively, insulating layers or reflection enhancement layers may be deposited in a manner discussed before. Metallic mirrors must be somewhat transmissive and therefore no more than several hundred angstroms thick. Insulator films can have thicknesses from one hundred to several thousand angstroms. Their thickness is determined by the kind of voltages expected in driving the devices.

Referring to FIG. 27B, a more elaborate configuration is shown. This is a compound conductor/mirror, with layer 900 as the substrate or the support membrane. The conductor 906 is either a transparent film such as indium tin oxide (ITO), or a very thin metallic layer such as gold. Either can be deposited using suitable film deposition methods. Thicknesses for the ITO should be in the range of several thousand angstroms, and metallic conductors less than 100 angstroms. 908 is a multilayer dielectric stack comprising the mirror. Such a mirror consists of alternating dielectric films with differing indexes of refraction deposited by a suitable PVD process. By choosing films with appropriate thicknesses and indexes, mirrors with tailorable spectral characteristics can be fabricated as is well known in the art. In general, the thickness of the individual layers is one quarter the wavelength of the light of interest.

Alternatively, these mirrors may be deposited using a technique known as codposition. In this case, PVD is used to deposit two materials with different refractive indices simultaneously. Using computer control the refractive index of the resulting film can be varied continuously between those of either film. This deposition technique makes possible mirrors with virtually any spectral characteristic.

The ability to design the characteristics of this mirror allow for devices with a greater variety of modes of operation. Unfortunately, because the conductive layer is not perfectly transparent, additional losses are incurred as a result.

Referring to FIGS. 27C and 27D, a dielectric mirror 908 is deposited directly on substrate 900. Metallic conductor 902 and insulator 904 are deposited and patterned such that they form a border around the periphery of the mirror. Using this configuration, it is possible to provide drive voltages to the devices without compromising throughput since the conductor can be placed outside the active area of the device. FIG. 27D shows a planar view of this mirror configuration.

Response times of this device may suffer as a result of decreased conductor area.

Referring to FIG. 28a, a linear tunable filter is shown which has been fabricated using the process sequence defined above. The major difference is the nature of the mask used to define the self-supporting membrane, which is comprised of support 1006 and 1008. The substrate, 1000, is transparent in the frequency region of interest, and electrodes 1004 are used to drive the device. Dielectric mirror 1002 are defined separately to produce a configuration like that of FIGS. 27c, 27d. Three filters are shown though many more can be fabricated. Each filter 1010, 1012, and 1014 is driven independently so that individual frequencies may be separated from an incident light beam. Such a device can find use in spectroscopic analysis, as a demultiplexer in a wavelength division multiplexed fiber optic communication system, a color printer, or any other application where independent frequency selection is required. FIG. 28b is a top view of the structure.

Referring to FIGS. 29a and 29b, a device known as a deformable mirror includes a self-supporting membrane

1102 fabricated on a substrate 1100. When a potential is applied between actuator electrodes 1104 and conducting mirror 1106, the surface of the mirror can be deformed in a controllable manner. Such a device can be used as a component in an adaptive optics system, or in any situation where control of an incident wavefront is required.

Other embodiments are within the scope of the following claims.

What is claimed is:

1. A device for modulating light in the visible spectrum comprising

an array of interferometric modulation elements formed integrally on a substrate, and

control circuitry connected to the array for controlling each of the modulation elements independently,

each of the modulation elements having two walls that define a cavity, one of the walls being movable relative to the other through a range of positions, the walls causing the cavity to operate interferometrically in at least two of the positions, at least one of the walls serving as a mirror and having at least two layers that cooperate to cause the element to exhibit, in at least one of the two positions, a predetermined optical response to light, each of the two layers contributing substantially to causing the element to exhibit the predetermined optical response.

2. The device of claim 1 wherein, in the one of the walls having layers, one of the layers comprises an opaque metallic layer.

3. The device of claim 1 wherein the optical response comprises reflection of particular frequencies of light.

4. The device of claim 1 wherein the optical response comprises transmission of particular frequencies of light.

5. The device of claim 1 wherein said optical response comprises incident electromagnetic radiation in the visible spectrum.

6. The device of claim 1 wherein said optical response comprises reflection of incident electromagnetic radiation in the visible spectrum.

7. The device of claim 1 wherein said optical response comprises the proportion of incident electromagnetic radiation of a given frequency band that is, on average, reflected.

8. The device of claim 1 further comprising electrodes connected to the control circuitry and to one of the cavity walls, the electrodes being defined separately from the cavity walls.

9. The device of claim 1 wherein one of the walls having layers comprises air as a dielectric material.

10. A tunable filter comprising the device of claim 1.

11. The device of claim 1 wherein both of the cavity walls comprise mirrors.

12. The device of claim 11 wherein one of the mirrors comprises a broadband mirror and the other of the mirrors comprises a narrow band mirror.

13. The device of claim 11 wherein both of the mirrors comprise narrow band mirrors.

14. The device of claim 11 wherein both of the mirrors comprise broad band, non metallic mirrors.

15. The device of claim 11 wherein one of the mirrors comprises a hybrid filter.

16. The device of claim 1 wherein one of the walls comprises a dielectric material, a metallic material, or a composite dielectric/metallic material.

17. The device of claim 1 wherein the movable one or the walls is under tensile stress.

18. The device of claim 1 wherein the control circuitry is connected for analog control of each of the elements.

19. The device of claim 1 wherein the control circuitry controls the motion of the movable one of the walls.

20. The device of claim 7 wherein said modulation element is responsive to a particular electrical condition to occupy either a state of higher reflectivity or a state of lower reflectivity, and said control circuitry generates a stream of pulses having a duty cycle corresponding to said proportion of incident radiation that is reflected and places the modulation element in said higher state of reflectivity during each said pulse and in said lower state of reflectivity in the intervals between said pulses.

21. The device of claim 7 wherein said modulation element is responsive to a particular electrical condition to occupy either a state of higher transmissivity or a state of lower transmissivity, and said control circuitry generates a stream of pulses having a duty cycle corresponding to said proportion of incident radiation that is transmitted and places the modulation element in said higher state of transmissivity during each said pulse and in said lower state of transmissivity in the intervals between said pulse.

22. The device of claim 21 wherein said characteristic comprises the proportion of incident electromagnetic radiation of a given frequency band that is, on average, transmitted by each of said modulation elements.

23. A device for modulating light in the visible spectrum comprising

an array of modulation elements, and

control circuitry connected to the array for controlling the amplitude of light delivered by each of the modulation elements independently by discrete digital signals,

each of the modulation elements having two walls that define a cavity, one of the walls being movable relative to the other through a range of positions, the walls causing the cavity to operate interferometrically in at least two of the positions, at least one of the walls serving as a mirror and having at least two layers that cooperate to cause the element to exhibit, in at least one of the two positions, a predetermined optical, response to light, each of the two layers contributing substantially to causing the element to exhibit the predetermined optical response.

24. The device of claim 23 in which each of the modulation elements is controlled independently by pulse code modulation.

25. A device for modulating light in the visible spectrum comprising

a deformable modulation element having a deformation mechanism and an optical portion independently imparting to the element respectively a controlled deformation characteristic and a controlled modulation characteristic,

the deformation mechanism and the optical portion being formed integrally on a substrate,

the deformation mechanism comprising a flexible membrane held in tensile stress, and the optical portion being formed on the flexible membrane, and

a wall which, together with the optical portion, defines an interference cavity,

the deformable modulation element being movable relative to the wall through a range of positions, the optical

portion and the wall causing the cavity to operate interferometrically in at least two of the positions, the optical portion serving as a mirror end having at least two layers that cooperate to cause the element to exhibit, in at least one of the two positions, a predetermined optical response to light, each of the two layers contributing substantially to causing the element to exhibit the predetermined optical response.

26. The device of claim 25 in which the optical portion comprises an induced absorber.

27. The display of claim 1, 23 or 25 further comprising an electronically active substrate.

28. A reflective or transmissive flat panel display comprising the device of claim 1, 23 or 25.

29. The display of claim 28 wherein the device is characterized by hysteresis.

30. The display of claim 28 in which pixels of different primary colors are displayed on a single plane.

31. The display of claim 30 in which pixels of different primary colors are displayed on separate planes.

32. The device of claim 1, 23, or 25 wherein said visible spectrum includes ultraviolet wavelengths in the visible spectrum.

33. The device of claim 1, 23 or 25 wherein said visible spectrum includes infrared wavelengths in the visible spectrum.

34. The device of claim 1, 23 or 25 wherein said layers comprise a quarter wave stack.

35. The device of claim 25 wherein the mirror has a narrow band that is sufficiently narrow so that light reflected from it represents a discernible color.

36. The device of claim 25 wherein the mirror has a broad band.

37. The device of claim 25 wherein the optical portion comprises a hybrid filter.

38. The device of claim 25 in which the deformation mechanism comprises one or more support arms.

39. The device of claim 25 wherein the modulation element is self-supporting.

40. The device of claim 25 wherein the modulation element is held on separate supports.

41. The device of claim 25 wherein the flexible membrane is supported along its edges by supports.

42. The device of claim 41 wherein the flexible membrane is generally planar and the supports are attached to at least two opposite edges of the membrane.

43. The device of claim 42 wherein the supports are orthogonal to the membrane.

44. The device of claim 25 wherein the deformable portion, under one mode of control is collapsed onto the wall.

45. The device of claim 25 further comprising control circuitry that controls the deformation mechanism by signals applied to the modulation element, and wherein the deformation of the mechanism is subject to hysteresis with respect to signals applied by the control circuitry.

46. The device of claim 42 wherein the membrane is rectangular.

## Novel prevention method of stiction using silicon anodization for SOI structure

Y. Matsumoto\*, T. Shinada, M. Ishida

Department of Electrical and Electronic Engineering, Toyohashi University of Technology, Tempaku-cho, Toyohashi 441-8580, Japan

Received 25 June 1998; revised 27 August 1998; accepted 4 September 1998

### Abstract

Silicon anodization process has been applied to prevent both 'after-rinse stiction' and 'in-use stiction' for the sensors with SOI structure. The anodization process roughened the silicon surface causing hillocks of a few tens of nanometer in height and a few hundreds of nanometer in diameter, resulting in increment of water contact angle above  $100^\circ$  as expected from a theory of fractal structure. Prevention effect for 'after-rinse stiction' was evaluated with silicon cantilever beam array fabricated by SOI structure. The maximum detachment length became three times longer than that of the beam on usual silicon surface. The roughening of silicon surface reduces the actual contact area, and hence, it is effective in preventing 'in-use stiction'. The anodization process was also performed using 73% HF solution without causing attack for aluminum metalization. © 1999 Elsevier Science S.A. All rights reserved.

**Keywords:** Silicon anodization; Stiction; Fractal; Water contact angle; SOI; 73% HF

### 1. Introduction

Surface micromachining devices using  $\text{SiO}_2$  sacrificial etching have advantages of integration with different type sensors, actuators and IC circuits with batch fabrication process [1]. Recently, micromachining sensors using SOI structure have been reported because the silicon structures above  $10\ \mu\text{m}$  thickness can be used with SDB-SOI structure [2–4]. The thick silicon structure results higher sensor capacitance, and the beams with single crystal silicon raises reliability because it does not have hysteresis and creep.

However, stiction is one of the most serious problem for the fabrication of surface micromachining devices and their long-term reliability [5]. The stiction is well known as 'after-rinse stiction' occurring in rinse/dry process after sacrificial wet etching process, and 'in-use stiction' caused by over-range shock or electrostatic force of static electricity etc. Many research groups made an effort to prevent stiction and carried out an analysis of the phenomenon [6]. For 'after-rinse stiction', techniques such as sublimation drying [7], supercritical carbon dioxide [8], photoresist-assisted release [9], SAM (Self-Assembled Mono layer) [10]

and Vapor HF etching [11] have been reported, whereas for preventing 'in-use stiction', methods namely, using dimple [7], fluorocarbon film [12,17], SAM [10], roughening silicon surface [14] have been reported.

The present paper shows the systematic study made on the application of silicon anodization process to prevent both 'after-rinse stiction' and 'in-use stiction' for SOI sensors. The anodized process roughened the silicon surface so that its water contact angle was increased to  $100^\circ$  from a theory of fractal structure. The prevention effect for 'after-rinse stiction' was evaluated, and the method was applied to the fabrication process of sensors.

### 2. Prevention of stiction

#### 2.1. Theory of stiction

The 'after-rinse stiction' occurred in rinse/dry process after the sacrificial  $\text{SiO}_2$  wet etching process is shown in Fig. 1. The phenomenon is divided into two processes, namely attracting process and adhesion process.

The attracting process is caused by capillary force of rinse liquid. Surface energy of liquid on solid can be divided to three components as illustrated in Fig. 2, where  $\alpha_{12}$ ,  $\alpha_{13}$  and  $\alpha_{23}$  denotes the interfacial tensions of the

\* Corresponding author

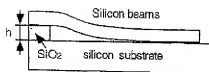


Fig. 1. Schematic diagram of stiction.

solid to liquid, the solid to air, and air to liquid interface, respectively [15].

The water contact angle  $\theta$  is derived from Young's equation as:

$$\cos \theta = \frac{\alpha_{13} - \alpha_{12}}{\alpha_{23}} \quad (1)$$

The capillary force  $F_p$  is derived from the stiction theory [5,6].

$$F_p = \frac{2\alpha_{23}\cos\theta}{h} \quad (2)$$

where  $h$  is gap of silicon structure and substrate. Eq. (2) implies that the capillary force becomes zero at  $\theta = 90^\circ$  and turns out to be negative for  $\theta > 90^\circ$ . Therefore, the attracting process does not occur on hydrophobic surface. In other words, if solid to air interfacial tension  $\alpha_{13}$  is smaller than solid to liquid interfacial tension  $\alpha_{12}$ , the structure is not attracted to the substrate.

The adhesion process is considered as the following process [5]. At first, hydrogen terminals are formed on silicon surface after HF etching process. However, these terminals are broken during rinse process by de-ionized water or upon exposure to atmospheric air. Then, hydroxyl groups are adhered by Van der Waals forces on silicon surface. If the structure get contacted to substrate by capillary force or over-range shock, etc., the structure get stuck to substrate by hydrogen bonding. The strength of hydrogen bonding is  $2\text{--}5 \text{ kg/cm}^2$  at room temperature, which is enough to make permanent adhesion to substrate.

## 2.2. Roughening surface and its water contact angle

As mentioned above, the capillary force becomes zero at  $\theta = 90^\circ$ , and for values of  $\theta$  greater than  $90^\circ$ , it turns out to be negative for values of  $\theta$  greater than  $90^\circ$  in accordance with Eq. (2). Although complete hydrogen terminated silicon surface is thought to be hydrophobic with a contact angle of around  $90^\circ$  [5], silicon surface after rinse and exposure to atmospheric air is slightly hy-

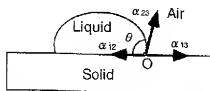


Fig. 2. Diagram of contact angle of liquid on solid.



Fig. 3. Illustration of water contact angle for mirror surface and roughening surface. (a) For mirror surface, (b) for roughening surface.

drophilic with water contact angle of around  $60^\circ$  because of the attachment of hydroxyl groups. Hence, formation of hydrophobic surface such as SAM or fluorocarbon film is one of the effective methods to prevent stiction although these methods require additional fabrication process or specific equipment.

The water contact angle also can be increased with roughening surface from the theory of fractal structure (roughening surface) as illustrated in Fig. 3 [16]. The water contact angle on roughening surface is given by the following equation [15,17]:

$$\cos \theta_r = r \cos \theta \quad (3)$$

where  $\theta_r$  is the water contact angle on roughening surface and  $r$  is a coefficient giving the ratio of the actual area of a roughening surface to the projected area. Usually, the coefficient  $r$  is very large on roughening surface, so that hydrophobic surface becomes ultrahydrophobic (super-water repellent) on roughening surface [16]. Therefore, if contact angle of roughening silicon surface after rinse/dry process becomes greater than  $90^\circ$ , the capillary force becomes negligible. This situation will be effective to prevent 'after-rinse stiction'.

## 2.3. Silicon anodization and its water contact angle

There are many methods to roughen silicon surface such as etch-back [11], making dimple [4] or chemical etching by  $\text{NH}_4\text{F}$  [2], etc. In the present study, silicon anodization process has been applied to roughen the silicon surface, because the process is simple and can be carried out in HF solution as shown in Fig. 4. HF solution is used in  $\text{SiO}_2$  sacrificial etching process, and the HF solution enters under SOI structure during the etching process, therefore, silicon anodization process can be continuously performed after sacrificial etching. The method

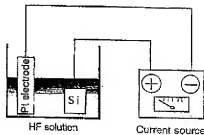


Fig. 4. Principle of silica anodization.

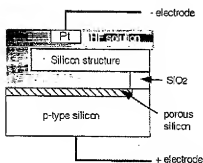


Fig. 5. Electrode contact to SOI structure for anodization process.

is also considered to be effective especially for high trench SOI sensors because entire liquid substitution in chemical treatment is usually difficult for the high aspect ratio SOI structures [19].

It is important to note that an electrode is connected to silicon p-type substrate as illustrated in Fig. 5. Therefore, current does not flow to silicon structure since it is isolated by SiO<sub>2</sub> layer. As a result, the silicon structure is not getting anodized during the process of anodization.

The anodization process is dependent on the doping level of silicon wafer, concentration of HF solution and current density, etc. [20]. In our case, the p-type ( $10^{19}/\text{cm}^3$ ) silicon was anodized in 16% HF (HF:H<sub>2</sub>O = 1:5) solution with a current density 20 mA/cm<sup>2</sup> for 60 min. Fig. 6 shows the SEM photograph of the anodized silicon surface. Small holes (hillocks) of size around a few tens of nanometer to a few hundreds of nanometer were formed on silicon surface. The surface profile was evaluated using AFM measurement. Fig. 7 shows the profile of anodized silicon surface. Many holes (hillocks) in the range of around a few hundreds of nanometer in diameter and a few tens of nanometer in height were formed on silicon surface.

The hydrophobicity of anodized silicon surface was evaluated with contact angle of water droplet. The varia-

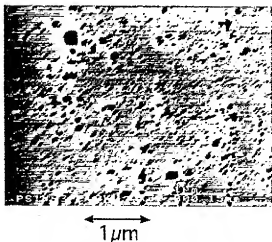


Fig. 6. SEM photograph of anodized silicon surface.

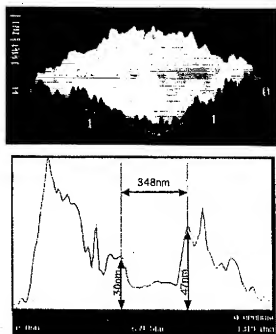


Fig. 7. Surface profile of anodized silicon surface by AFM measurement.

tion of the measured water contact angle in the relation of anodization time is shown in Fig. 8. As can be seen, the water contact angle increased with anodization time, and about 100° was attained over a 30-min duration. Fig. 9 shows the photograph of the water contact angle on silicon surface as well as on anodized silicon surface, where in the water contact angle of about 100° was clearly observed. The observed value satisfies the condition at which the capillary force can be negligible.

#### 2.4. Evaluation with cantilever beams

The effect of anti-stiction was evaluated using cantilever beam array fabricated by SOI structure. Figs. 10 and 11 show the structure and SEM photograph of silicon

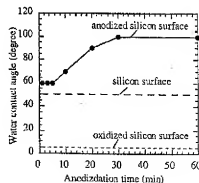


Fig. 8. Relation between water contact angle and anodization time.

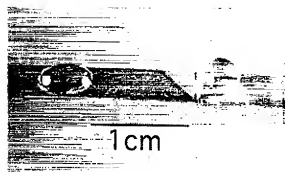


Fig. 9. Photograph of water contact angle on silicon surface (left) and on anodized silicon surface (right).

cantilever beams. The thickness of top silicon layer was 6  $\mu\text{m}$ , and thickness of  $\text{SiO}_2$  intermediate layer was 1  $\mu\text{m}$ . The width of beams was 20  $\mu\text{m}$ , and length was in range of 100  $\mu\text{m}$  to 2000  $\mu\text{m}$ . The substrate was high doped p-type ( $10^{19}/\text{cm}^3$ ) silicon and beams was low doped p-type ( $10^{15}/\text{cm}^3$ ) silicon. First, the silicon dioxide was sacrificial etched in 16% HF solution. Then, the sample was anodized with current density 20  $\text{mA}/\text{cm}^2$  in the same 16% HF solution. Further, the sample was rinsed in DI water, and dried in atmospheric air. The sticking probability was measured by SEM as shown in Fig. 12, or laser displacement measurement equipment. Fig. 13 shows the typical example of laser displacement measurement. The displacement between the substrate and beam's surface was measured by the equipment, so that gap between silicon beams and substrate can be calculated by subtracting the silicon thickness from the measured displacement.

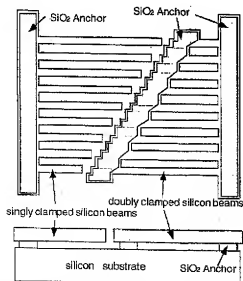


Fig. 10. Structure of SOI singly clamped cantilever beams and doubly clamped cantilever beams.

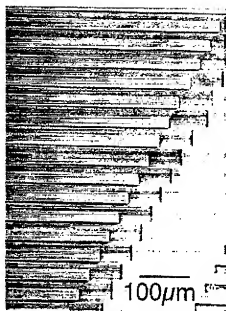


Fig. 11. SEM photograph of SOI cantilever beams.

Fig. 14 shows the relation between gap and beam's length for doubly clamped cantilever beams. From the results, it is evident that the maximum detachment length increases on anodized silicon surface.

The maximum detachment length of beams is calculated by the equations derived by Mastrangelo [6] as follows: For singly clamped cantilever beams:

$$N_p = \frac{3}{8} \frac{Eh^2t^3}{r_s L^4} \quad (4)$$

where  $N_p$  is peeling number,  $E$  is the Young modules of silicon,  $h$  is gap between beams and substrate,  $t$  and  $L$  are thickness and length of beams, and  $r_s$  is adhesion energy of silicon surface.

For doubly clamped cantilever beams:

$$N_p = \frac{128}{5} \frac{Eh^2t^3}{r_s L^4} \left[ 1 + \frac{4\sigma_R L^2}{21t^2} + \frac{256}{2205} \left( \frac{h}{t} \right)^2 \right] \quad (5)$$

where  $\sigma_R$  is the strain of beams.

By substituting  $N_p = 1$  in above the equation, maximum detachment length is calculated. The theoretical maximum detachment length on the usual silicon surface and measured maximum detachment length on anodized surface are summarized in Table 1. The maximum detachment length for each cantilever beams was increased with anodized time. For singly clamped beams, it increases 2 times compared to the beams on normal silicon surface with 30 min anodization treatment, and increases 3 times with 60 min anodization treatment.

From Fig. 8, the water contact angle of silicon wafer was maintained at the same value of  $100^\circ$  over 30 min, but

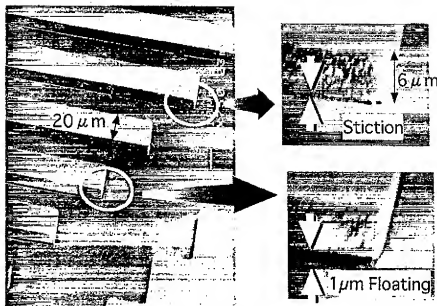


Fig. 12. Evaluation of stiction for SOI cantilever beams using SEM measurement method.

maximum detachment length of cantilever beams was increased with time over 30 min. Its difference was explained that the anodization speed was probably slow under cantilever beams structure because the substitution of HF solution was slow in the narrow gap between beams and substrate. However, it is evident that the maximum detachment length for each cantilever beams increases to about 3 times compared to the beams on normal silicon surface. From Eqs. (4) and (5), adhesion energy  $\gamma_s$  was calculated and found to be about a factor of 2 smaller than on normal silicon surface.

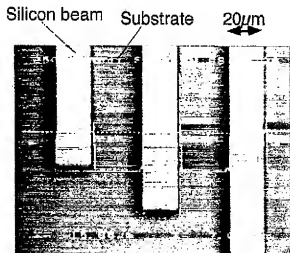


Fig. 13. Photograph of SOI cantilever beams under Laser displacement measurement equipment.

## 2.5. Long-term stability and thermal stability

The long-term stability of anodized silicon surface was evaluated. The anodized sample was exposed to atmosphere at room temperature for 3 months, and its water contact angle was evaluated. It was found that the water contact angle decreased from  $100^\circ$  to  $90^\circ$ . The slight decrease was probably caused by incomplete thin natural silicon di-oxide formation on anodized silicon surface.

The thermal stability of anodized silicon surface was also evaluated. The sample was placed on hot plate maintained at  $300^\circ\text{C}$  in atmosphere for 30 min duration, and its water contact angle was evaluated. The water contact angle decreased from  $100^\circ$  to  $5^\circ$  because of the formation of thick silicon di-oxide on anodized silicon surface. However, after dipping the sample in HF solution in a few

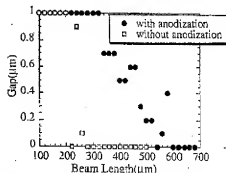


Fig. 14. Relation between gap and beam's length after rinse and drying process for doubly clamped cantilever beams.

Table 1  
Maximum detachment length for the different treatments

Maximum detachment length	For singly clamped cantilever beams	For doubly clamped cantilever beams
Theoretical length	94 $\mu\text{m}$	270 $\mu\text{m}$
Normal surface	less than 100 $\mu\text{m}$	less than 200 $\mu\text{m}$
Anodized (30 min)	180 $\mu\text{m}$	260 $\mu\text{m}$
Anodized (60 min)	380 $\mu\text{m}$	480 $\mu\text{m}$

seconds, the water contact angle was recovered to 100° because silicon dioxide was removed by HF solution and anodized fractal structure was not broken at 300°C. Further, the sample was annealed in ambient of nitrogen gas at 450° for 30 min duration. The annealing process results in the decrease of water contact angle to 5° due to formation of silicon di-oxide on anodized silicon surface with the remained oxygen gas or water in the anodized structure. However, the water contact angle also recovered to 100° with a dipping in HF solution. It indicates that the anodized fractal structure was not broken at high temperature 450°C. It is in contrast with SAM or fluorocarbon film which were broken at high temperature of over 300° [5,13].

### 3. Application for sensor

#### 3.1. Compatibility of anodization process with 73% HF solution

Recently, sacrificial etching methods without causing attack to aluminum metallization using 73% HF was reported by Gennissen and French [18]. If the anodized process can be performed with 73% HF without causing attack to aluminum, it is useful in view of the process compatibility for IC factory. Therefore, silicon anodization process with 73% HF (FLUKA Product #47610) was examined.

As mentioned before, the anodization process has to be carried out after SiO<sub>2</sub> sacrificial etching process of over 30 min. However, the etching rate of silicon di-oxide in conc.

73% HF solution was too fast (1.5  $\mu\text{m}/\text{min}$ ), it causes the attack to 'anchor' structure in SOI sensors. Therefore, 73% HF solution was diluted with IPA to 16% in order to reduce etching rate of silicon dioxide in which aluminum was not attacked [18]. The anodized process was performed for p-type ( $10^{19}/\text{cm}^3$ ) silicon with current density 20  $\text{mA}/\text{cm}^2$  for 60 min duration. As the results, holes with sizes of around a few tens of nanometer were observed, and also, an increase in the water contact angle was noticed.

#### 3.2. Sensor fabrication and durability for in-use stiction

The capacitive SOI accelerometers using SOI structure have been fabricated by adopting anodization process to prevent stiction. The thickness of top single-crystal silicon is 6  $\mu\text{m}$  with a sacrificial silicon di-oxide layer of 1  $\mu\text{m}$ . The substrate was p-type ( $10^{19}/\text{cm}^3$ ), and aluminum was used for metallization [21]. After removing silicon dioxide in 73% HF solution, the sample was anodized with current density 20  $\text{mA}/\text{cm}^2$  in the same 73% HF solution. It was possible to prevent 'after-rinse stiction', and yield of sensor can be increased using anodization method.

The anodized methods is considered to be effective in preventing 'in-use stiction' because the contact area is drastically decreased on roughened surface. Therefore, durability for in-use stiction was evaluated. Fig. 15 shows the relation between sensor capacitance of anodized sample and DC bias voltage applied to sensor. It was observed that the sensor capacitance was square proportional to bias voltage because of electro static force. The capacitance was saturated above 0.6 V because sensor structure come in contact with the substrate. The bias voltage of 5 V which was equivalent about 800 G was applied to sensor 50 times. After that, the initial capacitance was measured and found to be as of the same value. Further, it was changed by DC bias voltage almost in the same relation before contact test as shown in Fig. 15. The above observation conforms that the sensor structure was not stuck to substrate because of the decrement of contact area.

### 4. Conclusion

Silicon anodization process has been successfully applied to prevent both of 'after-rinse stiction' and 'in-use

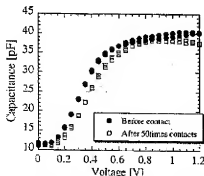


Fig. 15. C-V characteristics of SOI accelerometer using anodization method.



stiction' for SOI structure. The anodization process roughens silicon surface around a few tens of nanometer in height, so that water contact angle was increased over 100° after rise process from fractal theory. The anodized process was also performed using 73% HF solution and IPA without causing attack to aluminum metallization. Prevention effect for 'after-rise stiction' was evaluated with silicon cantilever beam array fabricated by SOI structure. The maximum detachment length becomes 3 times longer than that of on normal silicon surface. The reduction of actual contact area on roughening silicon surface made it effective in preventing 'in-use stiction'. Although it is difficult to prevent the formation of silicon di-oxide at high temperature, the anodized fractal structure was not broken at high temperature 450°C in ambient of nitrogen gas. The water contact angle was easily recovered to 100° with a few seconds dipping in HF solution.

#### Acknowledgements

This work has been partly supported by Japanese Ministry of Education, Science, Sports and Culture under a Grant-in-Aid for Encouragement of Young Scientists No. 10750065, and also partly supported by the Micromachine Technology Research Grant of Micromachine Center, Japan.

#### References

- [1] R.T. Howe, B.E. Boser, A.P. Pisano, Polysilicon integrated microsystems: technologies and applications, *Sensors and Actuators A* 56 (1996) 167–177.
- [2] V.M. Meneilly, M.J. Novack, M.A. Schmidt, Design and Fabrication of Thin-Film Microaccelerometers using Wafer Bonding, *Proc. 7th Int. Conf. Solid State Sensors and Actuators (Transducers'93)*, 1993, pp. 822–825.
- [3] Y. Matsumoto, M. Iwakiri, H. Tanaka, M. Ishida, T. Nakamura, A capacitive accelerometer using SDB-SOI structure, *Sensors and Actuators A* 53 (1996) 267–272.
- [4] T.J. Brodhan, J.M. Bustillo, A.P. Pisano, R.T. Howe, Embedded Interconnect and Electrical Isolation for High-aspect-ratio, SOI Inertial Instruments, *Proc. 1997 Int. Conf. Solid State Sensors and Actuators (Transducers'97)*, 1997, pp. 637–640.
- [5] R. Maboudian, R.T. Howe, Critical review: adhesion in surface micromechanical structures, *J. Vac. Sci. Technol. B* 15 (1) (1997) 1–20.
- [6] C.H. Mastrangelo, Mechanical stability and adhesion of micro structure under capillary forces: Part 1. Basic theory, *Journal of Micro-electromechanical Systems* 2 (1) (1993) 33–43.
- [7] C.-J. Kim, J.Y. Kim, B. Sridharan, Comparative evaluation of drying techniques for surface micromachining, *Sensors and Actuators A* 64 (1998) 17–26.
- [8] G.T. Mulhern, D.S. Soane, R.T. Howe, Supercritical Carbon Dioxide Drying of Microstructures, *The 7th Int. Conf. Solid State Sensors and Actuators*, 1990, pp. 296–299.
- [9] D. Kobayashi, C.-J. Kim, H. Fujita, Photocross-linked release of movable microstructures, *Jpn. J. Appl. Phys.* 32 (1993) 1642–1644.
- [10] M.R. Houston, R. Maboudian, R.T. Howe, Self-assembled Monolayer Films as Durable Anti-stiction Coating for Polysilicon Microstructures, *Solid-State Sensor and Actuator Workshop Hilton Head, SC, June 2–6, 1996*, pp. 42–47.
- [11] J.H. Lee, W.L. Jang, C.S. Lee, Y.I. Lee, C.A. Choi, J.T. Baek, H.J. Yoo, Characterization of anhydrous HF gas-phase etching with CH<sub>3</sub>OH for sacrificial oxide removal, *Sensors and Actuators A* 64 (1998) 27–32.
- [12] P.F. Mana, B.P. Gogoi, C.H. Mastrangelo, Elimination of Post-release Adhesion in Microstructures Using Thin Conformal Fluorocarbon Films, *Proc. IEEE Workshop on MEMS'96*, 1996, pp. 55–60.
- [13] Y. Matsumoto, K. Yoshida, M. Ishida, Fluorocarbon Film for Protection from Alkaline Etchant and Elimination of In-use Stiction, *Proc. 1997 Int. Conf. Solid State Sensors and Actuators (Transducers'97)*, 1997, pp. 695–698.
- [14] R.L. Alley, P. Mai, K. Konvopoulos, R.T. Howe, Surface Roughness Modification of Interfacial Contacts in Polysilicon Microstructure, *Proc. 7th Int. Conf. Solid State Sensors and Actuators (Transducers'93)*, 1993, pp. 288–291.
- [15] T. Onda et al., Super-water repellent fractal surfaces, *Langmuir* 12 (1996) 2115.
- [16] R.D. Hazlett, Fractal applications: wettability and contact angle, *J. Colloid Interface Sci.* 137 (1990) 527.
- [17] A.W. Adamson, *Physical Chemistry of Surfaces*, 5th edn., Chap. X, Section 4, Wiley, New York, 1990.
- [18] P.T.J. Geunissen, P.J. French, Sacrificial Oxide Etching Compatible with Aluminum Metallization, *Proc. 1997 Int. Conf. Solid State Sensors and Actuators (Transducers'97)*, 1997, pp. 225–228.
- [19] M. Nishimura, Y. Matsumoto, M. Ishida, The method to prevent stiction in a capacitive accelerometer using SDB-SOI structure, *Tech. Dig. of the 15th Sensor Symposium*, 1997, pp. 205–208.
- [20] Z.C. Feng, R. Tsu, Porous Silicon, Chap. 15, *World Scientific*, 1994.
- [21] Y. Matsumoto, M. Nishimura, M. Matsura, M. Ishida, Three-axis capacitive accelerometer using SDB-SOI structure, *Tech. Dig. of the 16th Sensor Symposium*, 1998, pp. 29–32.

Yoshinori Matsumoto was born in Shinjuku, Japan, in 1965. He received his BE and PhD degree in electronic engineering from Tohoku University, Sendai, Japan in 1988 and 1993, respectively. He worked on integrated capacitive pressure sensors and accelerometers. Since 1993 he has been a research associate at the Department of Electric and Electronic Engineering of Toyohashi University of Technology. His current research interest are sensors with SOI technology and smart sensors.

Taiji Shimada was born in Aichi, Japan, in 1975. He received his BE degree in Electronic Engineering from Toyohashi University of Technology, Toyohashi, Japan, in 1998. He is currently working towards an ME degree in Electronic Engineering at the same university.

Makoto Ishida was born in Hyogo, Japan, in 1950. He received his PhD degree in Electronics Engineering from Kyoto University, Kyoto, Japan, in 1978. Since 1979 he has been at Toyohashi University of Technology, and he is a professor of Electrical and Electronic Engineering. He is working on heteroepitaxial growth and processes of SOI material including SiGe, and their device applications including sensor and IC in electron device research center in Toyohashi University of Technology.



US006335224B1

(12) **United States Patent**  
**Peterson et al.**

(10) **Patent No.:** **US 6,335,224 B1**  
(45) **Date of Patent:** **Jan. 1, 2002**

(54) **PROTECTION OF MICROELECTRONIC DEVICES DURING PACKAGING**

(75) Inventors: **Kenneth A. Peterson**, Albuquerque;  
**William R. Conley**, Tijeras, both of  
NM (US)

(73) Assignee: **Sandia Corporation**, Albuquerque, NM  
(US)

(\*) Notice: Subject to any disclaimer, the term of this  
patent is extended or adjusted under 35  
U.S.C. 154(b) by 0 days.

(21) Appl. No.: **09/872,562**

(22) Filed: **May 16, 2000**

(51) Int. Cl.<sup>7</sup> ..... **H01L 21/44**

(52) U.S. Cl. .... **438/114; 438/460; 438/465;**  
438/113

(58) Field of Search ..... **359/223; 216/2;**  
216/1; **438/460, 462, 33, 68, 113, 114,**  
465; **83/906**

(56) **References Cited**

**U.S. PATENT DOCUMENTS**

5,107,328	A *	4/1992	Kinsman	.....	357/74
5,435,876	A	7/1995	Alfaro et al.	.....	156/247
5,516,728	A *	5/1996	Degant et al.	.....	438/465
5,605,489	A	2/1997	Gale et al.	.....	451/28
5,766,367	A *	6/1998	Smith et al.	.....	134/2
5,872,046	A *	2/1999	Kaeriyama et al.	.....	438/465
5,923,995	A	7/1999	Kao et al.	.....	438/460
5,951,813	A	9/1999	Warren	.....	156/305
5,958,510	A	9/1999	Sivaramakrishnam et al.	...	427/ 255.6
5,963,788	A	10/1999	Barron et al.	.....	438/48
6,025,767	A	2/2000	Kellam et al.	.....	335/128
6,063,696	A *	5/2000	Brenner et al.	.....	438/465

**OTHER PUBLICATIONS**

Wolf and Tauber; Silicon Processing for the VLSI Era vol.  
1: Process Technology, Lattice Press, Sunset Beach, CA,  
1986. pp. 542-550.\*

Tummala et al.; Microelectronics Packaging Handbook: Part  
II Semiconductor Packaging, ITP, New York, NY, 1997, pp.  
72-73 and 168-170.\*

M. Roth, S. Vogel, U. Schaber, H.-E. Endres, *Electrically  
Removable, Micromachined Encapsulation for Sensitive  
Materials*, Elsevier Science S.A., Sensors and Actuators  
A62 (1997) 633-635.

H. Krassow, F. Campabadal, E. Lora-Tamayo, *Photolitho-  
graphic Packaging of Silicon Pressure Sensors*, Elsevier  
Science S.A., Sensors and Actuators A66 (1998) 279-283.

\* cited by examiner

Primary Examiner—John F. Niebling  
Assistant Examiner—Christopher Lattin  
(74) Attorney, Agent, or Firm—Robert D. Watson

(57) **ABSTRACT**

The present invention relates to a method of protecting a  
microelectronic device during device packaging, including  
the steps of applying a water-insoluble, protective coating to  
a sensitive area on the device; performing at least one  
packaging step; and then substantially removing the protec-  
tive coating, preferably by dry plasma etching. The sensitive  
area can include a released MEMS element. The microelec-  
tronic device can be disposed on a wafer. The protective  
coating can be a vacuum vapor-deposited parylene polymer,  
silicon nitride, metal (e.g. aluminum or tungsten), a vapor  
deposited organic material, cyanoacrylate, a carbon film, a  
self-assembled monolayered material, perfluoropolyether,  
hexamethyldisilazane, or perfluorodecanoic carboxylic acid,  
silicon dioxide, silicate glass, or combinations thereof. The  
present invention also relates to a method of packaging a  
microelectronic device, including: providing a microelec-  
tronic device having a sensitive area; applying a water-  
insoluble, protective coating to the sensitive area; providing  
a package; attaching the device to the package; electrically  
interconnecting the device to the package; and substantially  
removing the protective coating from the sensitive area.

**49 Claims, 4 Drawing Sheets**

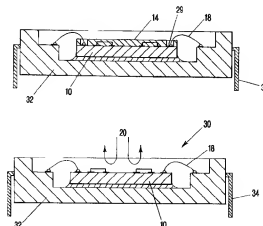




FIG-1A

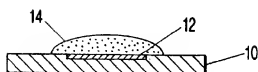


FIG-1B

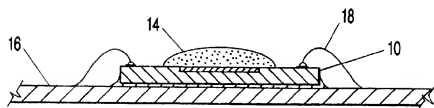


FIG-1C

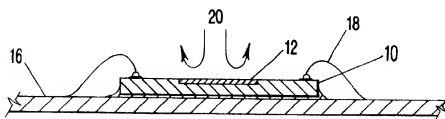


FIG-1D

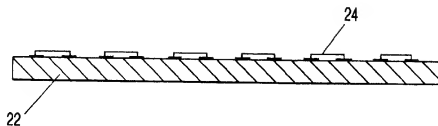


FIG-2A

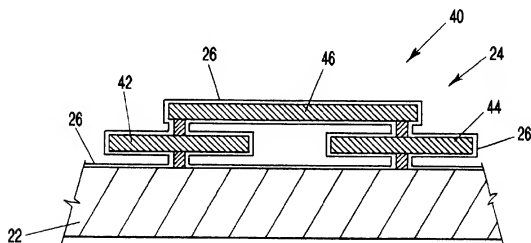


FIG-2B

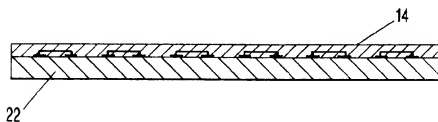


FIG-2C

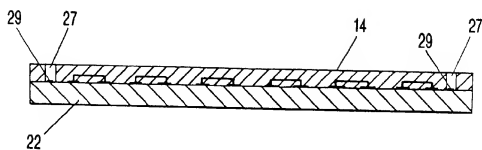


FIG-2D

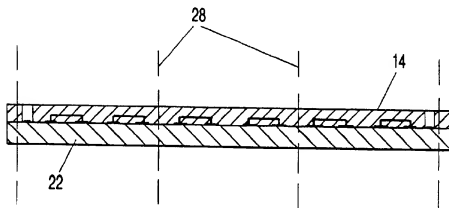


FIG-2E

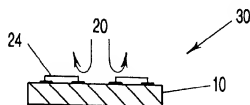


FIG-2F

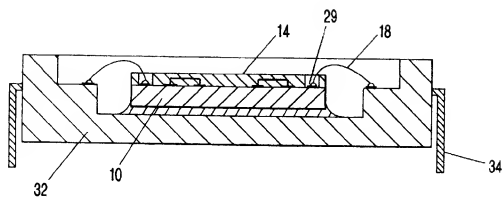


FIG-3A

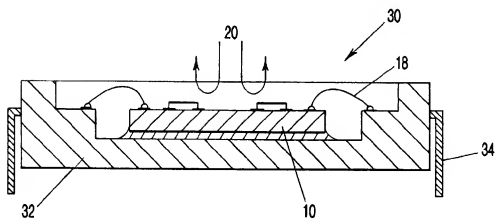


FIG-3B

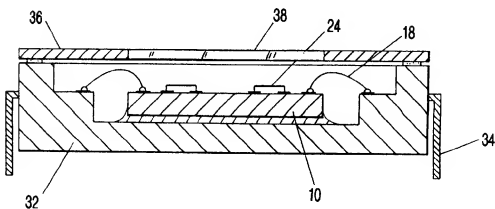


FIG-3C

1

# PROTECTION OF MICROELECTRONIC DEVICES DURING PACKAGING

## FEDERALLY SPONSORED RESEARCH

The United States Government has rights in this invention pursuant to Department of Energy Contract No. DE-AC04-94AL85000 with Sandia Corporation.

## CROSS-REFERENCE TO RELATED APPLICATIONS

None applicable

## BACKGROUND OF THE INVENTION

This invention relates generally to the field of microelectronics and more specifically to packaging of microelectromechanical systems (MEMS) and integrated microelectromechanical systems (IMEMS) devices.

Examples of MEMS and IMEMS devices include airbag accelerometers, microengines, optical switches, gyroscopic devices, sensors, and actuators. IMEMS devices can combine integrated circuits (IC's), such as CMOS or Bipolar circuits, with the MEMS devices on a single substrate, such as a multi-chip module (MCM). All of these devices use active elements (e.g. gears, hinges, levers, slides, and mirrors). These freestanding structures must be free to move, rotate, etc. Additionally, some types of microelectronics devices, such as microsensors, must be freely exposed to the environment during operation (e.g. for chemical, pressure, or temperature measurements).

For current commercially packaged MEMS and IMEMS components, the steps of packaging and testing can account for at least 70% of the cost. The current low-yield of MEMS packaging is a "show-stopper" for the eventual success of MEMS. Conventional electronic packaging methods, although expensive, are not presently adequate to carry these designs to useful applications with acceptable yields and reliability.

During conventional MEMS fabrication, silicon dioxide or silicate glass is a sacrificial material commonly used at the wafer scale to enable creation of complex three-dimensional structural shapes from polycrystalline silicon (e.g. polysilicon). The glass sacrificial layer surrounds and covers the multiple layers of polysilicon MEMS elements, preventing them from moving freely during fabrication. At this stage, the MEMS elements are referred to as being "unreleased".

The next step is to "release" and make free the MEMS elements. Conventionally, this is done by dissolving or etching the glass sacrificial coating in liquid mixtures of hydrofluoric acid, hydrochloric acid, or combinations of the two acids. This wet etching step is typically done at the wafer scale in order to reduce processing costs. Alternatively, a dry release etch may be performed by exposing the wafer to a plasma containing reactive oxygen, chlorine, or fluorine ions. Herein, the word "wafer" can include silicon; gallium arsenide (GaAs); or quartz wafers or substrates (e.g. for MEMS structures).

After releasing the active elements, the MEMS devices can be probed to test their functionality. Unfortunately, probed "good" MEMS are then lost in significant quantity due to damage during subsequent packaging steps. They can be damaged because they are unprotected (e.g. released). Subsequent processing steps can include sawing or cutting (e.g. dicing) the wafer into individual chips or device dies (e.g. dicing); attaching the device to the package (e.g. die

2

attach), wirebonding or other interconnection methods, such as flip-chip solder bumping, or direct metallization (e.g. interconnecting); pre-seal inspection; sealing of hermetic or dust protection lids; windowing; package scaling; plating; trim; marking; final test; shipping; storage; and installation. Potential risks to the delicate released MEMS elements include electrostatic effects, dust, moisture, contamination, handling stresses, and thermal effects. For example, ultrasonic bonding of wirebond joints can impart harmful vibrations to the fragile released MEMS elements.

One solution to this problem is to keep the original sacrificial glass coating intact for as long as possible. In one approach, the MEMS elements would be released after all of the high-risk packaging steps have been completed (including sawing of the wafer into chips). Another approach (which relates to the present invention) would be to release the MEMS elements at the wafer scale; apply any performance-enhancing coatings; re-apply a temporary, replacement protective coating prior to wafer sawing; and, finally, remove the protective coating after all of the high-risk packaging steps have been completed.

In order to reduce the costs of MEMS fabrication and packaging, it is desirable to perform as many fabrication steps at the wafer scale (e.g. before sawing the wafer into individual device dies). An example of a wafer scale process is deposition of performance-enhancing coatings on released MEMS elements (e.g. anti-stiction films and adhesion-inhibitors). Unfortunately, if these coatings are applied at the wafer scale (obviously, on released MEMS elements), then some of these performance-enhancing coatings may also be unintentionally deposited on the backside of the wafer. These unwanted coatings can interfere with the subsequent die attachment step. Also, the subsequent removal of these unwanted backside coatings can damage or contaminate the released MEMS elements.

Likewise, application of adhesion-promoting coatings (e.g. for die attachment) to the backside of the wafer may similarly damage the released MEMS elements by unintentional contamination or adsorption of harmful materials.

What is desired is a process that first releases the MEMS elements at the wafer scale; then applies all of the desired performance-enhancing coatings to the released MEMS elements; followed by re-application of a temporary protective coating; followed by cleanup of unwanted coatings unintentionally applied to the wafer's backside, followed by cutting the wafer into individual device dies.

Another desirable goal is to replace conventional wet etching processes with dry etching processes; to reduce costs, and because of an increasing emphasis on using environmentally friendly fabrication and cleaning processes. Especially for IMEMS devices, which can contain CMOS or Bipolar structures and other semiconductor materials, aggressive wet etchants used to release MEMS elements can damage the CMOS or Bipolar structures if they are not sufficiently protected. Standard photoresist protection used on CMOS or Bipolar chips may not provide sufficient protection from attack by acid etchants.

Wet etching processes can have other problems. Large hydrodynamic forces may be unintentionally applied to the fragile released MEMS elements, such as when agitating within a bath, and can fracture thin elements. Also, improper removal of any liquid film can create stiction problems resulting from capillary effects during the process of immersion in, removal from, and drying of liquid solutions. Using dry processing can eliminate these potential sources of damage.

3

What is also desired is using a dry etching process, preferably single-step, for removing protective coatings from MEMS devices. It is also desired that the dry etching process can be stopped before completely removing all of the protective coating, thereby leaving some desirable residual material that may reduce friction and may reduce tolerances between bearing surfaces, potentially reducing wobble in rotating gears and discs.

The list of desired objects described above could apply to microelectronics devices other than MEMS or IMEMS, such as microsensors. Microsensors also have a need for temporary protection of sensitive areas during packaging steps.

None of the approaches discussed above provides a low-cost, high-yield, high-capacity commercial wafer-scale, water-insoluble, protection film or coating that provides MEMS and IMEMS stabilization and protection during device packaging.

Use of the word "MEMS" is intended to also include "IMEMS" devices, unless specifically stated otherwise. Likewise, the word "plastic" is intended to include any type of flowable dielectric composition. The word "film" is used interchangeably with "coating", unless otherwise stated. The phrases "released MEMS elements", "released MEMS elements", "sensitive area", and "active MEMS elements" are used interchangeably to refer to the freely-movable structural elements, such as gears, pivots, hinges, sliders, etc.; and also to exposed active elements (e.g. flexible membranes) for microsensors (e.g. chemical, pressure, and temperature microsensors).

#### BRIEF DESCRIPTION OF THE DRAWINGS

The accompanying drawings, which are incorporated in and form part of the specification, illustrate various embodiments of the present invention and, together with the description, serve to explain the principles of the invention.

FIG. 1A shows a schematic cross-section view of a first example, according to the present invention, of a microelectronic device with a sensitive area.

FIG. 1B shows a schematic cross-section view of a first example, according to the present invention, that is similar to FIG. 1A, after a water-insoluble protective coating has been applied to the sensitive area.

FIG. 1C shows a schematic cross-section view of a first example, according to the present invention, that is similar to FIG. 1B, after the device has been attached and wirebonded to a substrate.

FIG. 1D shows a schematic cross-section view of a first example, according to the present invention, that is similar to FIG. 1C, after the protective coating has been removed by etching, thereby exposing the sensitive area to the surrounding environment.

FIG. 2A shows a schematic cross-section view of a second example, according to the present invention, of a wafer substrate with already released MEMS elements located on the wafer's topside.

FIG. 2B shows a schematic cross-section view of a second example, according to the present invention, that is similar to FIG. 2A, after an anti-stiction coating has been applied to the released MEMS elements.

FIG. 2C shows a schematic cross-section view of a second example, according to the present invention, that is similar to FIG. 2B, after a water-insoluble protective coating has been applied to the released MEMS elements, on top of the antistiction coating of FIG. 2B. The coating can be a vacuum vapor deposited parylene coating.

4

FIG. 2D shows a schematic cross-section view of a second example, according to the present invention, that is similar to FIG. 2C, after bond pads have been exposed by machining vias in the coatings.

FIG. 2E shows a schematic cross-section view of a second example, according to the present invention, that is similar to FIG. 2D, wherein the wafer is being cut into individual device dies by diamond saw cutting or laser dicing.

FIG. 2F shows a schematic cross-section view of a second example, according to the present invention, that is similar to FIG. 2E, wherein the protective coating is being removed by etching, thereby re-releasing the MEMS elements.

FIG. 3A shows a schematic cross-section view of a third example, according to the present invention, of a MEMS device attached and wirebonded to a package, with MEMS elements protected in a protective coating.

FIG. 3B shows a schematic cross-section view of a third example, according to the present invention, that is similar to FIG. 3A, wherein the protective coating is being removed by dry oxygen plasma etching, thereby re-releasing the MEMS elements.

FIG. 3C shows a schematic cross-section view of a third example, according to the present invention, that is similar to FIG. 3B, wherein a cover lid with a window has been attached to the package, thereby completing the packaging of the released MEMS device.

#### DETAILED DESCRIPTION OF THE INVENTION

The present invention relates to a method of protecting a microelectronic device during device packaging, comprising, in the order presented: providing a microelectronic device having a sensitive area; applying a water-insoluble, protective coating to the sensitive area; performing at least one packaging step; and then substantially removing the protective coating from the sensitive area.

FIG. 1A shows a schematic cross-section view of a first example, according to the present invention, of a microelectronic device 10 with a sensitive area 12. Examples of microelectronic device 10 can include an airbag accelerometer, a microengine, an optical switch, a gyroscopic device, a microsensor, and a microactuator. Microelectronic device 10 can include microelectromechanical systems (MEMS) that have MEMS elements (e.g. gears, hinges, levers, slides, and mirrors). These free-standing MEMS elements must be free to move, rotate, etc during MEMS operation. Microelectronic device 10 can also include IMEMS devices, which combine integrated circuits (IC's), such as CMOS or Bipolar circuits, with MEMS devices on a single substrate, such as a multi-chip module (MCM). Microelectronics device 10 can also include microsensors, which must be freely-exposed to the environment during operation (e.g. for chemical, pressure, or temperature measurements). Microelectronics device 10 can also include microfluidic systems, such as used in Chemical-Lab-on-a-Chip systems.

FIG. 1B shows a schematic cross-section view of a first example, according to the present invention, that is similar to FIG. 1A, after a water-insoluble protective coating 14 has been applied to the sensitive area 12. The application of protective coating 14 can potentially prevent damage due to external contamination, debris, moisture, cutting fluids, handling forces, electrostatic effects, etc. Sensitive area 12 can include a released MEMS element, an IC, an optically active surface, a chemically-sensitive surface, a pressure-sensitive surface, or a temperature-sensitive surface. Examples of



optically active devices include charge coupled devices (CCD), photocells, laser diodes, vertical cavity surface emitting lasers (VCSEL's), and UV erasable programmable read-only memory chips (E-EPROM's). While some of these devices emit light, and while others receive light, both are considered to be "optically active".

The ideal protective coating 14 would be water-insoluble, vacuum vapor-deposited, strong, pure, inert, defect-free, dry-etchable, and conformal. Coatings made from parylene generally satisfy these requirements. Other suitable protective coatings can include silicon nitride, metal (e.g. aluminum or tungsten), a vapor deposited organic material, cyanoacrylate, a carbon film, a self-assembled monolayered material, perfluoropolyether, hexamethyldisilazane, or perfluorodecanoic carboxylic acid, silicon dioxide, silicate glass, or combinations thereof. Other glass formulations (e.g. containing boron or phosphorus) can be used which have the desirable property of being more rapidly etched (e.g. fast-etch glass), even though other properties (e.g. dielectric strength) may not be as good as compared to pure silicon dioxide. Alternatively, amorphous carbon films, or diamond-like carbon films (DLC) can be used.

The preferred water-insoluble protective coating 14 is a material chosen from the family of vacuum vapor-deposited (e.g. CVD or PECVD) materials called "parylene". Other polymer coatings could be used, for example: epoxies, acrylics, urethanes, and silicones. However, those other coatings are generally applied in the liquid state, whereas parylene is applied in the vapor-phase. Liquid coatings generally do not conform as well to the complex 3-D shaped, multi-layer MEMS elements as vacuum vapor-deposited conformal coatings, such as parylene.

Parylene is the generic name for members of a unique polymer series originally developed by the Union Carbide Corporation. The basic member of the series is poly-paraxylylene; a completely linear, highly crystalline material called Parylene N. Parylene N is a primary dielectric, exhibiting a very low dissipation factor, high dielectric strength, and a dielectric constant invariant with frequency. Parylene C, the second commercially available member of the Union Carbide series, is produced from the same monomer, which has been modified by the substitution of a chlorine atom for one of the aromatic hydrogens. Parylene C has passed the NASA Goddard Space Flight Center outgassing test. Parylene C has a useful combination of electrical and physical properties plus a very low permeability to moisture and other corrosive gases. It also has the ability to provide a true pinhole-free conformal insulation. For these reasons, Parylene C is a preferred material for coating critical electronic assemblies.

Parylene D, the third member of the Union Carbide series, is produced from the same monomer, but modified by the substitution of the chlorine atom for two of the aromatic hydrogens. Parylene D has similar properties to Parylene C, but with the ability to withstand higher use temperatures. Due to the uniqueness of the vapor phase deposition, the parylene family of polymers can be formed as structurally continuous films as thin as a fraction of a micrometer, to as thick as several thousandths of an inch.

Vacuum vapor-deposited parylene coatings 14 are applied to specimens in an evacuated deposition chamber by means of gas phase polymerization. The parylene raw material, di-para-xylylene dimer, is a white crystalline powder manufactured by Union Carbide Corporation, Danbury, Conn. under the product name "Parylene Dimer DPX-N". First, the powder is vaporized at approximately 150 degrees C. Then

it is molecularly cleaved (e.g. pyrolyzed) in a second process at about 680 degrees C. to form the diradical, para-xylylene, which is then introduced as a monomeric gas that polymerizes on the specimens in the vacuum chamber at room temperature. There is no liquid phase in the deposition process, and specimen temperatures remain near ambient. The coating grows as a pure, defect-free, self-assembling, conformal film on all exposed surfaces, edges, and crevices.

During the deposition stage, the active (cured) monomeric gas polymerizes spontaneously on the surface of coated specimen at ambient temperature with no stresses induced initially or subsequently. In short, there are no cure-related hydraulic or liquid surface tension forces in the process. Parylenes are formed at a vacuum of approximately 0.1 torr, and under these conditions the mean-free-path of the gas molecules in the deposition chamber is in the order of 0.1 cm. In the free molecular dispersion of the vacuum environment, all sides of an object to be coated are uniformly impinged by the gaseous monomer, resulting in a high degree of conformity. Polymerization occurs in crevices, under devices, and on exposed surfaces at the same rate of about 0.2 microns per minute for Parylene C, and a somewhat slower rate for parylene N. The deposition rate depends strongly on processing conditions.

Parylene possesses useful dielectric and barrier properties per unit thickness, as well as extreme chemical inertness and freedom from pinholes. Since parylene is non-liquid, it does not pool, bridge, or exhibit meniscus or capillary properties during application. No catalysts or solvents are involved, and no foreign substances are introduced that could contaminate coated specimens. Parylene thickness is related to the amount of vaporized dimer and dwell time in the vacuum chamber, and can be controlled accurately to +/-5% of final thickness. The vacuum deposition process makes parylene coating relatively simple to control, as opposed to liquid materials, where neither thickness nor evenness can be accurately controlled. Parylene film meets typical printed wiring assembly coating protection and electrical insulating standards; as specified by MIL-I-46058. The coating's thickness is controllable from as little as 100 Angstroms, to hundreds of microns.

The parylene polymer coatings have fairly good adhesion to epoxy molding compounds. Interestingly, parylene monomer is soluble in epoxy gel-coat. Here, parylene polymer is formed under the surface of the epoxy, resulting in an interpenetrating polymer network and an especially effective mechanism for adhesion, if required.

Curing occurs during deposition; therefore no high temperature curing step is required. Since parylene is applied in a non-liquid state, there are no hydrodynamic forces that could damage the fragile released MEMS elements. Deposition also takes place at ambient temperatures, which minimize thermal or chemical cure stresses. Parylene's static and dynamic coefficients of friction are in the range of 0.25 to 0.33 (in air), which makes this coating only slightly less lubricious than TEFLON. Because the parylene deposition process is spontaneous, and does not require a cure catalyst, it is therefore extremely pure and chemically inert.

Parylene polymers resist attack and are insoluble in all organic solvents up to 150 C, including water. Parylene C can be dissolved in chloro-naphthalene at 175 C, and Parylene N is soluble at the solvent's boiling point of 265 C. Parylene coatings can be removed by many processes, including oxygen or ozone reactive ion plasma exposure; and laser ablation. Oxygen-based plasma exposure does not harm the polysilicon structural elements of MEMS devices.

Dry etching of parylene coatings is generally faster than dry etching of silicon dioxide glass coatings, which supports the preferred choice of parylene for use as the protective coating 14, as compared to using silicon dioxide glass.

Reactive parylene monomers can be blended with other reactive materials to form copolymer compounds, including silicon, carbon, and fluorine containing monomers (including siloxanes). Additional information on the formation and composition of thin parylene films on semiconductor substrates for use as a low-dielectric, insulating coating is contained in U.S. Pat. No. 5,958,510 to Sivaramakrishnan, et al., and in U.S. Pat. No. 6,030,706, to Eissa, et al. Both patents are herein incorporated by reference in their entirety.

FIG. 1C shows a schematic cross-section view of a first example, according to the present invention, that is similar to FIG. 1B, after device 10 has been conventionally attached to substrate 16, and electrically interconnected to substrate 16 with wirebonds 18. Other packaging steps, well-known to those skilled in the art, could be performed at this stage, such as encasing the wirebonds in a plastic material (not shown). Protective coating 14 protects sensitive area 12 during these packaging steps.

FIG. 1D shows a schematic cross-section view of a first example, according to the present invention, that is similar to FIG. 1C, after protective coating 14 has been substantially removed by using an etching process 20, thereby exposing sensitive area 12 to the surrounding environment.

A variety of etching solutions can be used to chemically remove coatings. Wet etching of silicon dioxide or silicate glass can use hydrofluoric or hydrochloric acid, followed by rinsing, and drying. Drying can include using supercritical drying and sublimation methods to reduce stiction problems. Etching solutions for removing plastic materials (e.g. epoxy resin and glob-top polymers) can include using fuming nitric acid, fuming sulfuric acid, or mixtures of the two acids.

Wet etching can be performed with a commercially available device conventionally called a "decapsulator", or "jet etcher", such a device removes material by directing a stream of (sometimes heated) acid etchant perpendicular to the surface being etched. A gasket can be used to confine the area being etched. The etching solutions can be heated to 250 C, and +/-1% temperature control is provided. An example of a decapsulator device is the "D Cap-Delta" dual acid system sold by B&G International, Santa Cruz, Calif., 95060. Other decapsulating devices are also described in U.S. Pat. No. 5,855,727 to Martin, et al.; and in U.S. Pat. No. 5,932,061 to Lam.

Alternatively, dry plasma etching can be used to substantially remove protective coating 14, instead of wet etching. Dry etching processes are generally less damaging to the fragile MEMS elements than wet processes. Plasma etching can include reactive ion etching and ion milling with chemically active ions (e.g. oxygen, chlorine, or fluorine ions). Exposure to ozone in the presence of UV radiation can also be used for dry etching. It is critical that the release process does not substantially damage other features on the micro-electronic device, such as metal interconnects.

Another dry etching process is exposure to gas or gases. For example, chlorine gas can be used to etch a tungsten protective coating, and xenon difluoride can be used to etch silicon.

FIG. 2A shows a schematic cross-section view of a second example, according to the present invention, of a wafer 22 with a plurality of already released MEMS elements 24 located on the wafer 22.

FIG. 2B shows a schematic cross-section view of a second example, according to the present invention, that is similar to FIG. 2A, after an optional anti-stiction coating 26 has been applied to the released MEMS elements 24. A schematic MEMS device 40 is shown, having MEMS elements 24 comprising two polysilicon gears 42, 44 and a linkage bar 46. Anti-stiction coating 26 in FIG. 2B is an example of a class of performance-enhancing and/or proprietary films that can be applied to released MEMS elements 24. Examples of performance-enhancing films include anti-stiction films, adhesion-inhibitors, lubricants (e.g. perfluoropolyether, hexamethyldisilazane, or perfluorodecanoic carboxylic acid), and nitrided-surfaces that reduce friction between moving (e.g. polysilicon) surfaces. In U.S. Pat. No. 5,766,367, "Method for Preventing Micromechanical Structures from Adhering to Another Object", Smith, et al. discloses the formation of an adhesion-inhibiting hydrophilic coating by immersing the MEMS components in a solvent containing hexamethyldisilazane. U.S. Pat. No. 5,766,367 is herein incorporated by reference in its entirety. Also, vapor-deposited, self-assembling monolayer (SAM) lubricants, such as perfluorodecanoic carboxylic acid, can be used. Finally, some degree of humidity can also help to increase lubricity.

FIG. 2C shows a schematic cross-section view of a second example, according to the present invention, that is similar to FIG. 2B, after water-insoluble protective coating 14 has been applied to the released MEMS elements 24, on top of the anti-stiction coating of FIG. 2B. Protective coating 14 substantially encapsulates the released MEMS elements 24, thereby inactivating them and protecting them with a durable coating. Coating 14 can be a vacuum vapor-deposited parylene coating. Coating 14 can be applied to the entire topside of wafer 22 without the need for masking or patterning. However, the backside of wafer 22 may be covered to prevent unwanted deposition thereon of coating 14. Preparation of the wafer's backside can include cleaning of unintentionally-deposited materials on the wafer's backside (such as anti-stiction films or MEMS lubricants); removing the native oxide film; and/or deposition of adhesion-enhancing layers to the backside, such as gold. Since MEMS elements 24 are stabilized and protected by protective coating 14, these optional backside preparation steps can be performed using conventional techniques, and without a requirement for extraordinary care.

FIG. 2D shows a schematic cross-section view of a second example, according to the present invention, that is similar to FIG. 2C, after bond pads 29 have been optionally exposed by machining via 27 in the coatings. Vias 27 can be defined by photolithography, and can be fabricated by using processes well-known in the art (e.g. e-beam ablation, laser ablation, and water-jet cutting).

FIG. 2E shows a schematic cross-section view of a second example, according to the present invention, that is similar to FIG. 2D, wherein wafer 22 is being cut into individual device dies 28 by using processes well-known in the art (e.g. diamond saw cutting, water-jet cutting, and laser dicing). MEMS elements 24 are protected by coating 14 from damage from cutting debris and lubricant fluids that are typically used during wafer dicing. Alternatively, protective coating 14 could be patterned in a manner to exclude coating 14 from the wafer saw streets (e.g. lines where the saw cuts along), prior to saw cutting. This would be desirable to avoid contaminating the dicing saw with unwanted debris (e.g. organic debris) generated by cutting of coating 14. Exclusion of coating 14 from the wafer saw streets can be accomplished by masking during deposition of the coating.

Alternatively, the coating can be removed from the wafer's saw streets by wet or dry etching using a patterned mask. An optional cleaning step can be performed after dicing wafer 22.

FIG. 2F shows a schematic cross-section view of a second example, according to the present invention, that is similar to FIG. 2E, wherein protective coating 14 is being substantially removed by etching process 20, thereby re-releasing the MEMS element 24, and producing a released MEMS device die 30. It is important that the etching process 20 does not also remove any performance-enhancing coatings, such as anti-stiction coating 26. Optional probe testing of each MEMS or IMEMS device die 30 can be performed at this stage to determine which ones are the "good" dies, since the released MEMS elements 24 are free and fully functional.

FIG. 3A shows a schematic cross-section view of a third example, according to the present invention, of a microelectronic device 10 attached and wirebonded to a package 32, with MEMS elements 24 protected in a protective coating 14. Package 32 has exterior electrical leads 34. Other interconnection methods, such as flip-chip solder bumps, or direct metallization, can be used in place of wirebonds. The use of protective coating 14 to encapsulate MEMS elements 24 permits a wide range of die attach processes and materials to be used without fear of adsorption of potentially harmful layers on the MEMS elements. Use of protective coating 14 also allows ultrasonic wirebonding or other interconnection steps to occur without damage due to mechanical vibrations or shock to the MEMS devices.

FIG. 3B shows a schematic cross-section view of a third example, according to the present invention, that is similar to FIG. 3A, wherein the protective coating 14 is substantially removed by a dry oxygen plasma etching process 20, thereby re-releasing the MEMS elements 24.

Alternatively, in FIG. 3B, the protective coating 14 can be only partially removed, whereby some residual amount of protective coating 14 remains. While sufficient amount of coating 14 must be removed so that MEMS element 24 is released, there are three reasons for not completely removing protective coating 14. Firstly, it might not be desirable to remove the performance-enhancing films 26 (e.g. anti-stiction and lubricants) applied previously. This can be prevented by not removing all of protective coating 14. Secondly, leaving a thin layer of protective coating 14 in place may be desirable if coating 14 can act as its own lubricant. This second option could possibly eliminate the extra step of applying performance-enhancing films 26 in FIG. 2B. Thirdly, leaving a thin layer of coating 14 can possibly reduce micromachining tolerances between bearing surfaces, whereby wobble in gears and discs can be reduced, for example.

FIG. 3C shows a schematic cross-section view of a third example, according to the present invention, that is similar to FIG. 3B, wherein a cover lid 36 has been attached to the package 32, thereby completing the packaging of the released MEMS device 30. Cover lid 36 can optionally include a window 38, for providing optical access to MEMS device 30. Optical access to operational MEMS devices can be useful for calibration, inspection, performance characterization, and failure analysis of MEMS elements.

The particular examples discussed above are cited to illustrate particular embodiments of the invention. Other applications and embodiments of the apparatus and method of the present invention will become evident to those skilled in the art. For example, although the figures illustrate only a single microelectronic device or MEMS device, the

method described herein applies equally well to packaging of multiple MEMS or IMEMS devices, which can be arrayed in a 1-D or 2-D array. Also, the method of perforating one side of a plastic package can also be applied to an opposite side. One example of this can be perforating both sides of a pressure-sensitive area on a microsensor device that is encapsulated in plastic. By perforating both sides, then a pressure differential can be sensed from one side of the device to the other side. The actual scope of the invention is defined by the claims appended hereto.

We claim:

1. A method of protecting a microelectronic device during device packaging, comprising, in the order presented:

providing a microelectronic device having a sensitive area;

vapor depositing a water-insoluble, protective coating on the sensitive area;

performing at least one packaging step; and substantially removing the protective coating from the sensitive area.

2. The method of claim 1, wherein the active area comprises a released MEMS element.

3. The method of claim 2, whereby removing the protective coating re-releases the MEMS element.

4. The method of claim 1, wherein the microelectronic device is disposed on a wafer.

5. The method of claim 4, wherein said wafer is patterned, whereby said protective coating is substantially removed from the wafer's saw streets before cutting said wafer into individual device dies.

6. The method of claim 5, wherein said wafer is masked during deposition of said protective coating, whereby said coating is substantially not deposited on to the wafer's saw streets, prior to cutting said wafer into individual device dies.

7. The method of claim 5, wherein said protective coating is substantially removed from said saw streets, before cutting said wafer into individual device dies.

8. The method of claim 5, further comprising cutting the wafer into a plurality of individual device dies.

9. The method of claim 1, wherein the step of applying a protective coating comprises vacuum vapor-depositing the coating.

10. The method of claim 9, wherein the vacuum vapor-deposited coating comprises a parylene polymer.

11. The method of claim 10, wherein the parylene coating is selected from the group of parylene polymers consisting of poly-para-xylylene, poly-para-xylylene which has been modified by the substitution of a chlorine atom for one of the aromatic hydrogens, and poly-para-xylylene which has been modified by the substitution of the chlorine atom for two of the aromatic hydrogens.

12. The method of claim 10, further comprising blending the parylene polymer with a reactive material to form a copolymer coating.

13. The method of claim 12, wherein the reactive material comprises a monomer containing an element selected from the group consisting of silicon, carbon, and fluorine, and combinations thereof.

14. The method of claim 1, wherein the protective coating comprises silicon dioxide, silicate glass, or silicon nitride.

15. The method of claim 1, wherein the protective coating comprises a metal.

16. The method of claim 15, wherein the metal comprises aluminum or tungsten.

17. The method of claim 1, wherein the protective coating comprises a vapor deposited organic material.

## 11

18. The method of claim 1, wherein the protective coating comprises cynoacrylate.

19. The method of claim 1, wherein the protective coating comprises a carbon film.

20. The method of claim 1, wherein the protective coating comprises a self-assembled monolayered material.

21. The method of claim 1, wherein the protective coating comprises a material selected from the group consisting of perfluoropolyether, hexamethyldisilazane, and perfluorodecanoic carboxylic acid.

22. The method of claim 1, further comprising exposing bond pads on the microelectronic device, after applying the protective coating.

23. The method of claim 8, further comprising exposing bond pads on the microelectronic device, after applying the protective coating, but before cutting the wafer.

24. The method of claim 1, wherein the removing step comprises using a dry etching process.

25. The method of 24, wherein using the dry etching process comprises exposing the active area to a reactive ion plasma.

26. The method of claim 25, wherein the reactive ion plasma comprises an element selected from the group consisting of oxygen, chlorine, and fluorine, and combinations thereof.

27. A method of packaging a microelectronic device, comprising, in the order presented:

providing a microelectronic device having a sensitive area;

applying a water-insoluble, protective coating to the sensitive area;

providing a package;

attaching the device to the package;

electrically interconnecting the device to the package; and substantially removing the protective coating from the sensitive area.

28. The method of claim 27, further comprising the step of attaching a cover lid to the package, after substantially removing the protective coating from the active area.

29. The method of claim 28, wherein the cover lid comprises a window.

30. The method of claim 27, wherein the interconnecting step comprises wirebonding.

31. A method of protecting at least one MEMS element during device packaging, comprising, in the order presented:

providing a wafer having a released MEMS element; applying a performance-enhancing coating to the released MEMS element;

applying a water-insoluble, protective coating on top of the performance-enhancing coating; cutting the wafer into a plurality of individual device dies; and

removing at least some of the water-insoluble protective coating, while not removing the performance-enhancing coating, whereby some residual amount of protective coating remains.

32. The method of claim 31, wherein all of the protective coating is removed.

33. The method of claim 31, wherein the performance-enhancing coating is selected from the group consisting of an anti-stiction film, an adhesion-inhibiting film, a lubricant, and a nitrided-surface.

34. The method of claim 31, wherein the performance-enhancing coating is selected from the group consisting of perfluoropolyether, hexamethyldisilazane, and perfluorodecanoic carboxylic acid.

35. The method of claim 31, wherein the residual remaining protective coating reduces friction.

36. The method of claim 31, wherein the residual remaining protective coating reduces tolerances between bearing surfaces of the MEMS element.

## 12

37. A method of protecting released MEMS elements during wafer dicing, comprising:

providing a wafer comprising a plurality of released MEMS elements fabricated thereon;

vapor depositing a water-insoluble, protective coating on the wafer such that the protective coating covers and encapsulates the released MEMS elements for protection during packaging steps subsequent to dicing; and then

dicing the wafer to form a plurality of individual dies.

38. The method of claim 37, further comprising removing the protective coating after dicing the wafer.

39. The method of claim 1, wherein vapor depositing comprises using a Chemical Vapor Deposition (CVD) process.

40. The method of claim 1, wherein vapor depositing comprises using a Plasma Enhanced Chemical Vapor Deposition (PECVD) process.

41. The method of claim 1, wherein vapor depositing comprises polymerizing a monomeric gas on the surface to be coated.

42. The method of claim 1, wherein the temperature of the sensitive area remains essentially at ambient temperature during vapor depositing.

43. The method of claim 24, wherein the dry etching process comprises exposure to chlorine gas.

44. The method of claim 24, wherein the dry etching process comprises ion milling.

45. The method of claim 24, wherein the dry etching process comprises exposure to ozone in the presence of UV radiation.

46. A method of protecting at least one MEMS element during device packaging, comprising, in the order presented:

providing a wafer having a released MEMS element;

applying a water-insoluble, performance-enhancing coating to the released MEMS element;

applying a water-insoluble, protective coating on top of the performance-enhancing coating;

dicing the wafer into a plurality of individual device dies; and

removing at least some of the protective coating, while not removing the performance-enhancing coating, whereby some residual amount of protective coating remains.

47. A method of protecting at least one MEMS element during device packaging, comprising, in the order presented:

providing a wafer having a released MEMS element;

applying a performance-enhancing coating directly to the released MEMS element;

applying a water-insoluble, protective coating directly on top of the performance-enhancing coating;

cutting the wafer into a plurality of individual device dies; and

removing at least some of the water-insoluble protective coating, while not removing the performance-enhancing coating, whereby some residual amount of protective coating remains.

48. The method of claim 1, wherein the microelectronic device having a sensitive area comprises a wafer having the sensitive area disposed thereon, and further wherein the step of performing at least one packaging step comprises dicing said wafer to form a plurality of individual dies.

49. The method of claim 4, wherein the step of performing at least one packaging step comprises dicing said wafer to form a plurality of individual dies.

\* \* \* \* \*



US005730792A

**United States Patent** [19]**Camilletti et al.**[11] **Patent Number:** **5,730,792**[45] **Date of Patent:** **Mar. 24, 1998**[54] **OPAQUE CERAMIC COATINGS**

5,492,958	2/1996	Haluska et al.	524/439
5,516,596	5/1996	Camilletti et al.	428/698
5,541,248	7/1996	Haluska et al.	524/420
5,635,249	6/1997	Haluska et al.	427/387

[75] **Inventors:** Robert Charles Camilletti; Loren Andrew Haluska; Keith Winton Michael, all of Midland, Mich.

[73] **Assignee:** Dow Corning Corporation, Midland, Mich.

*Primary Examiner*—David Brunnsman  
*Attorney, Agent, or Firm*—Sharon K. Severance

[21] **Appl. No.:** **725,791**[22] **Filed:** **Oct. 4, 1996**[51] **Int. Cl.<sup>6</sup>** ..... **C09D 183/04**[52] **U.S. Cl.** ..... **106/287.14; 427/96; 427/98; 427/99; 327/603; 420/433; 420/434; 420/447**[58] **Field of Search** ..... **106/287.14; 427/96, 427/98, 99; 327/603; 428/433, 434, 447**[56] **References Cited****U.S. PATENT DOCUMENTS**

3,986,997	10/1976	Clark	260/292
4,589,085	8/1987	Plueddemann	106/287
4,756,977	7/1988	Haluska	428/704
5,011,706	4/1991	Tatay	427/39
5,387,480	2/1995	Haluska et al.	428/698
5,399,441	3/1995	Beainger	428/689
5,436,083	7/1995	Haluska et al.	428/688
5,436,084	7/1995	Haluska	428/688
5,458,912	10/1995	Camilletti et al.	427/1264

[57] **ABSTRACT**

Thick opaque ceramic coatings are used to protect delicate microelectronic devices against excited energy sources, radiation, light, abrasion, and wet etching techniques. The thick opaque ceramic coating are prepared from a mixture containing tungsten carbide (WC), tungsten metal (W), and phosphoric anhydride, i.e., phosphorous pentoxide (P<sub>2</sub>O<sub>5</sub>), carried in an aqueous alkanol dispersion of colloidal silica and partial condensate of methylsilanetriol. The coating is pyrolyzed to form a ceramic SiO<sub>2</sub> containing coating. A second coating of plasma enhanced chemical vapor deposited (PECVD) silicon carbide (SiC), diamond, or silicon nitride (Si<sub>3</sub>N<sub>4</sub>), can be applied over the thick opaque ceramic coating to provide hermeticity. These coatings are useful on patterned wafers, electronic devices, and electronic substrates. The thick opaque ceramic coating is unique because the methyl silsesquioxane resin is resistant to etching using wet chemicals, i.e., acids such as H<sub>3</sub>PO<sub>4</sub> and H<sub>2</sub>SO<sub>4</sub>, or bases.

**23 Claims, No Drawings**

## OPAQUE CERAMIC COATINGS

## BACKGROUND OF THE INVENTION

This invention is directed to a method of forming coatings using compositions containing a methyl silsesquioxane resin, colloidal silica, and certain other opaque materials and/or obstructing agents. These protective coatings are useful on a variety of substrates, but especially electronic substrates.

The use of hydrogen silsesquioxane resin ( $\text{HSiO}_{3/2}$ )<sub>n</sub> derived ceramic coatings on substrates such as electronic devices is known. Thus, U.S. Pat. No. 4,756,977 (Jul. 12, 1988), discloses a process of forming a silica coating on an electronic substrate. According to the process, a solution of hydrogen silsesquioxane resin is applied to a substrate, followed by heating the coated substrate in air at a temperature in the range of 200°–1,000° C. The '977 patent, however, does not teach the use of opaque materials or obstructing agents within the coating, nor is the ( $\text{HSiO}_{3/2}$ )<sub>n</sub> resin derived ceramic coatings on the substrate taught to be resistant to wet etching techniques.

The use of silica within a protective coating is known. Thus, U.S. Pat. No. 3,986,997 (Oct. 19, 1976), describes a coating composition containing an acidic dispersion of colloidal silica, and partial condensate of methylsilanetriol in an alcohol-water medium. The coating composition can be used to apply transparent abrasion resistant coatings on a variety of substrates.

The '977 patent, however, does not describe the use of tungsten carbide, tungsten metal, or phosphoric anhydride, as an opaque material or obstructing agent; it does not describe applying the coating on an electronic substrate for the purpose of providing resistance to wet etching; nor does it describe pyrolysis of the coating at the high temperatures (i.e., 400° C. to 1,000° C.) as contemplated herein.

Accordingly, what we have discovered is that useful coatings can be formed from compositions containing colloidal silica and partial condensate of methylsilanetriol, and certain other additional opaque materials or obstructing agents; and that these coatings provide protection and resistance against various intrusion techniques, especially wet etching.

## BRIEF SUMMARY OF THE INVENTION

Our invention relates to a method of forming a coating on a substrate and to substrates coated thereby. The method comprises applying a coating composition containing an opaque material or obstructing agent carried in an aqueous alkaloid dispersion of colloidal silica and partial condensate of methylsilanetriol on the substrate. The coated substrate is then heated at a temperature sufficient to convert (pyrolyze) the coating composition to a ceramic coating. The method is especially valuable for forming protective coatings on a variety of electronic devices.

Our invention also relates to the coating composition containing an opaque material or obstructing agent carried in an aqueous alkaloid dispersion of colloidal silica and partial condensate of methylsilanetriol.

These and other features and objects of our invention will become apparent from a consideration of the detailed description.

## DETAILED DESCRIPTION

Our invention is concerned with preparation of a thick opaque protective ceramic coating that is effective against

various forms of energy, and which contains a solid reactive material that is a deterrent for preventing examination of an integrated circuit. The coating is effective against ozone, UV-ozone, gaseous free radicals and ions, any vapor or liquid borne reactive species, or plasmas. In addition, the coating is resistant to abrasion and is opaque to radiation and light.

The coating contains a combination of colloidal silica and partial condensate of methylsilanetriol, which is more resistant to being wet chemically etched with either an acid or a base, because it presents a surface that is more hydrophobic than a hydrogen silsesquioxane resin. This enhances the tamper-proof qualities of the coating. The coating may contain solid  $\text{P}_2\text{O}_5$  which further obstructs and acts as a deterrent to any attack by wet etching techniques. It functions in this capacity by generating phosphoric acid that would readily destroy the integrated circuit and its memory.

One embodiment of the coating is prepared from a combination of colloidal silica and partial condensate of methylsilanetriol, tungsten carbide (WC), tungsten metal (W) and solid  $\text{P}_2\text{O}_5$ . These components of the coating composition provide protection for any microelectronic device, and are useful for application on gallium arsenide (GaAs), silicon, metallic, or other electronic substrates, devices, or patterned wafers. If desired, a second hermetic coating, such as PECVD silicon carbide, diamond, or silicon nitride, can be applied to provide hermeticity.

As used herein, the expression "ceramic coating" is intended to describe a hard coating obtained after heating or pyrolyzing the coating composition. The ceramic coating may contain both amorphous silica ( $\text{SiO}_2$ ) materials, as well as amorphous silica-like materials that are not fully free of residual carbon and silanol ( $\text{SiOH}$ ), which are obtained upon heating the coating composition.

The expression "electronic device" is meant to include electronic substrates or electronic circuits such as silicon-based devices, gallium arsenide based devices, focal plane arrays, opto-electronic devices, photovoltaic cells, and optical devices.

In our process, a ceramic coating is formed on a substrate by applying a coating composition base containing a combination of colloidal silica and partial condensate of methylsilanetriol onto the substrate, and then heating and pyrolyzing the coated substrate at a temperature sufficient to convert the coating composition to a ceramic  $\text{SiO}_2$  containing coating.

One suitable coating composition base and method for its preparation is described in U.S. Pat. No. 3,986,997 (Oct. 19, 1976), incorporated herein by reference. This coating composition is a dispersion containing colloidal silica and a partial condensate of methylsilanetriol.

The silica component of the coating composition is present as an aqueous colloidal silica dispersion having a particle diameter of 5–150 millimicrons (nanometers). The partial condensate component of the coating composition is predominately derived from methylsilanetriol, but may contain other silanols of the formula  $\text{RSi(OH)}_3$ , in which R is an alkyl radical of 2 or 3 carbon atoms, the vinyl radical  $\text{CH}_2=\text{CH}-$ , the 3,3,3-trifluoropropyl radical  $\text{CF}_3\text{CH}_2\text{CH}_2-$ , the 3-glycidioxypropyl radical, or the 3-methacryloxypropyl radical  $\text{CH}_2=\text{C}(\text{CH}_3)\text{COOCH}_2\text{CH}_2\text{CH}_2-$ . At least 70 weight percent of the silanol is  $\text{CH}_3\text{Si(OH)}_3$ .

Preferably, the coating composition contains 10–50 weight percent solids, with the distribution being 10–70 weight percent colloidal silica and 30–90 weight percent of

the siloxanol. The siloxanol is carried in a lower aliphatic alcohol-water solvent, i.e., methanol, ethanol, isopropanol, n-butyl alcohol, or mixtures thereof.

The coating composition is prepared by adding a trialkoxysilane  $RSi(OR)_3$  to a colloidal silica hydrosol, and adjusting the pH to 3-6 with an organic acid such as acetic acid. Trisilanols are generated in situ by adding the trialkoxysilane to the acidic aqueous dispersion of colloidal silica. Upon generation of the silanol in the acidic aqueous medium, there occurs a partial condensation of hydroxyl substituents to form  $Si-O-Si$  bonding. Alcohol is also generated by hydrolysis of the alkoxy substituents of the silane. Depending upon the percent solids desired, additional alcohol, water, or water-miscible solvent can be added, to adjust the level of solids in the coating composition. This coating composition is a clear or slightly hazy low viscosity fluid which is stable for several days, but condensation of  $SiOH$  will continue at a very slow rate, and the coating composition eventually forms a gel structure.

What differentiates our invention from that described in the '997 patent (Clark), is that in our invention, at 400° C. the methyl groups on  $CH_3SiO_{1.5}$  are oxidized to form  $SiO_2$ . The oxidation may not be complete, however, due to the thickness of the coating composition, so that some methyl groups on silicon will remain. In Clark, by contrast, all of the methyl groups remain on silicon, and curing of the resin in Clark occurs through a condensation of the silanol and methoxy groups at temperatures in the range of 50°-150° C. By comparison, therefore, Clark employs a condensation cure, while in our invention, we utilize oxidation and thermal rearrangement, although some condensation may occur during the period of heating to reach 400° C.

If desired, the coating composition according to our invention may contain other ceramic oxide precursors, examples of which are compounds of various metals such as aluminum, titanium, zirconium, tantalum, niobium, or vanadium; and non-metallic compounds such as boron or phosphorus; any of which may be dissolved in solution, hydrolyzed, and subsequently pyrolyzed to form ceramic oxide coatings.

These ceramic oxide precursor compounds generally have one or more hydrolyzable groups bonded to the metal or non-metal depending on the valence of the metal. The number of hydrolyzable groups included in such compounds is not critical provided the compound is soluble in the solvent. Likewise, selection of an exact hydrolyzable substituent is not critical since it will be either hydrolyzed or pyrolyzed out of the system.

Typical hydrolyzable substituents include alkoxy groups such as methoxy, propoxy, butoxy and hexoxy; acyloxy groups such as acetoxy; and other organic groups bonded to the metal or non-metal through an oxygen atom such as acetylacetonate. Some specific compounds that can be used are zirconium tetracetylacetonate, titanium dibutoxy diacetylacetonate, aluminum triacetylacetonate, and tetra-butoxy titanium.

When the coating composition is combined with one of these ceramic oxide precursors, generally it is used in an amount such that the final ceramic coating contains 0.1-30 percent by weight of the modifying ceramic oxide precursor.

Our coating composition may contain a platinum, rhodium, or copper catalyst, to increase the rate and extent of conversion of the precursors to silica. Generally, any platinum, rhodium, or copper compound or complex which can be solubilized is appropriate, such as platinum acetylacetonate, rhodium catalyst  $RhCl_3 \cdot 3S$

$(CH_3CH_2CH_2CH_3)_2$ , a product of Dow Corning Corporation, Midland, Mich., or cupric naphthenate. These catalysts can be added in amounts of 5 to 1,000 parts per million of platinum, rhodium, or copper, based on the weight of the methyl silsesquioxane resin.

Our coating composition may also contain other opaque materials or obstructing agents, in addition to tungsten, tungsten carbide, and  $P_2O_5$ . For purposes herein, the terms opaque material or obstructing agent are used synonymously to describe a finely divided solid phase, which is distributed within the resin and the final ceramic coating, and which tends to (i) obstruct inspection, (ii) hinder inspection, or (iii) prevent reverse engineering of the device.

Specific materials useful in the instant invention include, but are not limited to, optically opaque materials, radiopaque materials, luminescent materials, oxidizing materials, abrasion resistant materials, magnetic materials, and conductive materials. Various inorganic and organic types of materials can be used in a variety of morphologies, including but not limited to, powders, particles, flakes, and microballoons.

Optically opaque materials are agents that when mixed with the preceramic silicon-containing material, render the resulting coating impenetrable to visual light. Optically opaque materials include but are not limited to, oxides, nitrides and carbides of silicon, alumina, metals, and inorganic pigments. Some preferred optically opaque materials are plasma alumina microballoons having an average particle size of about 6 microns, silica microballoons having an average particle size of about 5-40 microns, silicon nitride ( $Si_3N_4$ ) powder or whiskers; silicon carbide (SiC) powder or whiskers, aluminum nitride (AlN) powder, and black inorganic pigments such as black Ferro® F6331 having an average particle size of about 0.4 microns.

Radiopaque materials are agents that when mixed with the preceramic silicon-containing material, render the resulting coating impenetrable to radiation, such as x-rays, UV, IR, and visible light, as well as sound waves. Radiopaque materials include but are not limited to heavy metals such as lead, and insoluble salts of heavy metals such as barium, lead, silver, gold, cadmium, antimony, tin, palladium, strontium, and bismuth. The salts can include for example, carbonates, sulfates, and oxides.

Luminescent materials are agents that when mixed with the preceramic silicon-containing material, result in a coating that will absorb energy and emit electromagnetic radiation in excess of thermal radiation. These materials are typically phosphors such as sulfides (i.e., zinc sulfide and cadmium sulfide); selenides; sulfoselenides; oxyfluorides; oxygen dominate phosphors such as borates, aluminates, gallates, and silicates; and halide phosphors such as alkali metal halides, alkaline earth halides, and oxyhalides. Preferred are sulfides, and most preferred is zinc sulfide. The phosphor compound may be doped with an activator. Activators include, but are not limited to manganese, silver, and copper; and rare earth ions in the form of halides. The activator is generally present in amounts of about 0.1-10 mol percent based on the weight of the phosphor.

Abrasion resistant materials are agents that when mixed with the preceramic silicon-containing material, render the resulting coating impenetrable to removal by frictional means such as scraping. Abrasion resistant materials are exemplified by, but not limited to diamond, diamond dust, titanium nitride (TiN), tantalum carbide (TaC), and fibers of graphite, KEVLAR® (a DuPont trademark for aromatic polyamide fibers), NEXTEL® (a trademark of the 3M Company for boron-modified alumina-silica fibers), and aluminum oxide ( $Al_2O_3$ ).

Energy resistant materials are agents that when mixed with the preceramic silicon-containing material, react with energy sources such as ozone, UV-ozone, gaseous free radicals and ions, any vapor or liquid borne reactive species, and plasmas, to effectively cause degradation of the circuit and the memory. Energy resistant materials are exemplified by, but not limited to heavy metals such as lead, tungsten, tantalum, and antimony.

Magnetic materials are agents that when mixed with the preceramic silicon-containing material, render the resulting coating magnetic (i.e., magnetized by a magnetic field having a net magnetic moment). Magnetic materials are exemplified by carbon alloy ferrites, iron carbonyl, and alloys of metals such as iron, manganese, cobalt, nickel, copper, titanium, vanadium, molybdenum, magnesium, aluminum, chromium, zirconium, lead, and zinc. Some specific agents are  $\text{Fe}_3\text{O}_4$ ,  $\text{MnZn}$ ,  $\text{NiZn}$ , and  $\text{CuZn}$ .

Conductive materials are agents that when mixed with the preceramic silicon-containing material, render the resulting coating either electrically or thermally conductive. Conductive materials are exemplified by gold, silver, copper, aluminum, nickel, zinc, chromium, cobalt, and diamond.

Other opaque materials or obstructing agents useful herein include synthetic and natural materials such as oxides, nitrides, borides, and carbides of various metals and non-metals such as glass, phosphorous oxynitride (PON), alumina, titanium dioxide, zinc oxide, zirconium oxide ( $\text{ZrO}_2$ ), and ruthenium oxide ( $\text{RuO}_2$ ); titanates such as potassium titanate and barium titanate; niobates such as lithium niobate ( $\text{LiNbO}_3$ ) and lead niobate ( $\text{Pb}(\text{NbO}_3)_2$ ); barium sulfate; calcium carbonate; precipitated diatomite; aluminum silicate or other silicates; pigments and dyes such as crystal violet ( $\text{C}_{25}\text{H}_{20}\text{N}_4\text{Cl}$ ) and the cyanines; phosphors; metals such as silver, aluminum, or copper; wollastonite ( $\text{CaSiO}_3$ ); mica; kaolin; clay; tale; organic materials such as cellulose, polyimides, phenol resins, epoxies, polybenzocyclobutanes; fluorocarbon polymers such as polytetrafluoroethylene ( $\text{C}_2\text{F}_4$ )<sub>n</sub>; vinylidene fluoride  $\text{H}_2\text{C}=\text{CF}_2$ , and hexafluoropropylene  $\text{CF}_3\text{CF}_2\text{CF}_2$ ; high dielectric constant materials such as titanate, niobate, or tungstate salts of metals such as strontium, zirconium, barium, lead, lanthanum, iron, zinc, and magnesium, i.e., barium titanate ( $\text{BaTiO}_3$ ), potassium titanate ( $\text{K}_2\text{TiO}_3$ ), lead niobate, lithium titanate, strontium titanate, barium strontium titanate, lead lanthanum zirconium titanate, lead zirconium titanate, and lead tungstate.

The type of opaque material or obstructing agent employed will depend on the intended use of the coating. Thus, if the coating is to be used as an interlayer dielectric, a material such as alumina is desirable, so that the coating will have a low dielectric constant (DK). If a coating having a high DK is desired, a material such as barium titanate or lead niobate should be employed. If a conductive coating is desired, other types of metals can be added.

The particle size and shape of the opaque material or obstructing agent can vary over a wide range, depending on factors such as type of material and desired thickness of the coating. Our coatings are preferably less than about 500 microns in thickness, so a particle size of about 100 to less than about 500 microns is generally sufficient. A smaller particle size can be used, such as 50–100 microns, or even particle size from submicron (i.e., 5–150 millimicrons) to 10 microns.

The amount of opaque material or obstructing agent can be varied, depending on quality and electrical characteristics desired in the final coating. Generally, the opaque material

or obstructing agent is used in amounts of from one weight percent to less than about 94 weight percent, based on the weight of colloidal silica and partial condensate of methylsilanetriol. Sufficient resin must be employed to insure that enough resin is present to bind the opaque material or obstructing agent. Lesser amounts of opaque material or obstructing agent can also be employed, i.e., 1–5 weight percent.

If desired, the coating composition can contain a silane coupling agent to modify the surface of the opaque material or obstructing agent for better adhesion. Generally, silane coupling agents conform to the formula  $\text{A}_n\text{SiY}_3$ , where A is a monovalent organic radical such as an alkyl group, an aryl group, or a functional group such as methacryl, methacryloxy, epoxy, vinyl, or allyl; Y is a hydrolyzable radical such as an alkoxy group with 1–6 carbon atoms, an alkoxyalkoxy group with 2–8 carbon atoms, or an acetoxy group; and n is 1, 2, or 3, preferably 3.

Some examples of suitable silane coupling agents are 3-methacryloxypropyltrimethoxysilane of the formula  $\text{CH}_2=\text{C}(\text{CH}_3)\text{COO}(\text{CH}_3)_3\text{Si}(\text{OCH}_3)_3$ ; 3-glycidyloxypropyltrimethoxysilane; 3-mercaptopropyltrimethoxysilane of the formula  $\text{HSCH}_2\text{CH}_2\text{CH}_2\text{Si}(\text{OCH}_3)_3$ ; vinyltriethoxysilane of the formula  $\text{CH}_2=\text{CHSi}(\text{OOC}_2\text{H}_5)_3$ ; vinyltri-(2-methoxyethoxy) silane of the formula  $\text{CH}_2=\text{CHSi}(\text{OCH}_2\text{CH}_2\text{OCH}_3)_3$ ; and 2-(3,4-epoxycyclohexyl) ethyltrimethoxysilane. Reference may be to U.S. Pat. No. 4,689,085 (Aug. 25, 1987) for these and other suitable silane coupling agents that are appropriate.

According to our process, the coating composition is applied to the surface of a substrate such as an electronic device. Various facilitating measures such as stirring and heating may be used to dissolve or disperse the opaque material or obstructing agent in the base coating composition, and create a more uniform coating solution. For example, the coating solution can be prepared by mixing the resin, opaque material, or obstructing agent, solvent, and silane coupling agent, with a homogenizer, sonic probe, or colloid mill, to obtain a coating solution suitable for application to the surface of an electronic device.

Solvents which may be used include any agent or mixture of agents which will dissolve or disperse the resin and opaque material, to form a homogeneous liquid mixture without affecting the resultant coating. These solvents can include, for example, alcohols such as ethyl alcohol, isopropyl alcohol, and n-butanol; ketones; esters; and glycol ethers. The solvent should be present in an amount sufficient to dissolve or disperse the materials to the concentration desired for the application. Generally, enough solvent is used to form a 0.1–80 weight percent mixture, but preferably a 1–50 weight percent mixture.

The coating mixture is then coated onto the substrate. The coating composition can be applied by spin coating, dip coating, spray coating, or flow coating. Any other equivalent coating method can also be employed such as by applying the coating composition on a substrate or device by silk screening, screen printing, meniscus coating, or wave solder coating.

The solvent is allowed to evaporate from the coated substrate resulting in deposition of the resin and opaque material containing coating composition. Any means of evaporation may be used such as air drying by exposure to an ambient environment, or by application of vacuum or mild heat (i.e., less than 50° C.) during early stages of the

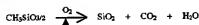


heat treatment. When spin coating is used, any additional drying period is minimized as spinning drives off the solvent to some extent.

Following removal of solvent, the resin and opaque material containing coating composition is converted to a ceramic coating by pyrolysis, i.e., heating it to a sufficient temperature to ceramify. Generally, this temperature is in the range of about 400° C. to about 1,000° C., depending on the pyrolysis atmosphere. Preferred temperatures are in the range of 400° C. to 800° C. Heating is conducted for a time sufficient to ceramify the coating composition. Generally, heating will require one to 6 hours, but typically less than about 3 hours will be adequate.

Heating to ceramify the coating composition may be conducted at atmospheric pressures varying from vacuum to superatmospheric, and under an oxidizing or non-oxidizing gaseous environment such as air, oxygen, an inert gas such as nitrogen, ammonia, an amine, moisture, or nitrous oxide. Heating can be carried out using a convection oven, a rapid thermal process, a hot plate, radiant energy, or microwave energy. The rate of heating is not critical although it is practical to heat the coating composition as rapidly as possible.

Pyrolysis results in removal of organic substituents and their replacement by oxygen. By this method, a ceramic coating is produced on the substrate, generally according to the scenario:



The thickness of the ceramic coating can vary over a wide range, but is typically from 1–500 microns. These ceramic coatings are able to smooth irregular surfaces of various substrates. The coatings are (i) relatively defect free, (ii) have excellent adhesive properties, and (iii) have a variety of electrical properties. I.e., DK's less than four and up to conductive coatings. As such, such coatings are particularly useful for electronic applications such as dielectric layers, protective layers, and conductive layers.

If desired, additional coatings may be applied over the ceramic coating. These additional coatings include SiO<sub>2</sub> coatings, SiO<sub>2</sub>/ceramic oxide layers, silicon-containing coatings, silicon carbon containing coatings, silicon nitrogen containing coatings, silicon oxygen nitrogen containing coatings, silicon nitrogen carbon containing coatings, and diamond-like carbon coatings. Methods for applying such coatings are described in U.S. Pat. No. 4,756,577, referred to previously. An especially preferred additional coating is silicon carbide.

The method of applying an additional coating such as silicon carbide is not critical, and such coatings can be applied by any chemical vapor deposition technique such as thermal chemical vapor deposition (TCVD), photochemical vapor deposition, plasma enhanced chemical vapor deposition (PECVD), electron cyclotron resonance (ECR), and jet vapor deposition. It could also be applied by physical vapor deposition techniques such as sputtering or electron beam evaporation. These processes involve either the addition of energy in the form of heat or plasma to a vaporized species to cause the desired reaction, or they focus energy on a solid sample of the material to cause its deposition.

For example, in thermal chemical vapor deposition, the coating is deposited by passing a stream of the desired precursor gas over a heated substrate. When the precursor gas contacts the hot surface, it reacts and deposits the

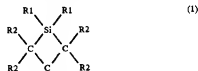
coating. Substrate temperatures in the range of 25° C. to 1,000° C. are sufficient to form these coatings in several minutes to several hours, depending on the precursor gas and the thickness of the coating. Reactive metals can be used in such a process to facilitate deposition.

In PECVD techniques, a precursor gas is reacted by passing it through a plasma field. Reactive species are formed and focused at the substrate where they readily adhere. The advantage of a PECVD process over a thermal CVD process is that in the former, lower substrate and processing temperatures can be used, i.e., 25° C. to 600° C.

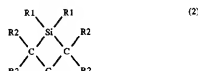
Plasma used in a PECVD process can be energy derived from electric discharges, electromagnetic fields in the radio-frequency or microwave range, lasers, or particle beams. In most plasma deposition processes, it is preferred to use radio frequency (i.e., 10 kHz to 10<sup>9</sup> MHz) or microwave energy (i.e., 0.1–10 GHz or 10<sup>9</sup> hertz) at moderate power densities (i.e., 0.1–5 watts/cm<sup>2</sup>). The frequency, power, and pressure are tailored to the precursor gas and equipment being used.

Some precursor gases that can be used include (1) mixtures of silanes or halosilanes such as trichlorosilane (HSiCl<sub>3</sub>) in the presence of an alkane of 1–6 carbon atoms such as methane, ethane, and propane; (2) an alkylsilane such as methylsilane (CH<sub>3</sub>SiH<sub>3</sub>), dimethylsilane (CH<sub>3</sub>)<sub>2</sub>SiH<sub>2</sub>, trimethylsilane (CH<sub>3</sub>)<sub>3</sub>SiH, and hexamethyldisilane (CH<sub>3</sub>)<sub>2</sub>Si-Si(CH<sub>3</sub>)<sub>2</sub>; or (3) a silacyclobutane or a disilacyclobutane of the type described in U.S. Pat. No. 5,011,706 (Apr. 30, 1991) incorporated by reference.

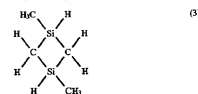
Examples of such silacyclobutanes (1) and disilacyclobutanes (2) are shown below. R1 is hydrogen, fluorine, or a hydrocarbon radical having 1–4 carbon atoms. R2 is hydrogen or a hydrocarbon radical having 1–4 carbon atoms. A preferred disilacyclobutane is 1,3-dimethyl-1,3-disilacyclobutane shown in formula (3).



(1)



(2)



(3)

When silicon carbide is used as a coating layer, it is capable of forming a hermetic and electrical barrier over the surface of the silica-containing ceramic layer on the electronic device, and inhibits damage from chemical and mechanical means.

In a preferred coating composition according to our invention, the matrix resin is colloidal silica and partial condensate of methylsilanetriol. Opaque material or obstructing agents for the coating composition are tungsten

carbide, tungsten, and  $P_2O_5$ . Tungsten metal is the material that functions as an energy barrier. Tungsten metal and tungsten carbide are each effective against radiation and light. Tungsten carbide has a Mohs' hardness rating greater than 9.5, and tungsten metal has a Mohs' hardness of about 6.5–7.5. Tungsten carbide is therefore the more effective against abrasion, although each are included in the coating composition and function to provide abrasion resistance.

Mohs' hardness, it is noted, is a comparison test involving the assignment of a relative number to known materials based on their ability to scratch one another. Some examples of the Mohs' hardness scale which ranks materials from 1–10, are graphite with a Mohs' hardness of 1, manganese with a Mohs' hardness of 5, quartz with a Mohs' hardness of 7, and diamond with a Mohs' hardness of 10.

As noted previously,  $P_2O_5$  protects the integrated circuit and its memory from invasion by wet etching techniques, and the silane coupling agent can be included in the coating composition to improve adhesion of the coating to the electronic device.

Following is an example illustrating our invention in terms of the method for the preparation of a coating composition containing (WC), (W), and ( $P_2O_5$ ).

#### EXAMPLE I

The materials listed below were mixed in a container for four periods of twenty seconds with a sonic probe to prepare a solution useful as a coating composition.

Amount	Component
1.0 g	Aqueous alkaline dispersion of colloidal silica and partial condensate of methylsilanetriol
15.0 g	Tungsten Carbide (WC) 0.83 $\mu$ m average particle diameter
3.0 g	Tungsten Metal (W) 0.6–0.9 $\mu$ m average particle diameter
0.08 g	$P_2O_5$ powder
0.4 g	3-glycidyloxypropyltrimethoxysilane
1.0 g	Isopropyl alcohol
20.48 g	Total

The resin component of this coating composition was a solution prepared generally according to the procedure set forth in Example 1 of U.S. Pat. No. 3,986,997. This component contained 31 percent solids, 40 percent of which was  $SiO_2$  and 60 percent partial condensate of  $CH_3Si(OH)_3$ . The remaining 69 percent of the resin component was a mixture containing water, acetic acid, isopropanol, and n-butanol.

A 4.5 inch square alumina panel with a thickness of 40 mils was coated with the solution using a 2 mil drawdown bar. The coated alumina panel was allowed to air dry for 50 minutes. The coating was then pyrolyzed at 400° C. for one hour in air. The coating was examined with a microscope under 1000 $\times$  magnification and no cracks were observable. The thickness of the coating was 7.2  $\mu$ m. The coating had a pencil hardness of 6H, a Vickers hardness of 633 N/mm<sup>2</sup>, and a modulus of 236 GPa (1 e giga or 10<sup>9</sup> Pascals).

The pencil test used to measure the hardness of the coating is a standard qualitative method of determining scratch resistance of coatings. According to the test procedure, a coated panel is placed on a firm horizontal surface. A pencil is held firmly against the coated film at a 45° angle pointing away from the technician conducting the test. It is pushed away by the technician in one-quarter inch (6.5 mm) strokes. The technician starts the process with the

hardest lead pencil, i.e., 9H, and continues down the scale of pencil hardness, i.e., 6B, to the pencil that will not cut into or gouge the film. The hardest pencil that will not cut through the film to the substrate for a distance of at least one-eighth of an inch (3 mm) is recorded, using the Bercel scale, i.e., Bercel Corporation, Brentwood, Tenn.:

6B, 5B, 4B, 3B, 2B, B, HB, F, H, 2H, 3H, 4H, 5H, 6H, 7H, 8H, 9H (softest)  $\rightarrow$  (hardest)

The Vickers test used in our evaluation of the coating is a measure of the resistance of a material to deformation. The test procedure is described in the American Society for Testing and Materials, Philadelphia, Pa., (ASTM) Standard Number E92. According to the test procedure, a pyramidal diamond is used as an indenter. The test is conducted using a flat specimen on which the indenter is hydraulically loaded. When the prescribed number of indentations have been made, the specimen is removed, the diagonals of the indentations are measured using a calibrated microscope, and then the values are averaged. A Vickers hardness number (VHN) can be calculated, or the VHN can be taken from a precalculated table of indentation size versus Vickers Hardness Numbers. The Vickers scale for VHN ranges from a low value of 100 which is a measure of the softest, to a high value of 900 which is a measure of the hardest.

Coating compositions most suitable for use according to our invention should contain 0.05–20 percent by weight of the combination of colloidal silica and partial condensate of methylsilanetriol, 5–30 percent by weight of tungsten metal, 30–80 percent by weight of tungsten carbide, 0.1–5 percent by weight of phosphoric anhydride, and 1–5 percent by weight of a silane coupling agent; the remainder of the coating composition being the solvent(s).

The amount of tungsten carbide can be varied from 1–91 volume percent. The amount of tungsten metal can also be varied from 1–91 volume percent minus the volume percent of tungsten carbide. In addition, the amount of phosphoric anhydride can be varied from 1–30 volume percent, minus the combined volume percent of tungsten carbide and tungsten metal.

Other variations may be made in the compounds, compositions, and methods described herein without departing from the essential features of our invention. The forms of our invention are exemplary only and not intended as limitations on its scope which is defined in the claims.

We claim:

1. A method of forming a coating on an electronic device comprising applying to a surface of the electronic device a coating composition containing an opaque material carried in an aqueous alkaline dispersion of colloidal silica and partial condensate of methylsilanetriol, and pyrolyzing the coating composition on the surface of the electronic device at a temperature in the range of 400° C. to 1,000° C., to convert the coating composition into a ceramic  $SiO_2$  containing coating.

2. A method according to claim 1 wherein the coating composition is applied to the surface of the electronic device by spray coating, dip coating, flow coating, spin coating, silk screening, screen printing, meniscus coating, or wave solder coating.

3. A method according to claim 1 wherein the coated surface of the electronic device is pyrolyzed at a temperature in the range of about 400° C. to about 800° C. for about one hour to less than about 3 hours.

4. A method according to claim 3 wherein the coated surface of the electronic device is pyrolyzed in an environment selected from the group consisting of air, oxygen, oxygen plasma, an inert gas, ammonia, an amine, moisture, and nitrous oxide.

5. A method according to claim 1 wherein the coating composition further comprises a silane coupling agent to modify the surface of the opaque material for better adhesion, the silane coupling agent having the formula  $A_{1-(4-n)}SiY_n$  where A is an alkyl group, an aryl group, or a functional substituent selected from the group consisting of methacryl, methacryloxy, epoxy, vinyl, or allyl; Y is a hydrolyzable radical selected from the group consisting of an alkoxy group with 1-6 carbon atoms, an alkoxyalkoxy group with 2-8 carbon atoms, or an acetoxy group; and n is 1, 2, or 3.

6. A method according to claim 5 wherein the silane coupling agent is selected from the group consisting of 3-methacryloxypropyltrimethoxysilane, 3-glycidoxypropyltrimethoxysilane, 3-mercaptopropyltrimethoxysilane, vinyltriethoxysilane, vinyltriethoxysilane, vinyl-tris(2-methoxyethoxy)silane, and 2-(3,4-epoxycyclohexyl)ethyltrimethoxysilane.

7. A method according to claim 1 wherein the opaque material is tungsten carbide, tungsten metal, or phosphoric anhydride.

8. A method according to claim 1 wherein the opaque material is tungsten carbide, tungsten metal, and phosphoric anhydride.

9. A method according to claim 1 wherein the opaque material is tungsten carbide and tungsten metal.

10. A method according to claim 1 wherein the opaque material is tungsten carbide.

11. A method according to claim 1 wherein the opaque material is tungsten metal.

12. A method according to claim 1 wherein the opaque material is phosphoric anhydride.

13. A method according to claim 1 wherein a second coating of silicon carbide, diamond, or silicon nitride, is applied over the ceramic coating by plasma enhanced chemical vapor deposition.

14. An electronic device coated by the method of claim 13.

15. An electronic device coated by the method of claim 1.

16. A coating composition for electronic devices comprising an opaque material carried in an aqueous alkanol dispersion of colloidal silica and partial condensate of methylsilanetriol, the coating composition having a pH of 3 to 6.

17. A coating composition according to claim 16 wherein the opaque material, colloidal silica, and partial condensate of methylsilanetriol comprise 0.5 to 80 weight percent of the coating composition.

18. A coating composition according to claim 16 further comprising a silane coupling agent of the formula  $A_{1-(4-n)}SiY_n$  where A is an alkyl group, an aryl group, or a functional substituent selected from the group consisting of methacryl, methacryloxy, epoxy, vinyl, or allyl; Y is a hydrolyzable radical selected from the group consisting of an alkoxy group with 1-6 carbon atoms, an alkoxyalkoxy group with 2-8 carbon atoms, or an acetoxy group; and n is 1, 2, or 3.

19. A coating composition according to claim 18 wherein the silane coupling agent is selected from the group consisting of 3-methacryloxypropyltrimethoxysilane, 3-glycidoxypropyltrimethoxysilane, 3-mercaptopropyltrimethoxysilane, vinyltriethoxysilane, vinyltriethoxysilane, vinyl-tris(2-methoxyethoxy)silane, and 2-(3,4-epoxycyclohexyl)ethyltrimethoxysilane.

20. A coating composition according to claim 16 further comprising a solvent selected from the group consisting of ketones, esters, and glycol ethers.

21. A method of protecting an electronic device from damage due to exposure of the device to excited energy sources, radiation, light, abrasion, and against wet etching techniques, comprising applying to a surface of the device the coating composition of claim 16.

22. A method according to claim 21 in which the coating composition is prepared by mixing the opaque material, aqueous alkanol dispersion of colloidal silica, and partial condensate of methylsilanetriol, with a homogenizer, sonic probe, or colloid mill.

23. A method according to claim 22 in which the coating composition is applied to the surface of the electronic device by spin coating, dip coating, spray coating, flow coating, silk screening, screen printing, meniscus coating, or wave solder coating.

\* \* \* \* \*



US006020047A

**United States Patent** [19][11] **Patent Number:** **6,020,047****Everhart**[45] **Date of Patent:** **\*Feb. 1, 2000****[54] POLYMER FILMS HAVING A PRINTED SELF-ASSEMBLING MONOLAYER**[75] Inventor: **Dennis S. Everhart**, Alpharetta, Ga.[73] Assignee: **Kimberly-Clark Worldwide, Inc.**,  
Nenah, Wis.

[\*] Notice: This patent issued on a continued prosecution application filed under 37 CFR 1.53(d), and is subject to the twenty year patent term provisions of 35 U.S.C. 154(a)(2).

[21] Appl. No.: **08/707,456**[22] Filed: **Sep. 4, 1996**[51] Int. Cl.<sup>7</sup> ..... **B32B 3/00**[52] U.S. Cl. .... **428/209; 428/212; 428/403;**  
**428/469; 428/704; 428/901**[58] Field of Search ..... **428/403, 204,**  
**428/212, 704, 901, 469, 476.1, 441; 252/512,**  
**518, 521****[56] References Cited****U.S. PATENT DOCUMENTS**

- Re. 33,581 4/1991 Nicoli et al. .  
 2,905,539 9/1959 Bowerman .  
 3,497,377 2/1970 Allingham .  
 3,641,354 2/1972 De Ment .  
 3,716,359 2/1973 Sheridon .  
 4,011,009 3/1977 Lama et al. .  
 4,173,075 11/1979 Stewart .  
 4,274,706 6/1981 Tangonan .  
 4,312,228 1/1982 Wohljen .  
 4,325,779 4/1982 Rossetti .  
 4,330,175 5/1982 Fujii et al. .  
 4,382,657 5/1983 Lemaître .  
 4,399,686 8/1983 Kindlund et al. .  
 4,477,158 10/1984 Pollock et al. .  
 4,512,848 4/1985 Deckman et al. .  
 4,528,260 7/1985 Kane .  
 4,561,286 12/1985 Sekler et al. .  
 4,562,157 12/1985 Lowe et al. .

(List continued on next page.)

**FOREIGN PATENT DOCUMENTS**

- 0 453 820 10/1991 European Pat. Off. .  
 0 657 737 6/1995 European Pat. Off. .  
 91,05999 5/1991 WIPO .  
 WO 95/12480 5/1995 WIPO .  
 96/20435 8/1996 WIPO .  
 96/33971 10/1996 WIPO .  
 WO 97/07429 2/1997 WIPO .

**OTHER PUBLICATIONS**

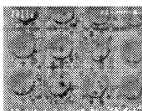
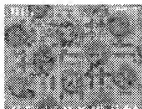
Copy of Search Report for PCT/US97/08522 dated Aug. 8, 1997.

R. Block et al., "Mechanical resonance gas sensors with piezoelectric excitation and detection using PVDF polymer foils", *Sensors and Actuators*, vol. B7, Mar. 1992, pp. 596-601.S.J. Martin, "Sensing liquid properties with thickness-shear mode resonators", *Sensors and Actuators A*, vol. A44, Sep. 1994, pp. 209-218.

(List continued on next page.)

*Primary Examiner*—Merrick Dixon  
*Attorney, Agent, or Firm*—Jones & Askew, LLP**[57] ABSTRACT**

The present invention comprises methods of contact printing of patterned, self-assembling monolayers of alkanethiolates, carboxylic acids, hydroxamic acids, and phosphonic acids on thermoplastic films metallized with an alloy such as nickel/gold, the compositions produced thereby, and the use of these compositions. Patterned self-assembling monolayers allow for the controlled placement of fluids thereon which contain a chemically reactive, indicator functionality. The optical sensing devices produced thereby when the film is exposed to an analyte and light, can produce optical diffraction patterns which differ depending on the reaction of the self-assembling monolayer with the analyte of interest. The light can be in the visible spectrum, and be either reflected from the film, or transmitted through it, and the analyte can be any compound reacting with the fluid on the self-assembling monolayer. The present invention also provides a flexible support for a self-assembling monolayer on a metal alloy.

**17 Claims, 5 Drawing Sheets**

## U.S. PATENT DOCUMENTS

- 4,582,566 4/1986 Grey .  
 4,587,213 5/1986 Molecki .  
 4,596,697 6/1986 Ballato .  
 4,690,715 9/1987 Allara et al .  
 4,728,591 3/1988 Clark et al .  
 4,731,155 3/1988 Napoli et al .  
 4,802,951 2/1989 Clark et al .  
 4,818,336 4/1989 Rossetti .  
 4,837,715 6/1989 Ungsiyakul et al .  
 4,842,633 6/1989 Kuribayashi et al .  
 4,844,613 7/1989 Batchelder et al .  
 4,851,816 7/1989 Macias et al .  
 4,868,034 9/1989 Steinberg ..... 428/403  
 4,877,747 10/1989 Stewart .  
 4,895,017 1/1990 Pyke et al .  
 4,897,325 1/1990 Akkapeddi et al .  
 4,983,436 1/1991 Bailey ..... 428/40  
 4,992,385 2/1991 Godfrey ..... 436/525  
 4,999,489 3/1991 Huggins .  
 5,018,829 5/1991 Ogawa .  
 5,020,879 6/1991 Kazuta et al .  
 5,023,053 6/1991 Finlan .  
 5,032,216 7/1991 Felten .  
 5,035,863 7/1991 Finlan et al .  
 5,055,265 10/1991 Finlan .  
 5,063,081 11/1991 Cozzette et al .  
 5,064,619 11/1991 Finlan .  
 5,076,094 12/1991 Frye et al .  
 5,079,600 1/1992 Schuur et al .  
 5,143,854 9/1992 Pirrung et al .  
 5,182,135 1/1993 Giesecke et al . ..... 427/98  
 5,189,902 3/1993 Groeninger .  
 5,202,227 4/1993 Matsuda et al .  
 5,235,238 8/1993 Nomura et al .  
 5,242,828 9/1993 Bergström et al .  
 5,255,273 10/1993 Nilsson et al .  
 5,259,926 11/1993 Kuwabara et al .  
 5,268,306 12/1993 Berger et al .  
 5,294,369 3/1994 Shigekawa et al .  
 5,315,436 5/1994 Lowenhan et al .  
 5,327,225 7/1994 Bader et al . ..... 356/445  
 5,334,303 8/1994 Muramatsu et al .  
 5,374,563 12/1994 Maule .  
 5,402,075 3/1995 Lu et al .  
 5,404,756 4/1995 Briggs et al .  
 5,415,842 5/1995 Maule .  
 5,418,136 5/1995 Miller et al .  
 5,436,161 7/1995 Bergström et al .  
 5,451,683 9/1995 Barrett et al .  
 5,455,475 10/1995 Josse et al .  
 5,468,606 11/1995 Bogart et al .  
 5,474,884 12/1995 Okazaki ..... 430/533  
 5,482,830 1/1996 Bogart et al .  
 5,482,867 1/1996 Barrett et al .  
 5,489,678 2/1996 Fodor et al .  
 5,512,131 4/1996 Kumar et al .  
 5,514,559 5/1996 Markert-Hahn et al .  
 5,527,711 6/1996 Ton-Moy et al .  
 5,554,541 9/1996 Malmqvist et al .  
 5,620,850 4/1997 Bamdad et al .  
 5,643,681 7/1997 Voohees et al .  
 5,658,443 8/1997 Yamamoto et al .
- Diamandis, EP et al., *Clin. Chem.*, vol. 37(5), 1991, pp. 625-633.  
 Bhatia, S.K. et al., 1992, *J. Am. Chem. Soc.*, vol. 114, p. 4432.  
 Bhatia, S.K. et al., *Analytical Biochem.*, vol. 208, pp. 197-205, 1993.  
 Häussling, L. et al., *Angew. Chem. Int. Ed. Engl.*, vol. 30, No. 5, 1991, pp. 569-572.  
 Larsen N.B. et al., "Order in Microcontact Printed Self-Assembled Monolayers", *J. Am. Chem. Soc.* vol. 119, pp. 3017-3026, 1997.  
 Abstract: 120:231703CA, "Scanning Probe Lithography.2. Selective Chemical Vapor Deposition of Copper into Scanning Tunneling Microscope-Defined Patterns", Schoer, Jonathan et al.  
 Abstract: Japan, JP2165933, (Seiko Epson Corp.), "Manufacture of Microlens Array", Jun. 26, 1990.  
 Abstract: Japan, JP2140702, (Fujitsu Ltd.), "Rotary Variable Focal Mirror", May 30, 1990.  
 Abstract: Japan, JP2210302, (Hamamatsu Photonics KK), "Focal Distance Variable Mirror", Aug. 21, 1990.  
 Abstract: Japan, 58-150148, (Toshiba Corp.), Sep. 6, 1983.  
 Moffat, T.P., et al., "Patterned Metal Electrodeposition Using an Alkanethiolate Mask", *J. Electrochem. Soc.*, vol. 142, No. 11, pp. 220-221 (Nov. 1995).  
 Dobisz, Elizabeth, A., et al., "Self-Assembled Monolayer Films for Nanofabrication", *Mat. Res. Soc. Symp. Proc.*, vol. 380, pp. 23-33 (1995).  
 Kim, Enoch, et al., "Combining Patterned Self-Assembled Monolayers of Alkanethiolates of Gold with Anisotropic Etching of Silicon to Generate Controlled Surface Morphologies", *J. Electrochem. Soc.*, vol. 142, No. 2, pp. 628-633 (Feb. 1995).  
 Laibinis, Paul, E., et al., "Comparison of the Structures and Wetting Properties of Self-Assembled Monolayers on n-Alkanethiols on the Coinage Metal Surfaces, Cu, Ag, Au", *Amer. Chem. Soc.*, vol. 113, No. 19, pp. 7152-7167 (1991).  
 Lopez, Gabriel P., et al., "Convenient Methods for Patterning the Adhesion of Mammalian Cells to Surfaces Using Self-Assembled Monolayers of Alkanethiolates on Gold", *Amer. Chem. Soc.*, vol. 115, No. 13, pp. 5877-5878 (1993).  
 Dulcey, Charles, S., et al., "Deep UV Photochemistry of Chemisorbed Monolayers: Patterned Coplanar Molecular Assemblies", *Science*, vol. 252, pp. 551-554 (Apr. 1991).  
 Jacobsen, S.C., et al., "Design, Analysis, and Experimental Results for the Wobble Motor: an Eccentric-Motion Electrostatic Microactuator", *Proc. Eng. Optim.*, vol. 1167, pp. 122-136 (1989).  
 Matsuda, T., et al., "Development of Micropatterning Technology for Cultured Cells", *Trans. Am. Soc. Artif. Int. Organs*, vol. XXXV, pp. 559-562 (1990).  
 Singhvi, Rahul, et al., "Engineering Cell Shape and Function", *Science*, vol. 264, pp. 696-698 (Apr. 1994).  
 Jacobsen, Stephen, C., et al., "Fabrication of Micro-Structures Using Non-Planar Lithography (NPL)", *Ctr. for Eng. Design*, 6 pages.  
 Westermark, Bengt, "Growth Control in Miniclones of Human Glial Cells", *Exp. Cell Res.*, vol. 111, pp. 295-299 (1978).  
 Lopez, Gabriel, P., et al., "Imaging of Features on Surfaces by Condensation Figures", *Science*, vol. 260, pp. 647-649 (Apr. 1993).

## OTHER PUBLICATIONS

- Abstract of EP 0 453 820 dated Oct. 30, 1991.  
 Muller, W. et al., *Science*, vol. 262, Dec. 10, 1993, pp. 1706-1708.  
 Jenneane, J. et al., *Can. J. Chem.* vol. 74, 1996, pp. 2509-2517.

- Parikh, Atul, N., et al., "An Intrinsic Relationship between Molecular Structure in Self-Assembled *n*-Alkylsiloxane Monolayers and Deposition Temperature", *J. Phys. Chem.*, vol. 98, No. 31, pp. 7577-7590 (1994).
- Ireland, G.W., et al., "Limitation of Substratum Size Alters Cytoskeletal Organization and Behavior of Swiss 3T3 Fibroblasts", *Cell Biol. Int.*, vol. 13, No. 9, pp. 781-790 (Sep. 1989).
- Abbott, Nicholas, L., "Manipulation of the Wettability of Surfaces on the 0.1-to-1-Micrometer Scale Through Micromachining and Molecular Self-Assembly", *Science*, vol. 257, pp. 1380-1382 (Sep. 1992).
- Brilland, Stephen, et al., "Micropatterned Substratum Adhesiveness: A Model for Morphogenetic Cues Controlling Cell Behavior", *Exp. Cell Res.*, vol. 198, pp. 124-129 (1992).
- Molecular Recognition at Self-Assembled Monolayers: Optimization of Surface Functionalization, *J. Chem. Phys.*, vol. 99, No. 9, pp. 7012-7019 (Nov. 1993).
- Vango, Terrence, G., "Monolayer Chemical Lithography and Characterization of Fluoropolymer Films", *Langmuir*, vol. 8, No. 1, pp. 130-134 (1992).
- O'Neill, Charles, et al., "Narrow Linear Strips of Adhesive Substratum are Powerful Inducers of Both Growth and Total Focal Contact Area", *Cell Science*, vol. 95, pp. 577-586 (1990).
- Kumar, Amit, et al., "Patterning Self-Assembled Monolayers: Applications in Materials Science", *Langmuir*, vol. 10, pp. 1498-1511 (1994).
- Abbott, Nicholas, L., et al., "Potential-Dependent Wetting Aqueous Solutions on Self-Assembled Monolayers Formed from 15-(Ferrocenylcarbonyl) pentadecanethiol on Gold", *Langmuir*, vol. 10, No. 5, pp. 1493-1497 (1994).
- Ponten, Jan, et al., "Proliferation Control in Cloned Normal and Malignant Human Cells", *Exp. Cell Res.*, vol. 129, pp. 367-375 (1980).
- McGovern, Mark, E., et al., "Role of Solvent on the Silanization of Glass with Octadecyltrichlorosilane", *Langmuir*, vol. 10, No. 10, pp. 3607-3614 (1994).
- Article: Cromie, William J., "Self-Assembling Molecules Manipulated by Chemists", pp. 1-30.
- Tiborio, R.C., et al., "Self-Assembled Monolayer Electron Beam Resist on GaAs", *Amer. Inst. Phys.*, (Feb. 1993).
- Biebuyck, Hans, A., et al., "Self-Organization of Organic Liquids on Patterned Self-Assembled Monolayers of Alkanethiols on Gold", *Langmuir*, vol. 10, No. 8, pp. 2790-2793 (1994).
- Huber, M.C.E., et al., "Toroidal Grating Obtained on an Elastic Substrate", *Applied Optics*, vol. 20, No. 12, pp. 2139-2142 (Jun. 1981).
- Gorman, Christopher, B., et al., "Use of a Patterned Self-Assembled Monolayer to Control the Formation of a Liquid Resist Pattern on a Gold Surface", *Chem. Mater.*, vol. 7, No. 2, pp. 252-254 (1995).
- Kumar, Amit, et al., "The Use of Self-Assembled Monolayers and a Selective Etch to Generate Patterned Gold Features", *Am. Chem. Soc.*, pp. 9188-9189 (1992).
- Tarlov, Michael J., et al., "UV Photopatterning of Alkanethiolate Monolayers Self-Assembled on Gold and Silver", *J. Am. Chem. Soc.*, vol. 115, No. 12, pp. 5305-5306 (1993).
- Whitesides, George, M., et al., "Wet Chemical Approaches to the Characterization of Organic Surfaces: Self Assembled Monolayers, Wetting, and the Physical-Organic Chemistry of the Solid-Liquid Interface", *Langmuir*, vol. 6, pp. 87-96 (1990).
- Jacobsen, S.C., et al., "The Wobble Motor: Design, Fabrication and Testing of an Eccentric-Motion Electrostatic Micromechanism", *IEEE*, vol. 8, pp. 1536-1546 (1989).
- Wilbur, James L., et al., "Microfabrication by Microcontact Printing of Self-Assembled Monolayers", *Adv. Mater.*, vol. 6, No. 7/8, pp. 600-604 (1994).
- Gorman, Christopher, B., et al., "Fabrication of Patterned, Electrically Conducting Polypyrrole Using a Self-Assembled Monolayer: A Route to All-Organic Circuits", *Chem. Mater.*, vol. 7, No. 3, pp. 526-529 (1995).
- Abbott, Nicholas, L., et al., "Active Control of Wetting Using Applied Electrical Potentials and Self-Assembled Monolayers", *Langmuir*, vol. 11, pp. 16-19 (1995).
- Gorman, Christopher, B., et al., "Control of the Shape of Liquid Lenses on a Modified Gold Surface Using an Applied Electrical Potential Across a Self-Assembled Monolayer", *Langmuir*, vol. 11, No. 6, pp. 2242-2246 (1995).
- Calvert, Jeffrey M., et al., "Deep Ultraviolet Patterning of Monolayer Films for High Resolution Lithography", *J. Vac. Sci. Techn.*, vol. 9, No. 6, pp. 3447-3450 (Nov/Dec. 1991).
- Calvert, Jeffrey M., et al., "New Surface Imaging Techniques for Sub-0.5 Micrometer Optical Lithography", *Solid State Tech.*, pp. 77-82 (Oct. 1991).
- Calvert, Jeffrey, M., "Deep Ultraviolet Lithography of Monolayer Films with Selective Electroless Metalization", *J. Electrochem. Soc.*, vol. 139, No. 6, pp. 1677-1681 (Jun. 1992).
- Bhatia, Suresh, K., et al., "Fabrication of Surfaces Resistant to Protein Adsorption and Application to Two-Dimensional Protein Patterning", *Biochem.*, vol. 208, pp. 197-205 (1993).
- Stenger, David A., et al., "Coplanar Molecular Assemblies of Amino- and Perfluorinated Alkylsilanes: Characterization and Geometric Definition of Mammalian Cell Adhesion and Growth", *J. Am. Chem. Soc.*, vol. 114, pp. 8435-8442 (1992).
- Dressick, Walter, J., et al., "Photopatterning and Selective Electroless Metalization of Surface-Attached Ligands", *Chem. Mater.*, vol. 3, pp. 149-150 (1993).
- Koloski, Timothy, S., et al., "Nucleophilic Displacement Reactions at Benzyl Halide Self-Assembled Monolayer Film Surfaces", *Langmuir*, vol. 10, No. 9, pp. 3122-3133 (1994).
- Potochnik, Stephen, J., et al., "Selective Copper Chemical Vapor Deposition Using Pd-Activated Organosilane Films", *Langmuir*, vol. 11, No. 6, pp. 1841-1845 (1995).
- Hartney M. A., et al., "Silylation of Focused Ion Beam Exposed Resists", *Appl. Phys. Lett.*, vol. 59, No. 4, pp. 485-487 (Jul. 1991).
- Ichinose, Nobuyuki, et al., "Immobilization of Protein on Micropatterns by the Use of Photoremovable Activated Ester", *Chem. Lett.*, pp. 237-238 (1995).
- Kang, Doris, et al., "Patterned Functionalization of Gold and Single Crystal Silicon via Photochemical Reaction of Surface-Confined Derivatives of  $(\eta^5\text{-C}_5\text{H}_5)\text{Mn}(\text{CO})_3$ ", *Langmuir*, vol. 7, No. 10, pp. 2169-2174 (1991).
- Lercel, M. J., et al., "Pattern Transfer of Electron Beam Modified Self-Assembled Monolayers for High-Resolution Lithography", *J. Vac. Sci. Techn.*, vol. 13, No. 3, pp. 1139-1143 (1995).
- Pritchard, David, J., et al., "Micron-Scale Patterning of Biological Molecules", *Angew. Chem. Int. Ed. Engl.*, vol. 34, No. 1, pp. 91-92 (1995).

- Rozsnyai, Lawrence, F., et al., "Selective Electrochemical Deposition of Polyaniline via Photopatterning of a Monolayer-Modified Substrate", *J. Am. Chem. Soc.*, vol. 116, pp. 5993-5994 (1994).
- Sondag-Huethorst, J.A.M., et al., "Generation of Electrochemically Deposited Metal Patterns by Means of Electro Beam (nano)lithography of Self-Assembled Monolayer Resists", *Appl. Phys. Lett.*, vol. 64, pp. 285-287 (1994).
- Wollman, Eric, W., et al., "Scanning Electron Microscopy for Imaging Photopatterned Self-Assembled Monolayers on Gold", *Langmuir*, vol. 9, No. 6, pp. 1517-1520 (1993).
- Wollman, Eric, W., et al., "Photosensitive Self-Assembled Monolayers on Gold: Photochemistry of Surface-Confining Aryl Azide and Cyclopentadienylmanganese Tricarbonyl", *J. Am. Chem. Soc.*, vol. 116, No. 10, pp. 4395-4404 (1994).
- Xia, Younan, et al., "Microcontact Printing of Octadecylsiloxane on the Surface of Silicon Dioxide and its Application in Microfabrication", *Am. Chem. Soc.*, pp. 9576-9577 (1995).
- Kumar, Amit, et al., "Features of Gold Having Micrometer to Centimeter Dimensions can be Formed through a Combination on Stamping with an Elastomeric Stamp and an Alkanethiol 'ink' followed by Chemical Etching", *Appl. Phys. Lett.*, vol. 63, pp. 2002-2004 (1993).
- Kleinfield, D., et al., "Controlled Outgrowth of Dissociated Neurons on Patterned Substrates", *J. Neurosci.*, vol. 8, pp. 4098-4120 (1988).
- Kelkar et al., "Acoustic Plate Waves for Measurement of Electrical Properties of Liquids", *Microchem. Journal*, vol. 43, pp. 155-164 (1991).
- Liedberg et al., "Molecular Gradients of  $\omega$ -Substituted Alkanethiols on Gold: Preparation and Characterization", *Langmuir*, vol. 11, pp. 3821-3827 (1995).
- Shana et al., "Analysis of electrical equivalent circuit of quartz crystal resonator loaded with viscous conductive liquids", *Journal of Electroanalytical Chemistry*, vol. 379, pp. 21-33 (1994).
- Shana et al., "Quartz Crystal Resonators as Sensors in Liquids Using the Acoustoelectric Effect", *Anal. Chem.*, vol. 66, pp. 1955-1964 (1994).
- Josse et al., "Electrical Surface Perturbation of a Piezoelectric Acoustic Plate Mode by a Conductive Liquid Loading", *IEEE Transactions on Ultrasonics, Ferroelectrics, and Frequency Control*, vol. 39, No. 4, (Jul. 1992).
- Josse et al., "On the use of ZX-LiNbO<sub>3</sub> acoustic plate mode devices as detectors for dilute electrolytes", *Sensors and Actuators B*, vol. 9, pp. 97-112 (1992).
- Daphint et al., "Probing of strong and weak electrolytes with acoustic wave fields", *Sensors and Actuators B*, vol. 9, pp. 155-162 (1992).
- Osada et al., "Intelligent Gels", *Scientific American*, pp. 82-87, May 1993.
- Saito et al., "Volume Phase Transition of N-Alkylacrylamide Gels", *Advances on Polymer Science*, vol. 109, pp. 207-232 (1993).
- Okano T. "Molecular Design of Temperature-Responsive Polymers as Intelligent Materials", *Advances in Polymer Science*, vol. 110, pp. 179-197 (1993).
- Shibayama et al., "Volume Phase Transition and Related Phenomena of Polymer Gels", *Advances in Polymer Science*, vol. 109, pp. 1-62 (1993).
- Kokufuta, E. "Novel Applications for Stimulus-Sensitive Polymer Gels in the Preparation of Functional Immobilized Biocatalysts", *Advances in Polymer Science*, vol. 110, pp. 157-177 (1993).
- Osada et al., "Stimuli-Responsive Polymer Gels and Their Application to Chemomechanical Systems", *Prog. Polym. Sci.*, vol. 18, pp. 187-266 (1993).
- Irie, M. "Stimuli-Responsive Poly(N-isopropylacrylamide) Photo- and Chemical-Induced Phase Transitions", *Advances in Polymer Science*, vol. 110, pp. 49-65 (1993).
- Tsai, et al., Letter to the Editor, "Comment on the Prediction of Segregation of Alloy Surfaces", *Journal of Catalysis*, vol. 50, pp. 200-202 (1977).
- Johnson et al., "Orientation Dependence of Surface Segregation in a Dilute Ni-Au Alloy", *J. Vac. Sci. Technol.*, vol. 15, No. 2, pp. 457-469 (Mar./Apr. 1978).
- Seah, M.P., "Quantitative Prediction of Surface Segregation", *Journal of Catalysis*, vol. 57, pp. 450-457 (1979).
- Kumar et al., "Patterned Condensation Figures as Optical Diffraction Gratings", *Science*, vol. 263, pp. 60-62 (Jan. 7, 1994).
- Folkers et al., "Self-Assembled Monolayers of Long-Chain Hydroxamic Acids on the Native Oxides of Metals", *Langmuir*, vol. 11, No. 3, pp. 813-824 (1995).
- Joon et al., "Patterned Self-Assembled Monolayers Formed by Microcontact Printing Direct Selective Metalization by Chemical Vapor Deposition on Planar and Nonplanar Substrates", *Langmuir*, vol. 11, No. 8, pp. 3024-3026 (1995).
- Abbott et al., "Using Micromachining, Molecular Self-Assembly, and Wet Etching to Fabricate 0.1-1- $\mu$ m-Scale Structures of Gold and Silicon", *Chem. Mater.*, vol. 6, No. 5, pp. 596-602 (1994).
- Mrkšich et al., "Patterning Self-Assembled Monolayers Using Microcontact Printing: A New Technology For Biosensors?" *Tibtech*, vol. 13, pp. 228-235 (Jun. 1995).
- Burton et al., "Prediction of Segregation of Alloy Surfaces from Bulk Phase Diagrams", *Physical Review Letters*, vol. 37, No. 21, pp. 1433-1436 (Nov. 22, 1976).
- Seah, M.P., "Quantitative Prediction of Surface Segregation", *Journal of Catalysis*, vol. 57, pp. 450-457 (1979).
- Glassman, A., ed. *Printing Fundamentals*, Tappi Press, Atlanta, Georgia (1981).
- Modern Plastics Encyclopedia*, McGraw-Hill Publishing Co., New York, New York, pp. 1923-1996.

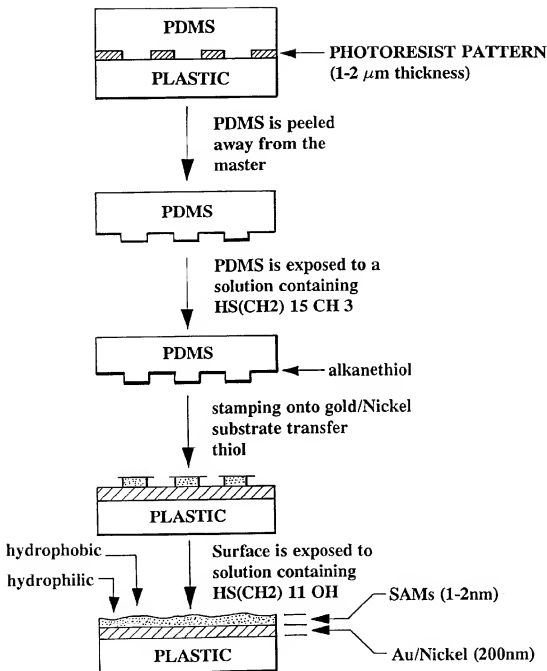




Fig. 2A

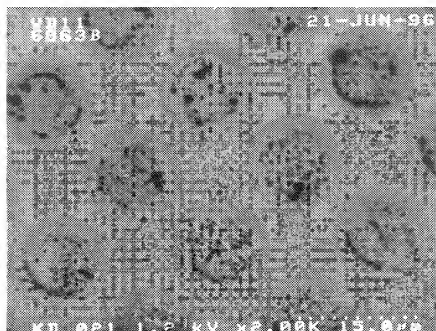


Fig. 2B

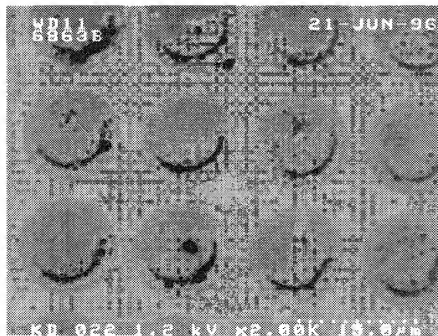


Fig. 3A

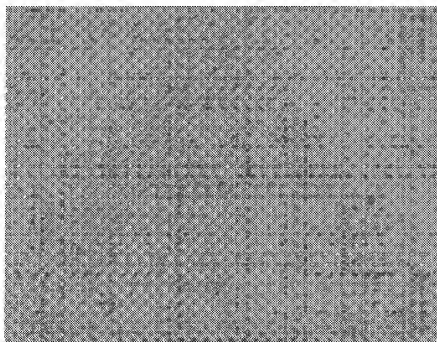


Fig. 3B

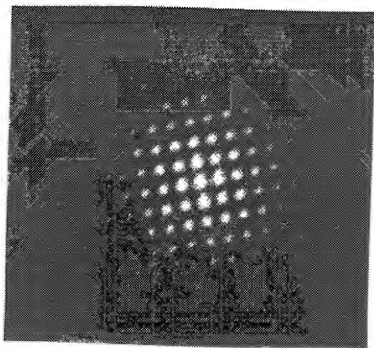
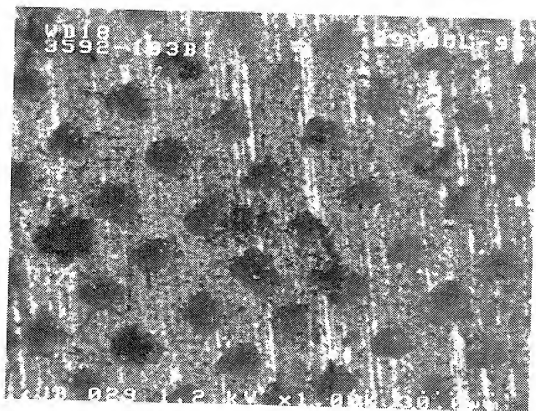
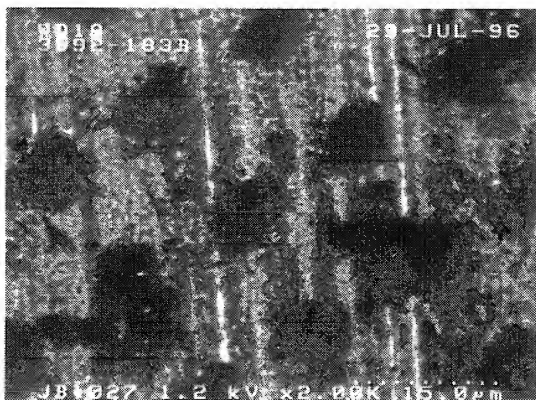


Fig. 4A



**Fig. 4B**

# POLYMER FILMS HAVING A PRINTED SELF-ASSEMBLING MONOLAYER

## TECHNICAL FIELD

The present invention is in the field of contact printing and, more specifically the present invention is in the field of microcontact printing on polymer films.

## BACKGROUND OF THE INVENTION

Microcontact printing is a technique for forming patterns of organic monolayers with  $\mu\text{m}$  and submicron lateral dimensions. It offers experimental simplicity and flexibility in forming certain types of patterns. It relies on the remarkable ability of self-assembled monolayers of long-chain alkane-thiols to form on gold and other metals. These patterns can act as nanometer resists by protecting the supporting metal from corrosion by appropriately formulated etchants, or, can allow for the selective placement of fluids on hydrophilic regions of the pattern. Patterns of self-assembled monolayers having dimensions that can be less than  $1\ \mu\text{m}$  are formed by using the alkane-thiol as an "ink," and by printing them on the metal support using an elastomeric "stamp." The stamp is fabricated by molding a silicone elastomer using a master prepared by optical or X-ray microlithography or by other techniques.

Microcontact printing of patterned self-assembled monolayers brings to microfabrication a number of new capabilities. First, microcontact printing makes it possible to form patterns that are distinguished only by their constituent functional groups; this capability permits the control of surface properties such as interfacial free energies with great precision. Second, because micro-contact printing relies on molecular self-assembly, it generates a system that is (at least locally) close to a thermodynamic minimum and is intrinsically defect-rejecting and self-healing. Simple procedures, with minimal protection against surface contamination by adsorbed materials or by particles, can lead to surprisingly low levels of defects in the final structures. The procedure can be conducted at atmospheric pressure, in an unprotected laboratory atmosphere. Thus, microcontact printing is especially useful in laboratories that do not have routine access to the equipment normally used in microfabrication, or for which the capital cost of equipment is a serious concern. Third, the patterned self-assembled monolayers can be designed to act as resists with a number of wet-chemical etchants.

Working with liquid etchants suffers from the disadvantages of handling solvents and disposing of wastes, but also enjoys substantial advantages: a high degree of control over contamination of surfaces; reduced damage to the substrate from energetic interactions with atoms or ions; the ability to manipulate complex and sensitive organic functionality. Because the self-assembled monolayers are only  $1\text{--}3\ \text{nm}$  thick, there is little loss in edge definition due to the thickness of the resist; the major determinants of edge resolution seem to be the fidelity of the contact printing and the anisotropy of etching the underlying metal. In the current best cases, features of size  $0.2\ \mu\text{m}$  can be fabricated; edge resolution in systems showing this resolution in feature size is less than  $50\ \text{nm}$ .

In the prior art, a gold film 5 to 2000 nanometers thick is typically supported on a titanium-primed  $\text{Si}/\text{SiO}_2$  wafer or glass sheet. The titanium serves as an adhesion promoter between gold and the support. However, the silicon wafer is rigid, brittle, and cannot transmit light. These silicon wafers are also not suitable for a large-scale, continuous printing

process, such as in letterpress, gravure, offset, and screen printing (see *Printing Fundamentals*, A. Glassman, Ed. (Tappi Press Atlanta, Ga. 1981); *Encyclopedia Britannica*, vol. 26, pp. 76-92, 110-111 (Encyclopedia Britannica, Inc. 1991)). In addition, silicon must be treated in a separate step with an adhesion promoter such as Cr or Ti, or Au will not adequately adhere, preventing formation of a stable and well-ordered self-assembling monolayer. Finally, silicon is opaque, so any diffraction pattern obtained must be created with reflected, not transmitted light. What is needed is an easy, efficient and simple method of contact printing on an optically transparent, flexible substrate, that is amenable to continuous processing.

## SUMMARY OF THE INVENTION

The present invention comprises methods of contact printing of patterned, self-assembling monolayers of alkane-thiols, carboxylic acids, hydroxamic acids, and phosphonic acids on thermoplastic films metallized with an alloy such as nickel/gold, the compositions produced thereby, and the use of these compositions.

Patterned self-assembling monolayers allow for the controlled placement of fluids thereon which can contain a chemically reactive, indicator functionality. The optical sensing devices produced thereby when the film is exposed to an analyte and light, can produce optical diffraction patterns which differ depending on the reaction of the self-assembling monolayer with the analyte of interest. The light can be in the visible spectrum, and be either reflected from the film, or transmitted through it, and the analyte can be any compound reacting with the self-assembling monolayer. The present invention also provides a flexible support for a self-assembling monolayer on a metal alloy.

The present invention includes a support for a self-assembling monolayer on a metal alloy which does not require an adhesion promoter for the formation of a well-ordered self-assembling monolayer. The present invention also provides a support for a self-assembling monolayer on a metal alloy which is suitable for continuous, rather than batch, fabrication. Finally the present invention provides a low-cost, disposable sensor which can be mass produced.

These and other objects, features and advantages of the present invention will become apparent after a review of the following detailed description of the disclosed embodiments.

## BRIEF DESCRIPTION OF THE FIGURES

FIG. 1 is a schematic of contact printing of self-assembling monolayers, using a nickel/gold coated polymer substrate as an example. A polydimethylsiloxane (PDMS; silicone elastomer 184; Dow Corning Corp., Midland, Mich.) is polymerized on a silicone master containing a pre-determined pattern. The PDMS is peeled away from the master, and then exposed to a solution containing  $\text{HS}(\text{CH}_2)_4\text{CH}_3$ . The alkane-thiol coated stamp is then stamped onto the nickel/gold-coated substrate. Then, the surface of the substrate is exposed to a solution containing a different alkane thiol such as  $\text{HS}(\text{CH}_2)_6\text{OH}$ .

FIG. 2 is a field emission secondary electron microscope image of 10 micron-diameter circles of hydrophilic self-assembling monolayers formed by printing of 16-mercaptohexadecanoic acid onto MYLAR® metallized with Ni/Au alloy, as described in Example 1.

FIG. 3a is an optical photomicrograph at 300x magnification of 10 micron-diameter circles of hydrophilic

self-assembling monolayers formed by printing of 16-mercaptohexadecanoic acid, as described in Example 1, below, and after exposure to a high surface energy, curable, optical adhesive. The adhesive was cured by ultraviolet light (UV) exposure.

FIG. 3b is a photograph of the diffraction pattern formed by visible light shown through the self-assembling monolayer pattern described by FIG. 3a.

FIGS. 4a and 4b are a field emission secondary electron micrograph image of 10 micron-diameter circles formed of self-assembled photoconductive polymers on hydrophilic self-assembling monolayers, printed as described in Example 1.

#### DETAILED DESCRIPTION

The present invention provides methods of contact printing of patterned, self-assembling monolayers of alkanethiols, carboxylic acids, hydroxamic acids, and phosphonic acids on polymer films metallized with an alloy such as nickel/gold, desirably thermoplastic polymer films, the compositions produced thereby, and the use of these compositions. Patterned self-assembling monolayers allow for the controlled placement of fluids thereon which can contain a chemically reactive, indicator functionality. The term "patterned self-assembling monolayers thereon" as used herein means the self-assembling monolayers in any pattern on the metallized polymer films including a solid pattern.

In one embodiment, optical sensing devices can be produced according to the present invention. When the film with the self-assembling monolayers thereon is exposed to an analyte that is capable of reacting with the self-assembling monolayer, the film will produce optical diffraction patterns which differ depending on the reaction of the self-assembling monolayer with the analyte of interest. The liquid may be a high surface tension fluid such as water. The light can be in the visible spectrum, and be either reflected from the film, or transmitted through it, and the analyte can be any compound reacting with the self-assembling monolayer.

Self-assembled monolayers of organic compounds on inorganic or metal surfaces are becoming increasingly important in many areas of materials science. Although there are many different systems of self-assembling monolayers based on different organic components and supports, desired systems are those of alkanethiols,  $\text{HS}(\text{CH}_2)_n\text{R}$ . Typically, a gold film, 5 to 2000 nm thick, is supported on a titanium-primed  $\text{Si}/\text{SiO}_2$  wafer or glass sheet. The titanium serves as an adhesion promoter between gold and the support. The alkanethiols chemisorb on the gold surface from a solution in which the gold film is immersed, and form adsorbed alkanethiolates with loss of hydrogen. Adsorption can also occur from the vapor. Self-assembling monolayers formed on gold from long-chain alkanethiols of structure  $\text{X}(\text{CH}_2)_n\text{Y}(\text{CH}_2)_m\text{S}$  are highly ordered and can be considered as crystalline or quasi-crystalline molecular arrays. A wide variety of organic functional groups (X,Y) can be incorporated into the surface or interior of the monolayer.

Self-assembling monolayers can therefore be tailored to provide a wide variety of material properties: wettability and protection against corrosion by chemical etchants are especially relevant to  $\mu\text{CP}$ . In one embodiment of the invention, there are two or more self-assembling monolayers with different chemical properties. In another embodiment of the invention, a first self-assembling monolayer is hydrophobic, and a second self-assembling monolayer is hydrophilic.

FIG. 1 outlines the procedure used for microcontact printing. An elastomeric stamp is used to transfer by contact

alkanethiol "ink" to a surface coated with a metal alloy. In a preferred embodiment, the alloy surface is predominantly gold. Preferred alloys are those such as nickel/gold, which are known to show an enrichment in the surface concentration of gold relative to its bulk concentration. Prediction of surface segregation of one metal of an alloy is described in M. P. Seah, "Quantitative Prediction of Surface Segregation," *Journal of Catalysis*, vol. 57, pp. 450-457 (1979), and J. J. Burton, et al., "Prediction of Segregation to Alloy Surfaces from Bulk Phase Diagrams," *Physical Review Letters*, vol. 37, No. 21, pp. 1433-1436 (Nov. 22, 1976), both incorporated herein by reference. In one embodiment of the invention, the metal alloy has surface enrichment of a metal reacting with the self-assembling monolayer. If the stamp is patterned, a patterned self-assembling monolayer forms. The stamp is fabricated by casting polydimethylsiloxane (PDMS) on a master having the desired pattern. Masters are prepared using standard photolithographic techniques, or constructed from existing materials having microscale surface features.

In a typical experimental procedure, a photolithographically produced master is placed in a glass or plastic Petri dish, and a 10:1 ratio (w:w or v:v) mixture of SYLGARD® silicone elastomer 184 and SYLGARD® silicone elastomer 184 curing agent (Dow Corning Corporation) is poured over it. The elastomer is allowed to sit for approximately 30 minutes at room temperature and pressure to degas, then cured for 1-2 hours at 60° C., and gently peeled from the master. "Inking" of the elastomeric stamp is accomplished by exposing the stamp to a 0.1 to 1.0 mM solution of alkanethiol in anhydrous ethanol, either by pouring the solution over the surface of the stamp, or by rubbing the stamp gently with a Q-TIP® (that has been saturated with the inking solution). The stamp is allowed to dry until no liquid is visible by eye on the surface of the stamp (typically about 60 seconds), either under ambient conditions, or by exposure to a stream of nitrogen gas. Following inking, the stamp is applied (typically by hand) to a metal alloy, e.g., nickel/gold surface. Very light hand pressure is used to aid in complete contact between the stamp and the surface. The stamp is then gently peeled from the surface. Following removal of the stamp, the surface is washed of excess thiol and the patterned metal alloy surface can be subjected to chemical etchants (see below) that selectively remove underivatized areas of the metal alloy surface, and if desired, the underlying support(s). Alternatively, further derivatization of unstamped areas can be accomplished, either by using a second stamp, or by washing the entire surface with a different alkanethiol.

The elastomeric character of the stamp is essential to the success of the process. Polydimethylsiloxane (PDMS), when cured, is sufficiently elastomeric to allow good conformal contact of the stamp and the surface, even for surfaces with significant relief; this contact is essential for efficient contact transfer of the alkanethiol "ink" to the alloy-coated film. The elastomeric properties of PDMS are also important when the stamp is removed from the master: if the stamp were rigid (as is the master) it would be difficult to separate the stamp and master after curing without damaging one of the two substrates. PDMS is also sufficiently rigid to retain its shape, even for features with sub-micron dimensions: we have successfully generated patterns with lines as small as 200 nm in width. The surface of PDMS has a low interfacial free energy ( $\gamma=22.1$  dynes/cm), and the stamp does not adhere to the metal alloy coated film. The stamp is durable: we have used the same stamp up to 100 times over a period of several months without

significant degradation in performance. The polymeric nature of PDMS also plays a critical role in the inking procedure, by enabling the stamp to absorb the alkanethiol ink by swelling.

Microcontact printing on metal alloy surfaces can be conducted with a variety of alkanethiol "inks". Alkanethiols that do not undergo reactive spreading (after application to the metal alloy film) are required for formation of small features with high resolution. For stamping in air, one can use autophobic alkanethiols such as hexadecanethiol. Microcontact printing of other non-autophobic alkanethiols, for example,  $\text{HS}(\text{CH}_2)_{15}\text{COOH}$ , can be conducted by stamping under a liquid such as water. Patterned self-assembling monolayers of alkanethiols on metal alloy provide excellent resist character with a number of wet-chemical etchants.

In one embodiment of the present invention, the self-assembling monolayer is formed of a carboxy-terminated alkane thiol stamped with a patterned elastomeric stamp onto a nickel/gold-surfaced thermoplastic film such as MYLAR®. The alkanethiol is inked with a solution of alkanethiol in ethanol, dried, and brought into contact with a surface of nickel/gold. The alkanethiol is transferred to the surface only at those regions where the stamp contacts the surface, producing a pattern of self-assembling monolayer which is defined by the pattern of the stamp. Optionally, areas of unmodified nickel/gold surface next to the stamped areas can be rendered hydrophobic by reaction with a methyl-terminated alkane thiol.

A more detailed description of the methods and compositions of the present invention follows. All publications cited herein are incorporated by reference in their entirety.

Any thermoplastic film upon which a metal substrate can be deposited is suitable for the present invention. These include, but are not limited to polymers such as: polyethylene-terephthalate (MYLAR®), acrylonitrile-butadiene-styrene, acrylonitrile-methyl acrylate copolymer, cellphane, cellulosic polymers such as ethyl cellulose, cellulose acetate, cellulose acetate butyrate, cellulose propionate, cellulose triacetate, cellulose triacetate, polyethylene, polyethylene-vinyl acetate copolymers, ionomers (ethylene polymers) polyethylene-nylon copolymers, polypropylene, methyl pentene polymers, polyvinyl fluoride, and aromatic polysulfones. Preferably, the plastic film has an optical transparency of greater than 80%. Other suitable thermoplastics and suppliers may be found, for example, in reference works such as the *Modern Plastics Encyclopedia* (McGraw-Hill Publishing Co., New York 1923-1996).

In one embodiment of the invention, the thermoplastic film with the metal coating thereon has an optical transparency of between approximately 5% and 95%. A more desired optical transparency for the thermoplastic film used in the present invention is between approximately 20% and 80%. In a desired embodiment of the present invention, the thermoplastic film has at least an approximately 80% optical transparency, and the thickness of the metal coating is such as to maintain an optical transparency greater than about 20%, so that diffraction patterns can be produced by either reflected or transmitted light. This corresponds to a metal coating thickness of about 20 nm. However, in other embodiments of the invention, the gold thickness may be between approximately 1 nm and 1000 nm.

The preferred metal alloy for deposition on the film is gold and another metal. However, alloys of silver, aluminum, copper, iron, zirconium, platinum, nickel may also be used. Preferred metals are ones that do not form

oxides, and thus assist in the formation of more predictable self-assembling monolayers. Alloys such as Ni/Au, Pt/Au, and Cu/Au, which show surface enrichments of Au, are suitable.

In principle, any surface with corrugations of appropriate size could be used as masters. The process of microcontact printing starts with an appropriate relief structure, from which an elastomeric stamp is cast. This "master" template may be generated photolithographically, or by other procedures, such as commercially available diffraction gratings. In one embodiment, the stamp may be made from polydimethylsiloxane.

In one embodiment of the present invention, the self-assembling monolayer has the following general formula:



X is reactive with metal or metal oxide. For example, X may be asymmetrical or symmetrical disulfide (—RSSR, —RSSR), sulfide (—RSR, —RSR), diselenide (—RSe—SeR), selenide (—RSeR, —RSeR), thiol (—SH), nitrile (—CN), isocyanide, nitro (—NO<sub>2</sub>), selenol (—SeH), trivalent phosphorus compounds, isothiocyanate, xanthate, thiocarbamate, phosphine, thiosulfate or dithiosulfate, carboxylic acids, hydroxylic acids, and hydroxamic acids.

R and R' are hydrocarbon chains which may optionally be interrupted by hetero atoms and which are preferably non-branched for the sake of optimum dense packing. At room temperature, R is greater than or equal to seven carbon atoms in length, in order to overcome natural randomizing of the self-assembling monolayer. At colder temperatures, R may be shorter. In a preferred embodiment, R is —(CH<sub>2</sub>)<sub>n</sub>— where n is between 10 and 12, inclusive. The carbon chain may optionally be perfluorinated.

Y may also have any surface property of interest. For example, Y could be any among the great number of groups used for immobilization in liquid chromatography techniques, such as hydroxy, carboxyl, amino, aldehyde, hydrazide, carbonyl, epoxy, or vinyl groups. Examples of sensing layer materials are set forth in "Patterning Self-Assembled Monolayers Using Microcontact Printing: A New Technology for Biosensors?" by Milan Mrksich and George M. Whitesides, published in *TIBTECH*, June, 1995 (Vol. 13), pp. 228-235, hereby incorporated by reference.

Self-assembling monolayers of alkyl phosphonic, hydroxamic, and carboxylic acids may also be useful for the methods and compositions of the present invention. Since alkanethiols do not adsorb to the surfaces of many metal oxides, carboxylic acids, phosphonic acids, and hydroxamic acids may be preferred for X to the metal oxides. See J. P. Folkers, G. M. Whitesides, et al., *Langmuir*, 1995, vol. 11, pp. 813-824.

R may also be of the form (CH<sub>2</sub>)<sub>a</sub>—Z—(CH<sub>2</sub>)<sub>b</sub>, where a ≥ 0, b ≥ 7, and Z is any chemical functionality or compound of interest, such as sulfones, urea, lactam, etc.

The stamp may be applied in air, or under a fluid such as water to prevent excess diffusion of the alkanethiol. For large-scale or continuous printing processes, it is most desirable to print in air, since shorter contact times are desirable for those processes.

In one embodiment of the present invention, the pattern is formed on the metallized thermoplastic polymer with the self-assembling monolayer. In another embodiment of the present invention, the relief of the pattern is formed with the self-assembling monolayer. After the stamping process, the metallized areas on the plastic may optionally be passivated, for example, with a methyl-terminated self-assembling monolayer such as hexadecylmercaptan.

This invention is further illustrated by the following example, which is not to be construed in any way as imposing limitations upon the scope thereof. On the contrary, it is to be clearly understood that resort may be had to various other embodiments, modifications, and equivalents thereof, which, after reading the description herein, may suggest themselves to those skilled in the art without departing from the spirit of the present invention.

#### Example 1

Printing of nickel/gold-coated MYLAR® (polyethylene terephthalate) with patterns of 16-mercaptohexadecanoic acid and hexadecanethiol

A nickel/gold alloy was sputter-coated onto 7 mil MYLAR® of 15.9 nm thickness. The composition had 65% visible light transmittance, and 65 ohms/cm<sup>2</sup> resistance. The following results from XPS surface analysis were obtained.

Sputter Time (sec)	% C	% O	% Au	% Ni
0	51.5	8.0	40.5	ND
15	33.3	6.4	60.3	ND
30	20.2	ND	71.7	8.0
60	19.3	ND	72.4	8.3

ND means "not detected", i.e., less than 0.2 atom-percent.

These results show that the outermost surface of the Ni/Au alloy is predominantly Au, i.e., Ni is not detected until after approximately 5.0 nm of Au is removed. Thus, the alloy presents a surface that resembles pure gold and can be used as a "pure gold" surface for contact printing.

MYLAR® film modified with a sputter-deposited nickel/alloy topcoat was obtained from Courtaulds Performance Films (21034 Osborne Street, Canoga Park, Calif. 91304). Patterns of hydrophilic, carboxy-terminated alkane thiols were stamped onto the Ni/Au unutilized MYLAR® using CH<sub>3</sub>(CH<sub>2</sub>)<sub>15</sub>SH and HOC(O)(CH<sub>2</sub>)<sub>15</sub>SH acid by the following method. (See FIG. 1). An exposed and developed photoresist pattern of 10 micron diameter circles on a silicon wafer was used as the master. Polydimethylsiloxane (PDMS; silicone elastomer 184; Dow Corning Co., Midland, Mich.), was polymerized on a master to produce a stamp with ten micron-diameter circles spaced five microns apart. The stamp was inked by exposure to a solution (1 to 10 mM in ethanol) of 16-mercaptohexadecanoic acid, and allowed to air-dry. The substrate was contacted with the stamp for 50 seconds and washed for 2 to 4 seconds with a solution of hexadecanethiol (1 to 10 mM in ethanol). The substrate was finally washed for 10 seconds in ethanol and dried in a stream of nitrogen. The results of this printing are shown in FIG. 2.

These hydrophilic self-assembling monolayer circles allow for selective placement of high surface tension fluids such as water, triethylene glycol, or ultraviolet light curable urethane acrylic adhesives. These liquids can contain dissolved and suspended reagents that react chemically or physically with targeted analytes, thus making the coated plastic film a collection of 10 micron microreactors suitable for low-cost, disposable chemical sensors. An example of such a device is shown in FIG. 3a.

Diffraction of visible light was shown with these compositions. Both reflected and transmitted diffraction patterns were observed when using 5 mW, 670 nm laser illumination. FIG. 3b is a photograph of the diffraction pattern formed by visible light shown through the self-assembling monolayer pattern of FIG. 3a. Rainbow diffraction colors were observed with transmitted white light.

#### Measurement of Contact Angles

Contact angles were measured on a Rame-Hart Model 100 goniometer at room temperature and ambient humidity. Water for contact angles was deionized and distilled in a glass and TEFLON® apparatus. Advancing and receding contact angles were measured on both sides of at least three drops of each liquid per slide; data in the figures represents the average of these measurements. The following method was used for measuring contact angles: A drop approximately 1–2 microliters in volume was grown on the end of a pipette tip (Micro-Electropipette syringe; Matrix Technologies; Lowell, Mass.). The tip was then lowered to the surface until the drop came in contact with the surface. The drop was advanced by slowly increasing the volume of the drop (rate approximately 1 microliter/second). Advancing contact angles of water were measured immediately after the front of the drop had smoothly moved a short distance across the surface. Receding angles were taken after the drop had smoothly retreated across the surface by decreasing the volume of the drop.

#### X-ray Photoelectron Spectroscopy (XPS)

X-ray photoelectron spectra were collected on a Surface Science SSX-100 spectrometer using a monochromatized Al K-alpha source (hv=1486.6 electron volts). The spectra were recorded using a spot size of 600 micrometers and a pass energy on the detector of 50 electron volts (acquisition time for one scan was approximately 1.5 minutes). For the monolayers, spectra were collected for carbon and oxygen using the 1s peaks at 285 and 530 eV, respectively; the binding energies for elements in the monolayer were referenced to the peak due to hydrocarbon in the C 1s region, for which we fixed the binding energy at 284.6 eV. Spectra for the solid hydroxamic acid were collected using an electron flood gun of 4.5 eV to dissipate charge in the sample. The binding energies for the substrates were not standardized to a reference sample. All spectra were fitted using an 80% Gaussian/20% Lorentzian peak shape and a Shirley background subtraction. See J. P. Folgers, G. M. Whitesides, et al., *Langmuir*, vol. 11, no. 3, pp. 813–824 (1995).

#### Condensation Figures

Condensation figures (CFs) are arrays of liquid drops that form upon condensation of vapor onto a solid surface. The examination of condensation figures has historically been used as a method to characterize the degree of contamination on an otherwise homogeneous surface. One is able to impose a pattern on arrays of condensed drops by patterning the surface underlying them into regions of different solid-vapor interfacial free energy and to characterize the patterned CFs by photomicroscopy and optical diffraction. It can be demonstrated that appropriately patterned CFs can be used as optical diffraction gratings and that examination of the diffraction patterns provides both a rapid, nondestructive method for characterizing patterned self-assembling monolayers and an approach to sensing the environment. Because the form of the CFs—that is, the size, density, and distribution of the drops is sensitive to environmental factors, CFs of appropriate size and pattern diffract light and can be used as sensors. This principle is demonstrated by correlating the temperature of a substrate patterned into hydrophobic and hydrophilic regions, in an atmosphere of constant relative humidity, with the intensity of light diffracted from CFs on these regions.



Appropriate patterns are formed from self-assembled monolayers (self-assembling monolayers) on gold/nickel by using combinations of hexadecanethiol [ $\text{CH}_3(\text{CH}_2)_{15}\text{SH}$ ], 16-mercaptohexadecanoic acid [ $\text{HS}(\text{CH}_2)_{15}\text{COOH}$ ], and 11-mercaptoundecanol [ $\text{HS}(\text{CH}_2)_{10}\text{OH}$ ]. Several techniques are now available for preparing patterns of two or more self-assembling monolayers having 0.1- to 10- $\mu\text{m}$  dimensions.

At 20° C., an incident beam of light from a laser (helium-neon laser, wavelength=632.8 nm) produced a single transmitted spot because no water had condensed on the surface, and the transmittance of the regions covered with different self-assembling monolayers were effectively indistinguishable. As the surface was exposed to warm, moist air, droplets of water condensed preferentially on the hydrophilic regions. Diffraction patterns appeared in the light transmitted from the surface. Under these conditions, light was transmitted coherently from the regions where no water had condensed and was scattered by the regions where water had condensed. The condensation figures disappeared within several seconds as the water droplets which condensed on the self-assembling monolayers evaporated.

The ability to form condensation figures can be ascertained by the relative contact angles of water on the hydrophobic and hydrophilic self-assembling monolayers. Unpatterned monolayers of the appropriate thiol were prepared by immersion of the substrate in a dilute solution for one hour, followed by rinsing with ethanol and air drying.

The contact angles of water on Au(Ni)/MYLAR reacted with  $\text{Cl}_3(\text{CH}_2)_3\text{SH}$  and  $\text{HOOC}(\text{CH}_2)_3\text{SH}$  were 100° and 62°, respectively. The untreated Au(Ni)/MYLAR contact angle for water was 73-77°. The water contact angle is similar to that obtained for Au coated SiOx wafers, which is 73-74° (data not shown).

Condensation Figures [Science, Vol. 263, 60 (1994), incorporated herein by reference] with equivalent optical diffraction can be formed on Au/Ni:MYLAR®, relative to known art with Au:SiOx. The chemistry of alkane-thiols reacting with Au/Ni:MYLAR is similar to that reported in the literature for Au:SiOx.

A field emission secondary electron microscope image of 10 micron-diameter circles of hydrophilic self-assembling monolayers formed by printing of 16-mercaptohexadecanoic acid onto MYLAR® metallized with Ni/Au alloy is shown in FIG. 2. FIG. 3a is an optical photomicrograph at 300x magnification of 10 micron-diameter circles of hydrophilic self-assembling monolayers formed by printing of 16-mercaptohexadecanoic acid, and after exposure to a high surface energy, curable, optical adhesive. The adhesive was cured by ultraviolet light (UV) exposure.

FIG. 3b is a photograph of the diffraction pattern formed by visible light shown through the self-assembling monolayer pattern described by FIG. 3a.

FIGS. 4a and 4b are field emission secondary electron micrograph images of 10 micron-diameter circles formed of self-assembled photocurable polymers on hydrophilic self-assembling monolayers.

Those skilled in the art will now see that certain modifications can be made to the invention herein disclosed with respect to the illustrated embodiments, without departing from the spirit of the instant invention. And while the invention has been described above with respect to the preferred embodiments, it will be understood that the invention is adapted to numerous rearrangements, modifications, and alterations, all such arrangements, modifications, and alterations are intended to be within the scope of the appended claims.

What is claimed is:

1. A film with patterned self-assembling monolayers thereon comprising:

a polymer film coated with a metal alloy; and

a self-assembling monolayer printed onto the polymer film.

2. The film of claim 1, wherein the metals to be alloyed are selected from the group consisting essentially of gold, silver, nickel, platinum, aluminum, iron, copper, and zirconium.

3. The film of claim 1, wherein the alloy coating is between approximately 1 nanometer and 1000 nanometers in thickness.

4. The film of claim 1, wherein the polymer film is selected from the group consisting of polyethylene-terephthalate, acrylonitrile-butadiene-styrene, acrylonitrile-methyl acetate copolymer, cellophane, cellulose polymers such as ethyl cellulose, cellulose acetate, cellulose acetate butyrate, cellulose propionate, cellulose triacetate, polyethylene, polyethylene-vinyl acetate copolymers, ionomers (ethylene polymers) polyethylene-nylon copolymers, polypropylene, methyl pentene polymers, polyvinyl fluoride, and aromatic polysulfones.

5. The film of claim 4, wherein the polymer film is polyethylene-terephthalate.

6. The film of claim 1, wherein the polymer film is optically transparent.

7. The film of claim 1, wherein the polymer film has an optical transparency between 5% and 95%.

8. The film of claim 1, wherein the polymer film has an optical transparency between 20% and 80%.

9. The film of claim 1, wherein the self-assembling monolayer comprises compounds with the following general formula:



wherein:

X is reactive with the metal or metal oxide on the polymer film;

R is a hydrocarbon chain; and

Y is a compound with any property of interest;

wherein the self-assembling monolayer compound is attached to the polymer film through reaction of X with the metal or metal oxide on the polymer film.

10. The film of claim 9, wherein:

X is selected from the group consisting of an asymmetrical or symmetrical disulfide ( $-\text{SSY}$ ), sulfide ( $-\text{SY}$ ), diselenide ( $-\text{SeSeY}$ ), selenide ( $-\text{SeY}$ ), thiols ( $-\text{SH}$ ), nitrile ( $-\text{CN}$ ), isonitrile, nitro ( $-\text{NO}_2$ ), selenol ( $-\text{SeH}$ ), trivalent phosphorus compounds, isothiocyanate, xanthate, thiocarbamate, phosphine, thioacid, dithioacid, carboxylic acids, hydroxylic acids, and hydroxamic acids;

R and R' are selected from hydrocarbon chains hydrocarbon chains interrupted by hetero atoms, hydrocarbon chains which are perfluorinated, or hydrocarbons which are non-branched; and

Y and Y' are selected from hydroxy, carboxyl, amino, aldehyde, hydrazide, carbonyl, epoxy, or vinyl groups.

11. The film of claim 9, wherein R is greater than 7 carbon atoms in length.

12. The film of claim 9, wherein R is a compound of the form  $(\text{CH}_2)_a-\text{Z}-(\text{CH}_2)_b$ , wherein  $a \geq 0$ ,  $b \geq 7$ , and Z is any chemical functionality of interest.

13. The film of claim 12, wherein Z is selected from the group consisting of sulfones, lactams, and urea.

## 11

14. The film of claim 1, wherein the polymer film comprises a first self-assembling monolayer stamped on the polymer film and a second self-assembling monolayer located in unstamped areas of the polymer film, further wherein each self-assembling monolayer has different 5 chemical properties.

15. The film of claim 14, wherein the first self-assembling monolayer is hydrophobic, and the second self-assembling monolayer is hydrophilic.

16. A film with patterned self-assembling monolayers 10 thereon comprising:

## 12

a polymer film coated with a metal alloy; and  
a self-assembling monolayer printed onto the polymer film;

wherein the metal alloy has surface enrichment of a metal reacting with the self-assembling monolayer.

17. The film of claim 16 wherein the metal alloy is selected from the group consisting of Ni/Au, Pt/Au, and Cu/Au.

\* \* \* \* \*